UNIVERSITEIT VAN PRETORIA
UNIVERSITY OF PRETORIA
YUNIBESITHI YA PRETORIA

Desert soil microbial communities across a xeric stress gradient

Vincent Scola

Submitted in partial fulfillment of the requirements for the degree of
Magister Scientiae (M.Sc.),
in the Faculty of Natural and Agricultural Sciences, Department of Microbiology,
University of Pretoria,
Pretoria
January 2016

UNIVERSITEIT VAN PRETORIA
UNIVERSITY OF PRETORIA
YUNIBESITHI YA PRETORIA
Denkleiers • Leading Minds • Dikgopolo tša Dihlalefi

Supervisor: Prof. D. A. Cowan
Co-supervisors: Dr. J.B. Ramond and Dr. A. Frossard

Abstract

Deserts are the largest terrestrial ecosystem (Laity, 2009). It is estimated that 69% of desert lands that are used for agriculture around the world are either degraded or undergoing desertification as a consequence of climatic variation or intensive human activity (UNEP, 1992; Souvignet *et al.*, 2012). Additionally, climate change models predict that the variability of rainfall events will intensify in desert regions (Faramarzi *et al.*, 2013). Because desert environments contain a limited range of higher plants and animals, soil microbial communities are likely the most productive component of these systems as well as the dominant drivers of biogeochemical cycling (Makhalanyane *et al.*, 2015). As a result, understanding how microbial communities respond to varying degrees of moisture input and xeric stress is important for developing sustainable resource management and agriculture practices, as well as predicting the impacts of global climate change on terrestrial systems (Paul, 2014).

This study focuses on the Namib Desert in western Namibia, the oldest and one of the driest deserts on the planet (Prestel *et al.*, 2008). In the Namib Desert, sporadic rainfall events provide 25 mm of mean annual rainfall a year; however, near the coast, consistent fog formation provides a form of available water to an area that would otherwise be hyperarid (Eckardt *et al.*, 2013b). We examined the effect of xeric stress on microbial community structure and function in these desert soils, taking advantage of the naturally occurring gradient of water availability. Soil samples were collected every 10 km on a 190 km transect from the fog-dominated coastal region, through an inland area of high aridity, into a region of increased rainfall. Soil physicochemical properties and microbial community structure and function were assessed across the transect.

Both microbial community structures and functions differentiated based on three *a priori* defined zones of differing xeric stress (i.e., the 'Fog', 'Dry', and 'Rain' zones). Water availability was indicated as significantly shaping the microbial community structure and function in the central Namib Desert. In the fog dominated regions, stochastic processes dominated community assembly, while the deterministic effects of environmental filtering shaped community structure in the rest of the transect. In addition, a significant relationship between community structure and function was found (Mantel $r = 0.2$; $p < 0.01$), indicating changes in community structure coincided with changes in function.

Declaration

I, Vincent Scola, declare that the thesis/dissertation 'Desert soil microbial communities across a xeric stress gradient', which I hereby submit for the degree Magister Scientiae (M.Sc.) at the University of Pretoria, is my own work and has not previously been submitted by me for a degree at this or any other tertiary institution, and that all the sources I have used or quoted have been indicated and acknowledged by complete references throughout.

Vincent Scola
M.Sc. candidate
January 2016

Acknowledgments

First, I must thank Prof. Don Cowan for bringing me to the University of Pretoria. You truly embody the spirit of the modern day explorer and I am forever grateful for having been given the opportunity to learn from you.

Thank you to my supervisors J.B. and Aline, my lab mates, and my friends for their guidance, advice, comfort, road trips, and braais that made my time here feel like home. I arrived in South Africa knowing no one and I have left with a second family.

I must also thank my parents, grandparents, brother, sisters, and friends back in Chicago for everything while I was away. Your encouragement, inspiration, and support made this all possible.

Finally, I would like to thank the National Research Foundation (NRF) for financial assistance of this project.

"…these plains are pronounced by all wretched and useless. They can be described only by negative characters; without habitations, without water, without trees, without mountains, they support merely a few dwarf plants.

Why, then, and the case is not peculiar to myself, have these arid wastes taken so firm a hold on my memory?

…If, as the ancients supposed, the flat earth was surrounded by an impassable breadth of water, or by deserts heated to an intolerable excess, who would not look at these last boundaries to man's knowledge with deep but ill-defined sensations?"

-Charles Darwin
The Voyage of the Beagle, 1839

Table of contents

List of figures

List of tables

Chapter 1: Literature review

1.1 Deserts

Deserts cover more than one-third of the Earth's total land surface, representing the largest terrestrial ecosystem (Peel *et al.*, 2007; Laity, 2009; Pointing and Belnap, 2012). When combined with the dry subhumid regions of the desert's peripheries, desert drylands cover approximately 47% of the Earth's land surface (Figure 1) (UNEP, 1992; Laity, 2009). Abiotic pressures such as ultraviolet radiation exposure, temperature extremes, high diurnal temperature variation, and xeric conditions converge in these poly-extreme environments (Table 1). Of these pressures, xeric stress exerts the greatest strain on living organisms. Water is integral for plasma membrane functionality, required for protein folding, and is the solvent of the cellular metabolism that defines life (Rothschild and Mancinelli, 2001; Wharton, 2002; Alpert, 2005; Collet, 2011).

Water availability is widely used as a criterion to define deserts. The aridity index adopted by the United Nations Environmental Programme (UNEP) estimates the water deficit of an area based on meteorological data. This aridity index takes into consideration both precipitation (P) and potential evapotranspiration (PET) (the potential amount of water unavailable due to evaporation and plant transpiration) (Thornthwaite, 1948). Areas where the ratio of precipitation to potential evapotranspiration (P/PET) is less than 1 are classified as deserts (UNEP, 1992; Makhalanyane *et al.*, 2015). Four subcategories of the desert classification have been described: hyperarid (P/PET < 0.05), arid (0.05 to 0.20), semiarid (0.20 to 0.50), and subhumid (0.50 to 0.65) (Table 2) (UNEP, 1992).

Up to 2.1 billion people live in desert areas, and 5.2 billion hectares of desert lands are used for agriculture around the world (Souvignet *et al.*, 2012). It is estimated that 69% of these agriculturally used desert areas are either degraded or undergoing desertification as a consequence of climatic variation or intensive human activity (UNEP, 1992). The loss of this arable land is estimated to cost US$42 billion a year (UNEP, 1992; Pointing and Belnap, 2012). In addition, deserts contain 27% the global soil organic carbon reserves, and desertification has been shown to decrease soil carbon sequestering capability (Corvalan *et al.*, 2005, Pretty *et al.*, 2005, Trumper *et al.*,

Table 1: Record desert environmental extremes.

Desert Environmental Stress		Location	Reference
Temperature high	70.7°C	Lut Desert, Iran	(Mildrexler *et al.*, 2011)
Temperature low	-93.2°C	East Antarctic Plateau	(NASA, 2013)
Diurnal temperature variation	57°C (8°C to −49°C)	Browning, Montana	(Ahrens, 2011)
Aridity	0.3 mm annual rainfall	Atacama Desert, Chile	(Mooney *et al.*, 1980)
Radiation	>9 $kWh \cdot m^{-2} \cdot day^{-1}$	Atacama Desert, Chile	(Romero, 2008)

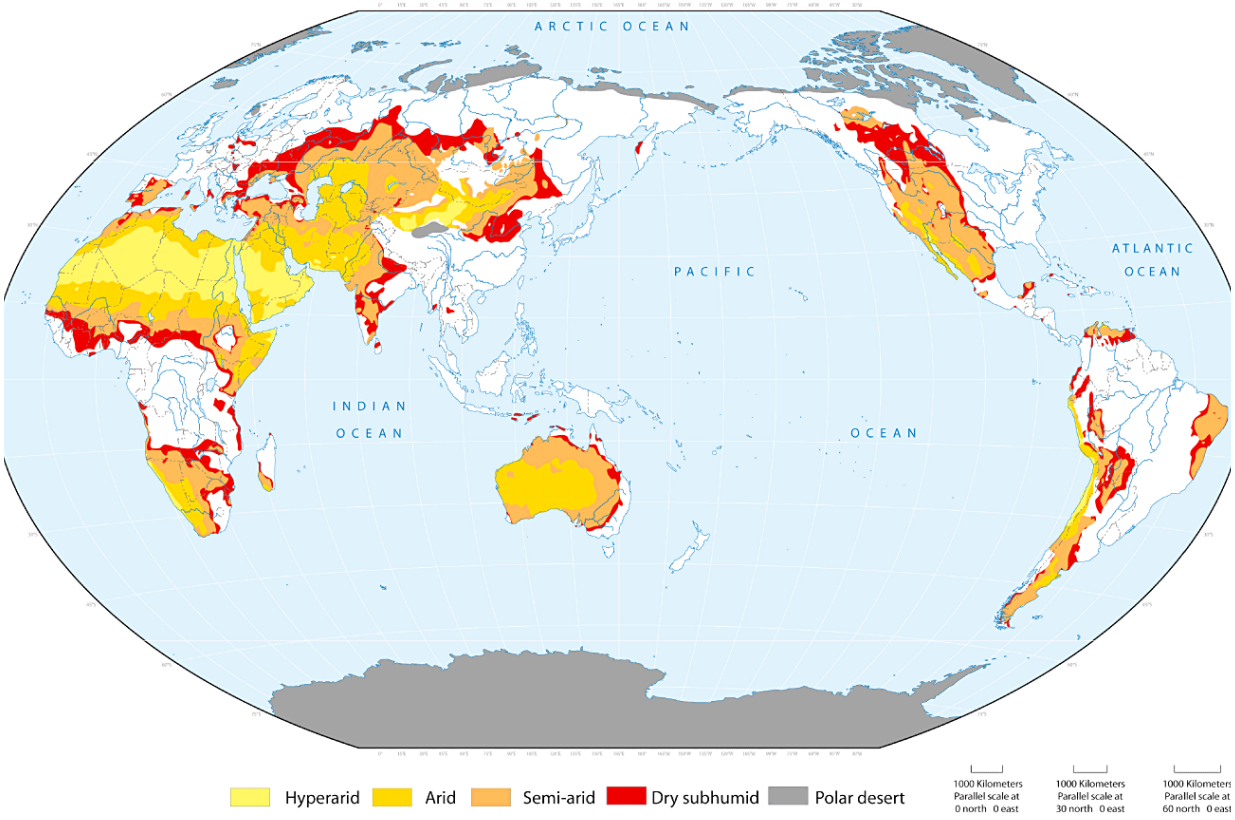

Figure 1: The distribution of arid regions on Earth (Chan *et al.*, 2012).

Table 2: Dryland categories as defined by P/PET and rainfall (UNEP, 1992).

Classification	P/PET	Annual Rainfall (mm)	Worldwide Area (%)
Hyperarid	< 0.05	< 200	7.5
Arid	0.05 < P/PET < 0.20	< 200 (winter) or < 400 (summer)	12.1
Semiarid	0.20 < P/PET < 0.50	200-500 (winter) or 400-600 (summer)	17.7
Dry subhumid	0.50 < P/PET < 0.65	500-700 (winter) or 600-800 (summer)	9.9
			Total: 47.2%

2008). Increased understanding of desert systems is critical for sustainable land management practices, conservation efforts, and water resource planning in regions that are susceptible to continued and future desertification (UNEP, 2006; Makhalanyane *et al.*, 2015).

1.2 The Namib Desert

The Namib Desert is 2 000 km long coastal desert in southwestern Africa that covers over 130 000 km^2 (Figure 2). It lies west of Great Escarpment of southern Africa, forming a 50 to 150 km wide strip from the Olifants River in South Africa (31°S), across the Atlantic coast of Namibia, to the Rio Bentiaba in Angola (14°S) (Henschel and Lancaster, 2013). The Namib Desert is among the oldest deserts on the planet. Although some controversy exists in establishing a date for the onset of aridity in the Namib Desert, geological evidence suggests the emergence of arid to semiarid conditions 80 million years (Ma) ago during late Cretaceous (Table 3) (Ward *et al.*, 1983; Ward and Corbett, 1990; Wilkinson, 1990; Goudie and Eckardt, 1999; Seely and Pallett, 2008). The present hyperarid conditions of the Namib Desert are thought to have been in place since the upwelling of the Benguela current began, 15 Ma ago (Table 3) (Siesser, 1978; Tankard and Rogers, 1978; Siesser, 1980; Van Zinderen Bakker, 1984; Pickford *et al.*, 1995; Senut and Pickford, 1995; Van der Wateren and Dunai, 2001). This longstanding aridity has resulted in the relatively limited denudation of geologic features in the Namib Desert (Bierman and Caffee, 2001).

1.2.1 Geology of the Namib Desert

The rocks that underlay the Namib Desert have a large temporal spread that reflects the complex and long-lived geology of the area (Table 3). The oldest rocks are 2 600 Ma old and found in the Northern Namib (Seth *et al.*, 1998). These Archean metamorphic rocks are part of the southwestern margin of the Congo Craton, an area of continental crust that has been tectonically stable since its formation approximately 3 000 Ma ago (Table 3; Figure 3b) (Dirks *et al.*, 2003). The rifting of the Congo and Kalahari cratons 850 Ma ago initiated the formation of the Damara Sequence, which constitutes a significant portion of Namib Desert geology (Table 3; Figure 3a) (Milner *et al.*, 1992). Damaran rocks are comprised of gneisses, granites, marbles, migmatites, schists, and amphibolites (Goudie and Eckardt, 1999). The Damara Sequence's formation concluded with the

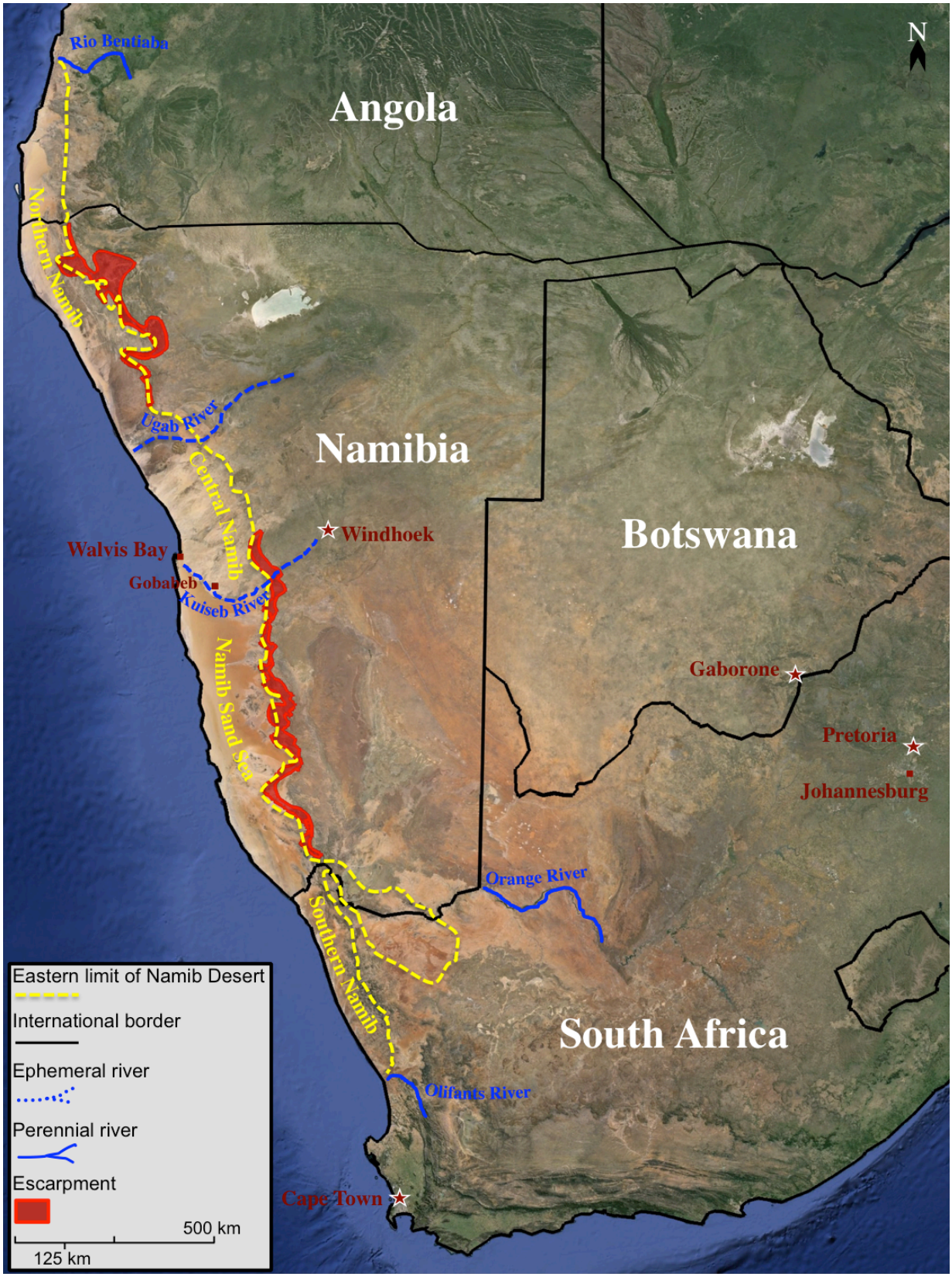

Figure 2: Map of the 2 000 km long Namib Desert of southern Africa. The dashed yellow line indicates the eastern boundary (Figure adapted by author from Google Earth, 2013; Henschel and Lancaster, 2013).

rejoining of Congo and Kalahari cratons 550 Ma ago during the forming of the Gondwana supercontinent (Table 3). The orogen created at the intersection of the two cratons resulted in rock deformation, metamorphism, and the formation of the Naukluft Mountains in southern Namibia (Martin and Porada, 1977; Gray *et al.*, 2008). During the breakup of Gondwana 132 Ma ago, southern Africa began to separate from South America as the South Atlantic opened (Table 3). This continental rifting led to the deposition of flood basalts and the distinctive Damaraland Igneous Province in the Northern Namib (Figure 3a). During this time, the formation of the sedimentary Kalahari Group initiated (Table 3; Figure 3a). The deposition of these fluvial calcretes and aeolian surface sands has continued into recent times (Wanke and Wanke, 2007).

Fission-track and cosmogenic-nuclide data has shown that the geological features of the Namib Desert have experienced low erosion rates over the past 20 Ma, evidence of the long-standing arid conditions in the region (Bierman and Caffee, 2001; Garzanti *et al.*, 2014). This slow change is evident in the current landscape of the Namib Desert, which can be subdivided into four major landscape types: the 'Southern Namib', the 'Namib Sand Sea', the 'Central Namib', and the 'Northern Namib' (Figure 2; Figure 4) (Jürgens *et al.*, 1997; Stone and Thomas, 2013).

1.2.2 The Southern Namib

The Southern (or Transitional) Namib consists largely of sand covered plains intermittently spaced by low hills and outcrops of rock (Figure 4a). These rock outcrops include the Dwyka Group sedimentary geological formations (the oldest unit of the 320 Ma old Karoo Supergroup) and the 1 050 to 1 400 Ma old Namaqua metamorphic complex (Table 3; Figure 3a). The Southern Namib extends north from the Olifants River in South Africa and includes the coastal portions of Namaqualand, a part of the Succulent Karoo that is recognized as one of the world's 25 biodiversity hotspots (Figure 2; Figure 4a) (Myers *et al.*, 2000; Burke, 2004). This area is also known as the 'Diamond Coast', where diamond mining in the Sperrgebiet occurs under heavily restricted access (Pallett, 1995). The Southern Namib branches inland around the Orange (or Gariep) River, and reaches north along the coast to form an integrated aeolian system of deposition, erosion, and transport with the Namib Sand Sea (Figure 2) (Corbett, 1993).

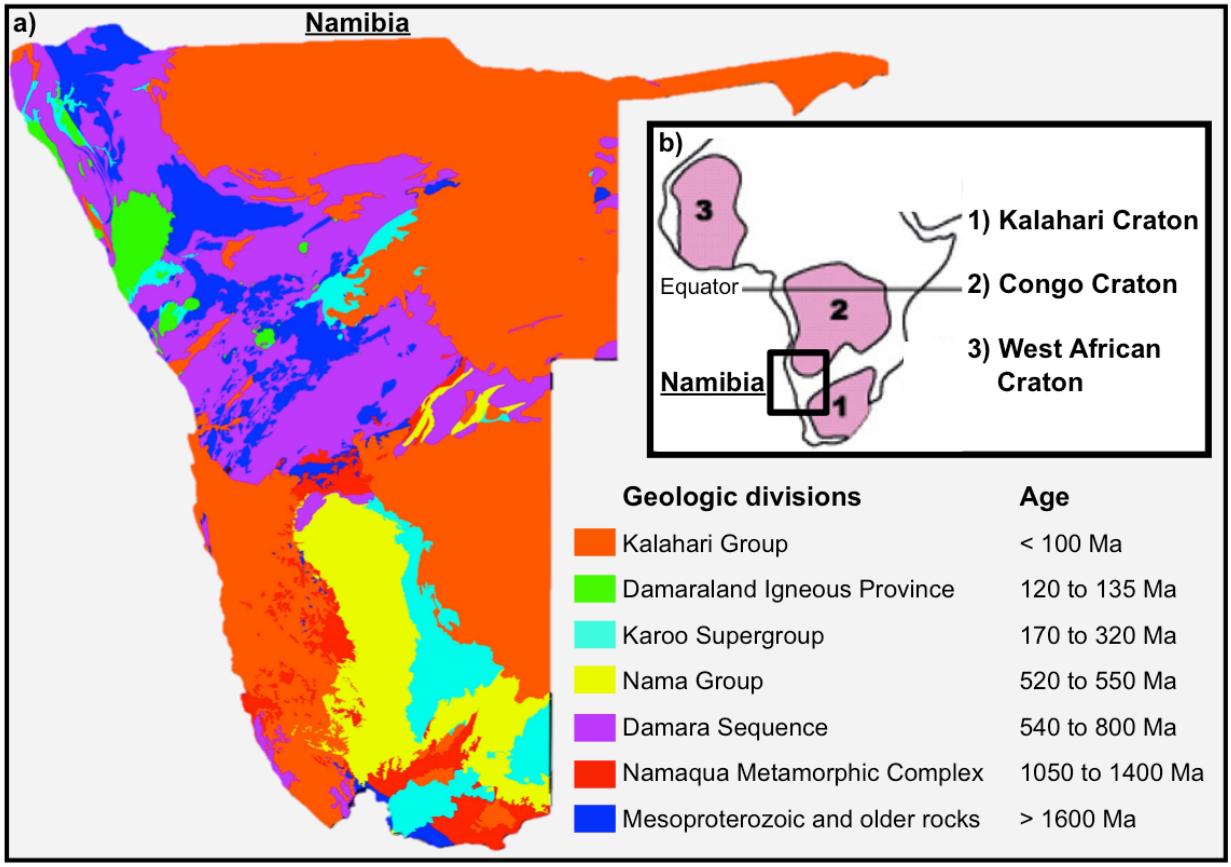

Figure 3: a) The location and ages of major geologic features of the Namib Desert. b) Approximate location of the Mesoproterozoic (>1 300 Ma) cratons of Africa (Figure adapted by author from Directorate of Environmental Affairs, 2002; Clifford, 2008; Google Earth, 2013).

Table 3: Outline of the geologic history of the Namib Desert, highlighting key events that have shaped the current landscape (Table adapted by author from Ward et al., 1983; Goudie and Viles, 2015).

Eon/Era	Period	Time (Ma ago)	Event
Archean		3000—2000	Formation of Kalahari, Congo, and West African cratons
		2600	Oldest rocks in Namibia formed
Proterozoic		1400—1050	Namaqua metamorphic complex formation
		850—600	Rifting of Kalahari and Congo cratons; Damara Sequence formation
		550	Formation of Gondwana supercontinent
Paleozoic	Cambrian	542	End of Precambrian, start of Paleozoic
	Mississippian	320	Karoo Supergroup formation initiated (cessation 170 Ma ago)
Mesozoic	Cretaceous	132—120	Breakup of Gondwana and opening of South Atlantic Ocean; eruption of Damaraland flood basalts and igneous complexes; Kalahari Group sedimentation initiated.
		80	Emergence of arid to semiarid conditions in the Namib Desert
Cenozoic	Neogene	26	Start of Miocene epoch; formation of Tsondab Sandstone
		15	Upwelling of the Benguela current and hyperarid conditions in the Namib Desert initiated
		7	Start of Pliocene
	Quaternary	2.58	Central Namib Desert dune sedimentation
		1.8	Start of Pleistocene epoch
		0.8	Northern margin of the Namib Sand Sea stabilizes

Figure 4: a) The Southern Namib (Bruenken, 1996), b) The Namib Sand Sea (Scola, 2012), c) The Central Namib (public domain), and d) The Northern Namib (Didrik, 2014).

1.2.3 The Namib Sand Sea

The Namib Sand Sea, also called the Sossus Sand Formation, has been a UNESCO World Heritage site since 2013 (Seely, 2012). Extensive aeolian dune fields cover an area of approximately 34 000 km^2, and are the largest active dune fields in southern Africa (Figure 4b) (Walter *et al.*, 1986; Livingstone, 2013). The Namib Sand Sea stretches over 400 km, delimited in the east by the Great Escarpment and in the west by the Atlantic Ocean (Figure 2). A diverse array of dune types are found in the Namib Sand Sea. Compound transverse and barchanoid dunes are found along the coast, and star dunes can be found on the sand sea's eastern margin (Lancaster, 1989). However, large linear dunes dominate the landscape, with multiple dunes reaching over 300 m in height representing some of the tallest dunes on Earth (Laity, 2009). The linear dunes are separated by interdune areas of exposed, partially lithified Tsondab sandstone (Garzanti *et al.*, 2014). The entire sand sea lies on top of the this Tsondab sandstone, a 26 Ma old aeolian analogue of the present day sand sea (Table 3) (Eckardt *et al.*, 2013a; Goudie and Viles, 2015). The deposition of the modern

sand sea, which contains over 3.75×10^{11} m^3 of sand, is estimated to have taken over 1 Ma to accumulate (White *et al.*, 2007; Vermeesch *et al.*, 2010; Garzanti *et al.*, 2012). Primary sources of sedimentation for the dune fields are thought to be the sand sheets of the Southern Namib and the catchment of the Orange River (Livingstone, 2013; Gehring *et al.*, 2014). The ephemeral Kuiseb River forms the northern boundary of the main sand sea, although some dunes near the coast extend north across the Kuiseb delta (Figure 2).

1.2.4 The Northern Namib

The Northern Namib, which stretches from the ephemeral Ugab River to the Rio Bentiaba in Angola, contains two additional dune fields smaller in size than the Namib Sand Sea; the Skeleton Coast and Kunene sand seas (Figure 2; Figure 4d). The Northern Namib is also known as the Kaokoveld Desert, or the Moçâmedes Desert where it crosses into Angola. The Skeleton Coast sand sea is approximately 2 000 km^2 and runs 150 km along the Namibian Atlantic coast. A large portion the Skeleton Coast sand sea sand originates from the Orange River (≥ 80%; Figure 2) (Bluck *et al.*, 2007). The sediment is carried 1 750 km by longshore ocean currents and is the longest littoral sand transport yet documented (Garzanti *et al.*, 2014). The Skeleton Coast sand sea is also the result of the slow erosion of Damara Sequence rocks (Table 3; Figure 3a).

The Kunene sand sea is approximately 2 000 km^2 and dominated by barchan, transverse, and linear dunes (Goudie and Viles, 2015). It straddles the mouth of the Kunene River, extending north into southern Angola (Garzanti *et al.*, 2014). Beyond the sand seas, the Northern Namib is comprised of dissected pediplains with lava-capped plateaus and hills in an area known as the Kaokoveld. The relative inaccessibly of the Northern Namib, and the issues of access in the diamond areas of the Southern Namib, has led to the predominance of the research being carried out in the Central Namib portion of the Namib Desert (Lancaster, 2002; Krapf *et al.*, 2003; Stone and Thomas, 2013).

1.2.5 The Central Namib

Bounded by the ephemeral Kuiseb and Ugab Rivers, the Central Namib is an expanse of ancient gravel plains containing a large temporal spread of geologic features (Figure 2; Figure 4c).

Inselbergs of Precambrian rock (550 Ma old) and scattered dunes of Quaternary sedimentation (1 Ma old) share a landscape marked by the tectonic opening of the South Atlantic Ocean during the Cretaceous 132 Ma ago (Table 3) (Goudie and Eckardt, 1999). Periodic flooding of the Kuiseb River flushes away the aeolian sand from the Namib Sand Sea to the south and prevents dune migration from advancing northward (Figure 2) (Ward, 1987). The Kuiseb River has impeded the dune fields from extending northward since the late Pleistocene, 0.8 Ma ago (Table 3) (Bierman and Caffee, 2001). The elevation of the Central Namib plains rises at a 1° gradient from the sea inland to approximately 1 000 m at the Great Escarpment (the eastern boundary of the Namib Desert; Figure 2). Fluvial gravel and sands up to 125 m deep border the coast and gypcrete soils up to 1.5 m deep dominate the coastal plains that reach approximately 70 km inland (Figure 5) (Eckardt *et al.*, 2001; Viles and Goudie, 2013). The soil fertility of these gypsum laden soils is very low and vegetation cover in the coastal plain is almost nonexistent (Mendlesohn *et al.*, 2002). Inland, the coastal plain transitions to a gravel plain. The gravel plains of the Central Namib are interspersed with exposed bedrock, scattered dunes, marble, and dolerite ridges (Eckardt *et al.*, 2013a; Viles and Goudie, 2013). Large expanses of calcrete also cover the gravel plains (the result of carbonate rock weathering) (Figure 5). The calcrete serves as a barrier to erosion and reduces the denudation rates in this area (Viles and Goudie, 2013). Soil alkalinity is higher in the gravel plain than the coastal plain, and the calcisols offer an increased degree of soil fertility. However, vegetation cover is still relatively low on the gravel plains because of low nutrient levels and high concentrations of calcium, which reduce the bioavailability of iron and zinc (Mendlesohn *et al.*, 2002). East of the gravel plains, leptosols and regosols are found at the base of the Great Escarpment and Central Plateau (Figure 5). The water holding capacity in the soils of these actively eroding regions is low, and vegetation cover is generally sparse and subject to drought (Mendlesohn *et al.*, 2002). The regosols are fine-textured and particularly susceptible to erosion, and the coarse-textured leptosols are the shallowest soils found in Namibia (Mendlesohn *et al.*, 2002). Throughout the Central Namib, nutrient rich, deep soils are largely absent as a direct result of the Namib Desert's long history of climatic aridity (Van der Wateren and Dunai, 2001; Eckardt *et al.*, 2013a; Viles and Goudie, 2013).

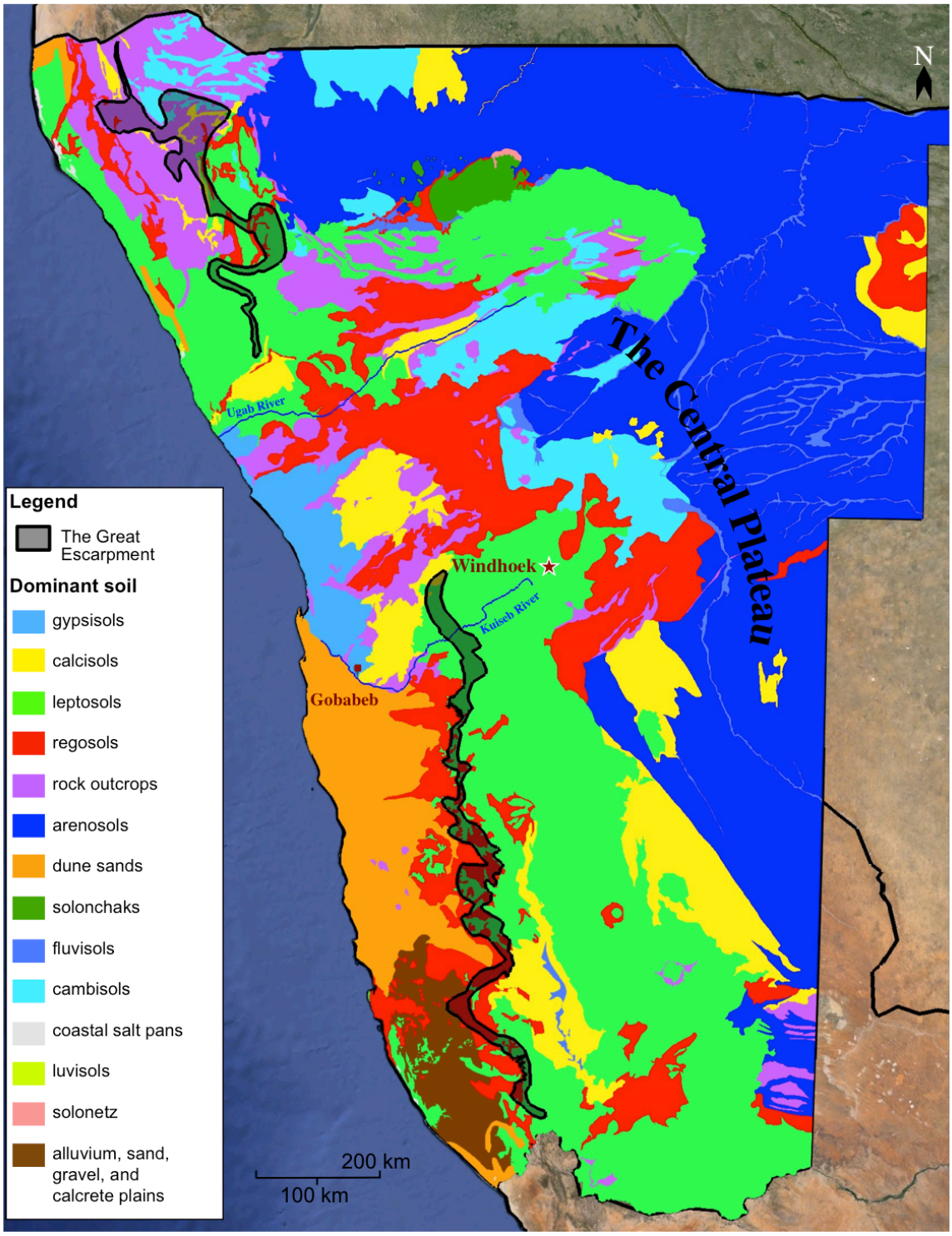

Figure 5: Dominant soil types in Namibia and across the Namib Desert (Figure adapted by author from Directorate of Environmental Affairs, 2002; Google Earth, 2013).

1.2.6 Climate of the Namib Desert

In addition to being one of the oldest, the Namib Desert is also one of the driest deserts in the world, receiving 25 mm of mean annual rainfall (data from 1960 to 2010) (Eckardt *et al.*, 2013b). In

comparison, the Atacama Desert, which is the driest desert on Earth, has a long-term mean annual rainfall of 5 to 25 mm (Warren-Rhodes *et al.*, 2006). However, the extreme aridity of the Namib Desert is balanced by two sources of water availability: fog and rainfall. Fog events in the Namib Desert are a consequence of the Benguela current, which cycles cold water from the Antarctic up the western coast of Africa (Figure 6). This cold water lowers the temperature of the coastal air making it cool, dense, and stable. The cool, moist coastal air is unable to rise to the elevations necessary to create rain-bearing clouds, instead creating fog (Mendlesohn *et al.*, 2002). The Benguela current is very efficient at producing and sustaining fog, which can occasionally reach the base of the Great Escarpment (< 10 days a year). More often, the fog drifts up to 75 km inland (up to 100 days out of the year; Figure 6) (Eckardt *et al.*, 2013b). The shading effect of the fog and low-lying cloud cover also reduces the solar radiation near the coast compared to the relatively high levels received inland (Figure 7). At the central Namib coast, where over 125 fog days are recorded each year, up to 34 mm of moisture is precipitated from fog annually (Viles and Goudie, 2013). This exceeds the total moisture contribution of rain in the coastal region for most years (Olivier, 1995; Goudie and Eckardt, 1999; Robinson and Barrows, 2013).

Rainfall in Namibia is mainly tied to the hot, moist air of the Intertropical Convergence Zone (ITCZ) (Figure 8). In the austral winter, the high pressure cell of the South Atlantic anticyclone pushes air from the southwest inland (Figure 8). This prevents the moist air in the ITCZ from moving southward, creating a dry season in Namibia from June to November (Hachfeld, 2000; Okitsu, 2005). In the austral summer (December to March) the South Atlantic anticyclone moves to the south, allowing the moist air of the ITCZ to move southward as well. The moist air condenses as rain as it moves down from the north of the country (where the mean annual rainfall is greatest) (Figure 9). Rain-bearing clouds that reach the Great Escarpment from the north precipitate much of their moisture at this high elevation point before reaching the lower elevations of the Namib Desert in the west (Figure 9; Figure 10). Strong onshore winds also push rain-bearing weather systems inland, further impeding their penetration into the Namib Desert (Figure 8) (Robertson, 2012). In addition, rainfall in Namibia has the highest coefficient of variation in all of southern Africa, with a large degree of variability seen specifically in the central and northern Namib Desert (Figure 11) (Southgate *et al.*, 1996; Mendlesohn *et al.*, 2002; Muller *et al.*, 2008; Eckardt *et al.*, 2013b).

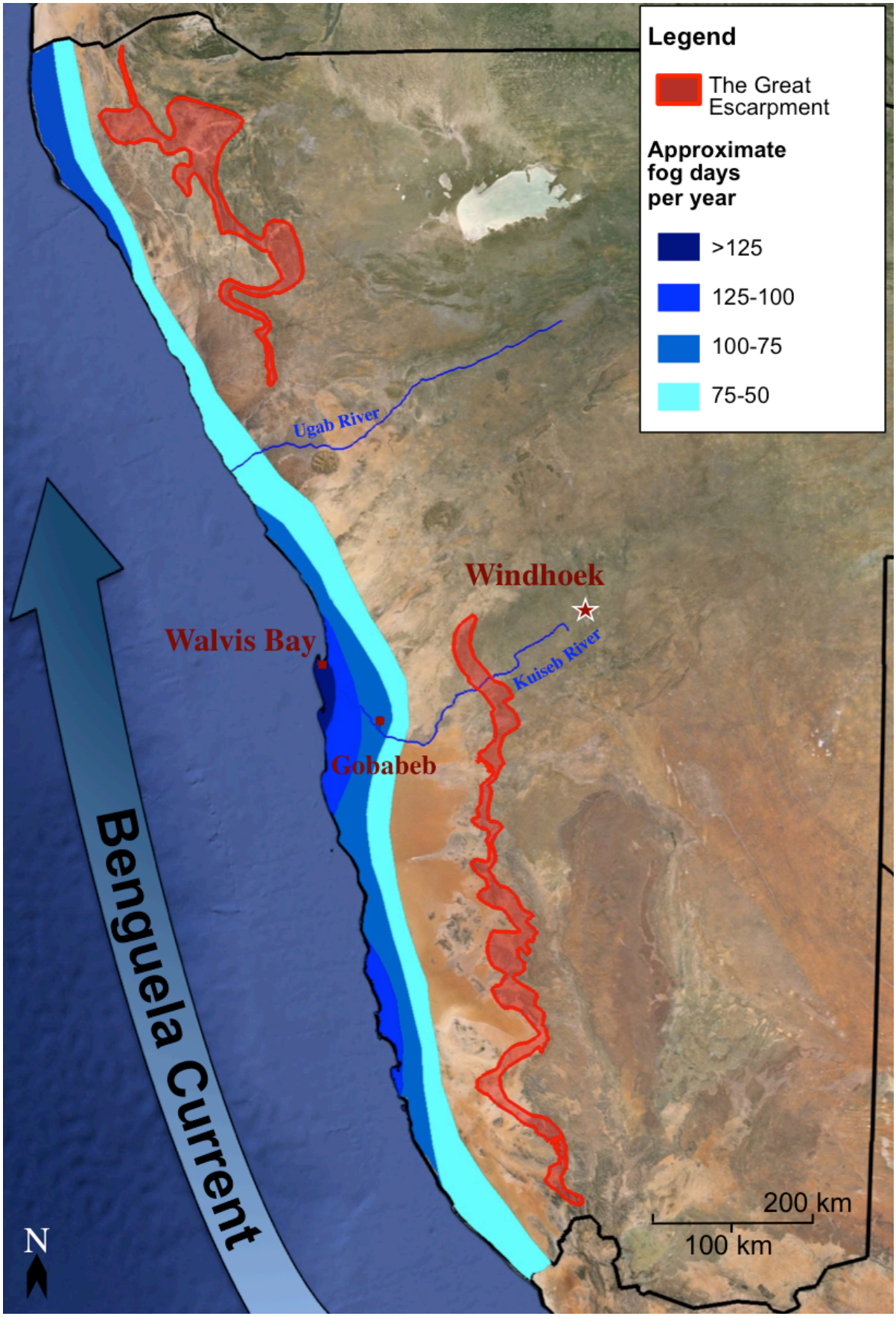

Figure 6: Approximate number of fog days per year in Namibia (Figure adapted by author from Directorate of Environmental Affairs, 2002; Eckardt *et al.*, 2013b; Google Earth, 2013).

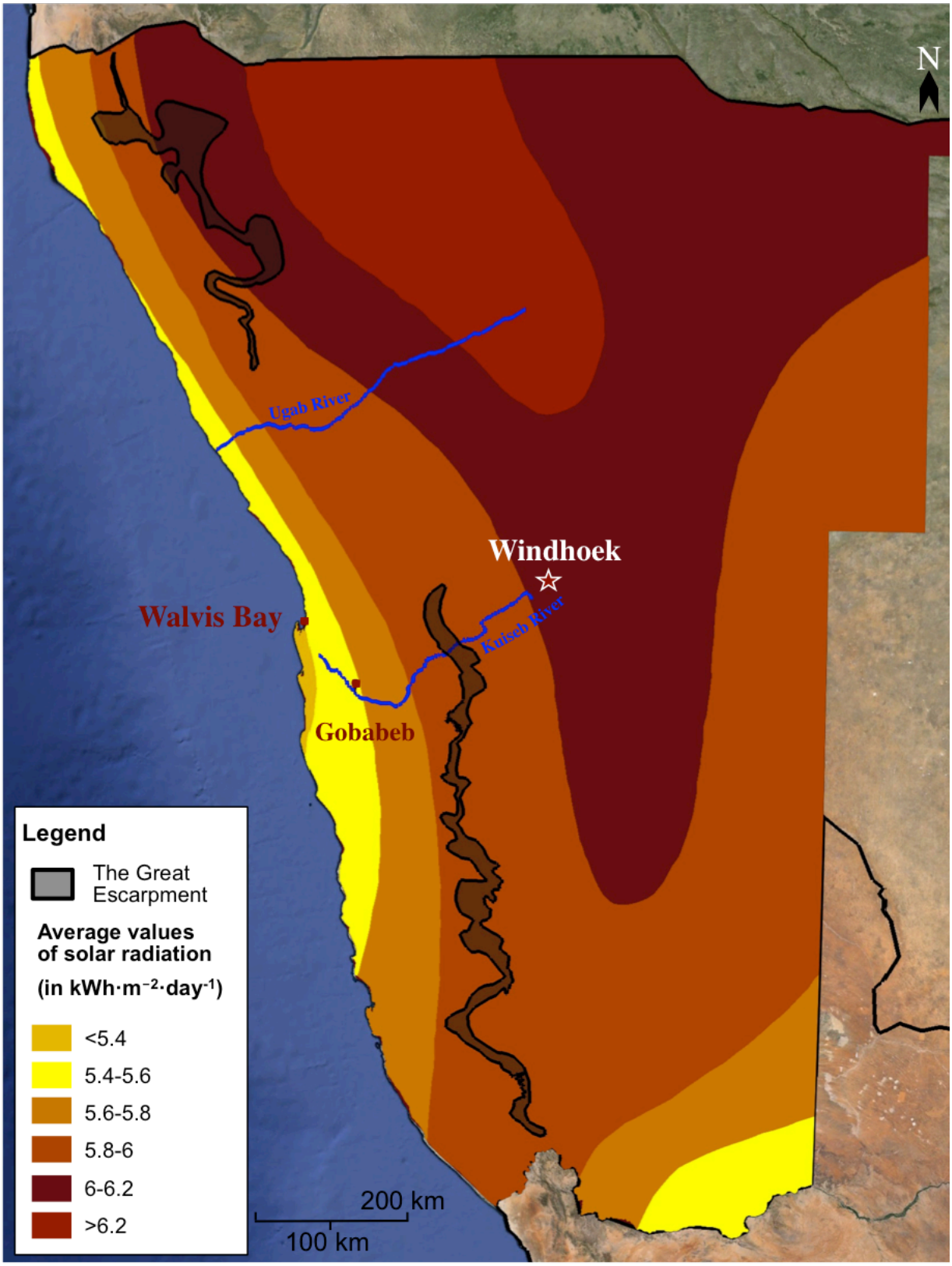

Figure 7: Average values of solar radiation in Namibia (in kWh·m^{-2}·day^{-1}) (Figure adapted by author from Directorate of Environmental Affairs, 2002; Google Earth, 2013).

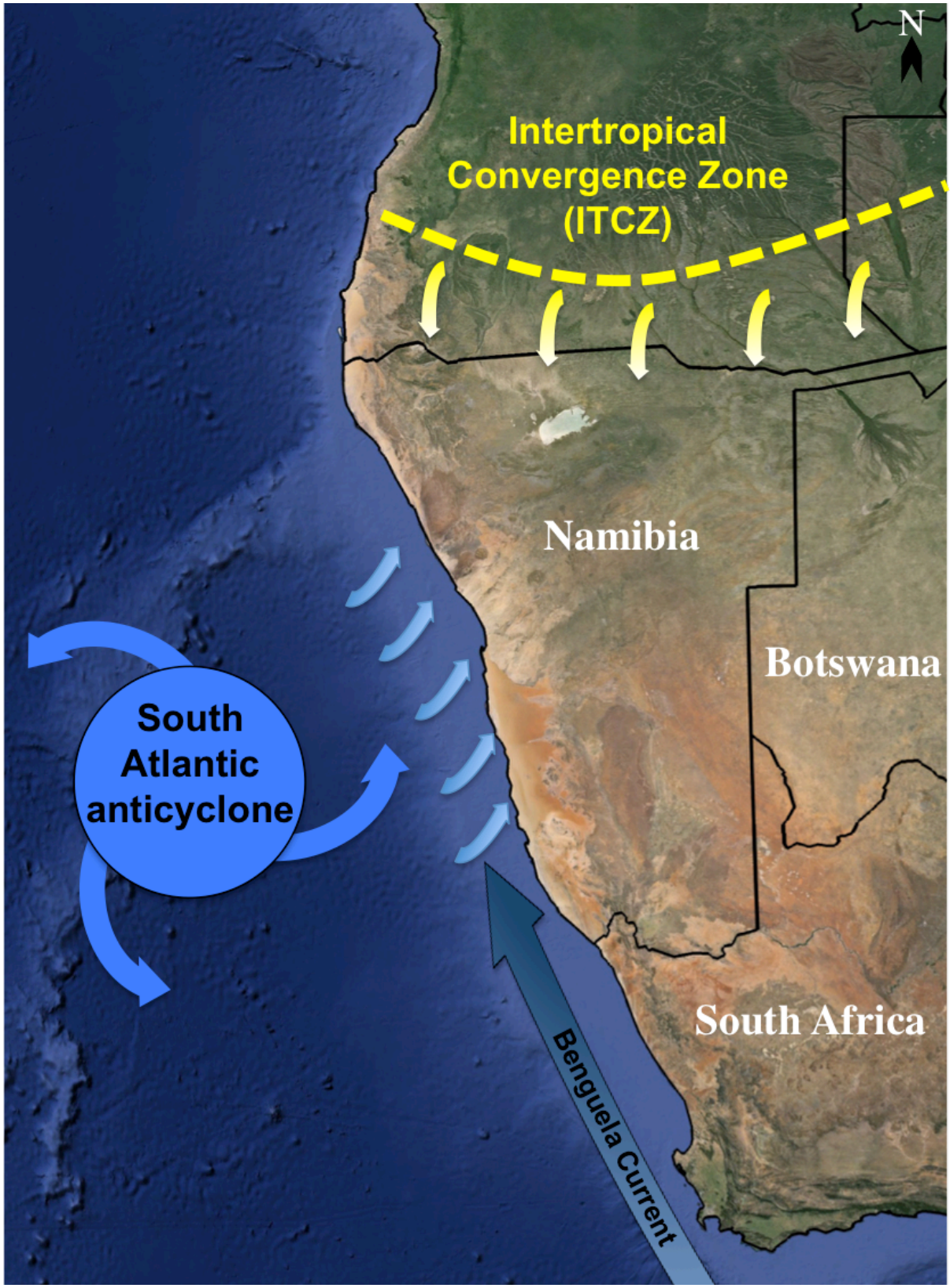

Figure 8: The major air pressure and convergence zones of Namibia (Figure adapted by author from Mendlesohn et al., 2002; Google Earth, 2013).

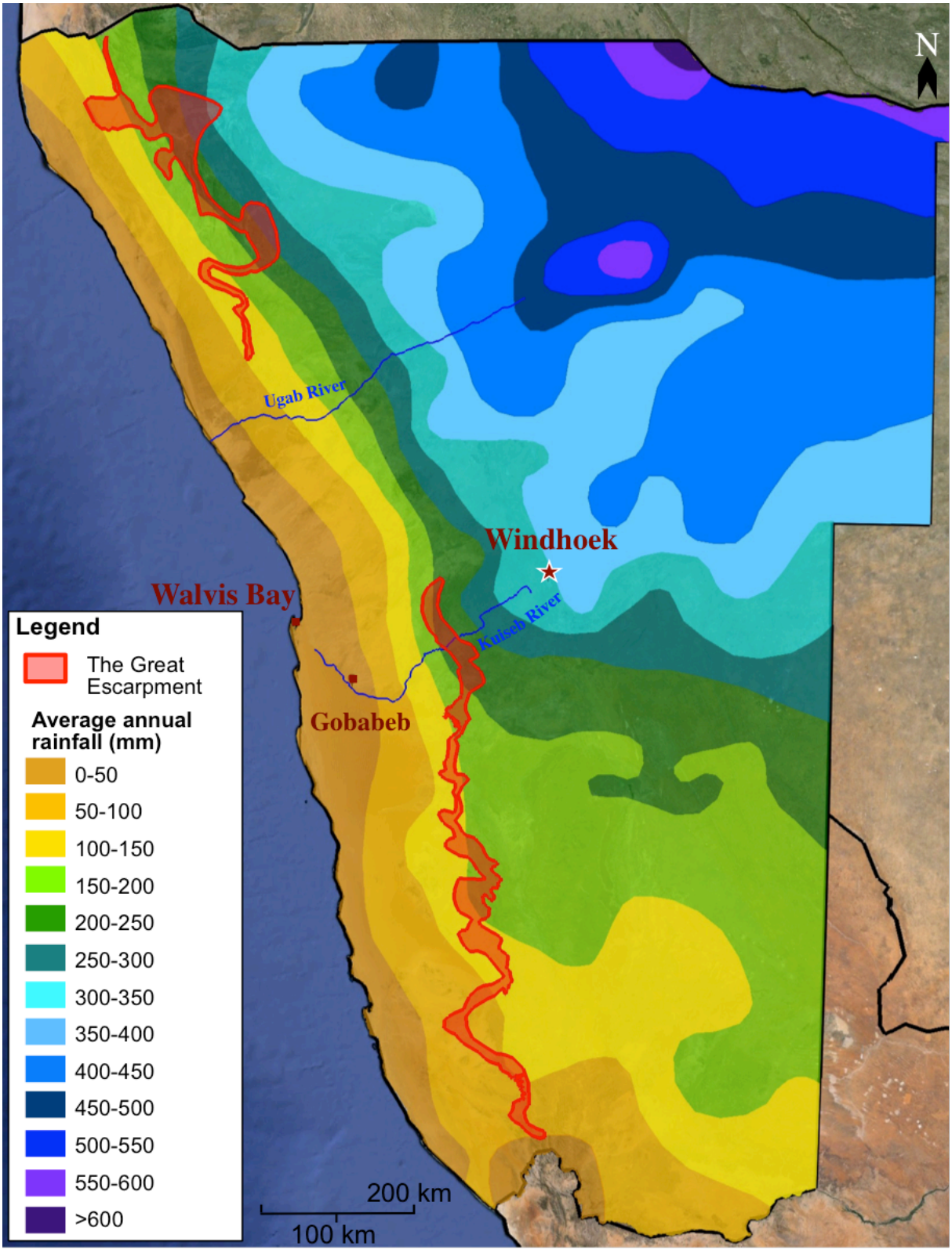

Figure 9: Mean annual rainfall in Namibia (Figure adapted by author from Directorate of Environmental Affairs, 2002; Google Earth, 2013).

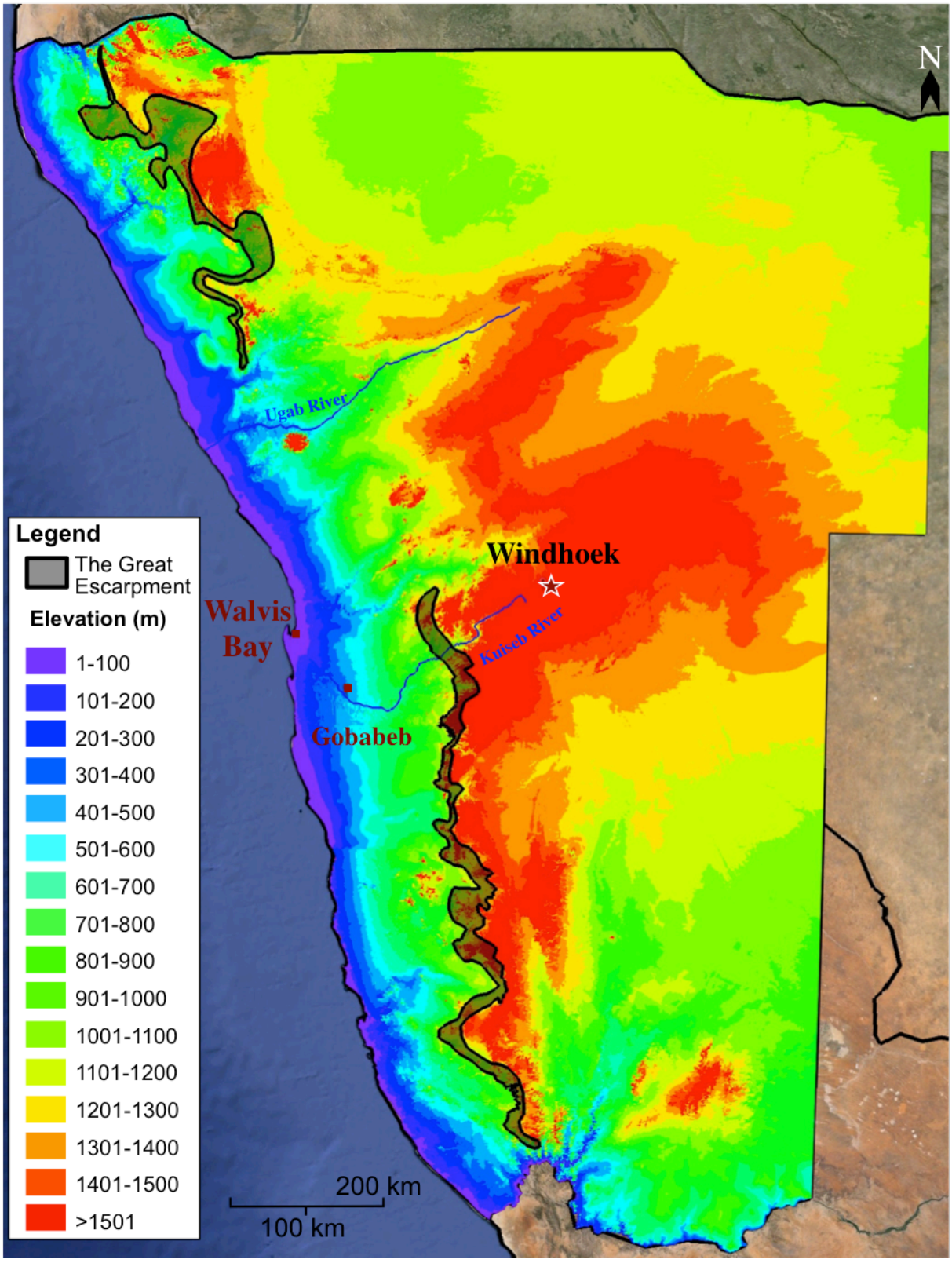

Figure 10: Elevations and relief in Namibia (Figure adapted by author from Directorate of Environmental Affairs, 2002; Google Earth, 2013).

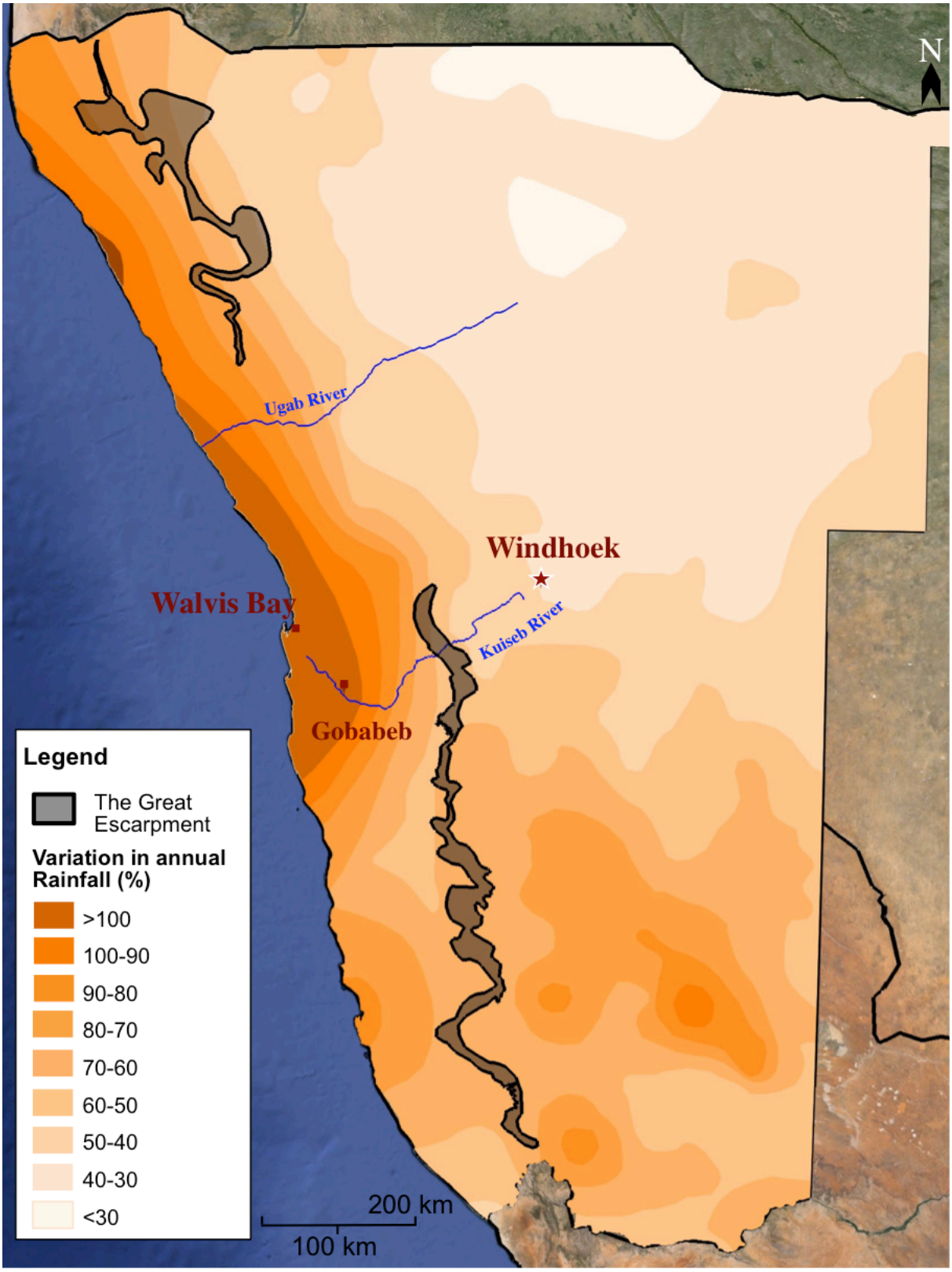

Figure 11: Coefficient of variation in rainfall in Namibia (Figure adapted by author from Directorate of Environmental Affairs, 2002; Google Earth, 2013).

This variation results in strong fluctuations of water availability in the region across years and decades (Henschel and Lancaster, 2013). Despite this temporal variability, a spatial rainfall gradient occurs from the coast inland in the Namib Desert, and the mean annual rainfall steadily increases with increasing elevation (Figure 9; Figure 10).

1.3 Microbial ecology of desert soils

The vast majority Earth's biomass is comprised of microorganisms, with 350 to 550 Pg of organic carbon (C) contained in prokaryotic life alone (Whitman *et al.*, 1998; Forney *et al.*, 2004). Worldwide, prokaryotes also contain 9 to 14 Pg of phosphorus (P) and 85 to 130 Pg of nitrogen (N) (Whitman *et al.*, 1998). This is 10 times the amount found in plants and represents the largest reservoir of these nutrients in all living organisms (Whitman *et al.*, 1998).

Within the edaphic systems of terrestrial soils, microorganisms are abundant; 10^9 bacterial cells can be found per gram of soil (2.6×10^{29} total prokaryotic cells in soils worldwide) (Bakken, 1985). The biological activity in soil is non-homogenous, localized around aggregates with differing physicochemical properties (Sexstone *et al.*, 1985). In addition, the physicochemical properties in soil systems change spatially and temporally. In these dynamic systems, shifting C sources, mineral nutrients, ionic composition, water availability, temperature, and pH affect microbial ecology, activity, and population dynamics (Nannipieri *et al.*, 2003). As a result, the microbial communities of edaphic systems are thought to be the most complex on Earth (Torsvik *et al.*, 1990; Urich *et al.*, 2008). Developing a better understanding of the factors that determine microbial community composition and function in soils will further our understanding of the soil biogeochemical processes for C, N, and P cycling, which are critical for overall soil quality (Yao *et al.*, 2000; Calderon *et al.*, 2001; Keith-Roach *et al.*, 2002; Drenovsky *et al.*, 2004). This is of particular importance in arid environments and their peripheries as susceptibility to desertification adversely affects the soil quality in these regions (Doran and Zeiss, 2000; Pointing and Belnap, 2012).

Owing to their complexity, soil microbial communities contain immense genetic diversity (Torsvik and Øvreås, 2002). Understanding the mechanisms that control the assembly of these microbial

communities is a major target of ecological research (Valverde *et al.*, 2015). Microbial communities may be shaped by the deterministic forces of abiotic and biotic selection (Coleman and Chisholm, 2010), or by the random stochastic processes of chance colonization and ecological drift conceptualized in neutral theory (Hubbell, 2001). Analysis of global patterns in community assembly have suggested that deterministic processes play a dominant role in shaping communities (Lozupone and Knight, 2007; Tamames *et al.*, 2010). However, stochastic processes have been shown to shape community structure in high productivity environments (Chase, 2010), while deterministic processes are thought to shape the communities of high stress habitats (Wang *et al.*, 2013). Likely, a combination these two mechanisms of assembly are what determine microbial communities composition (Hanson *et al.*, 2012; Lindström and Langenheder, 2012; Valverde *et al.*, 2015).

Desert edaphic microbial communities may be well suited to analyze the mechanisms of community assembly, as well as microbial functional capacities (López-Lozano *et al.*, 2013). Due to the limited range of higher plants and animals, desert microbial communities are likely the dominant drivers of biogeochemical processes and primary production in these systems (Friedmann and Ocampo, 1976; Makhalanyane *et al.*, 2015). However, the harsh conditions of deserts environments require special adaptations for the microbial communities present in the soil.

1.3.1 Biological soil crusts

One of the most common adaptations of microbial associations in deserts is the formation of cohesive, macroscopic soil-surface communities known as biological soil crusts (BSCs), which can cover up to 70% of the desert soil's surface (Belnap, 2003). BSCs generally include groupings of different organisms, such as chlorophyte algae, filamentous cyanobacteria, fungi, heterotrophic bacteria, and mosses (Pointing and Belnap, 2012). The communities of the BSCs take on a layered structure, where UV susceptible organisms are protected beneath heavily pigmented fungal or cyanobacterial species (Pointing and Belnap, 2012). The protected photoautotrophs have been shown to move to the surface of the crust during wetting events and retreat below the protective layer upon drying. This is a common protective mechanism among surface microbial communities in stress inducing environments (Pointing and Belnap, 2012). The cohesive structure of BSCs is mostly

due to filamentous cyanobacteria, predominantly of the genus *Microcoleus* (Belnap, 2003), and the polysaccharides extruded by the BSC communities that link the loose particles into larger stabilized soil aggregates. This stabilization protects the soil from the wind and water erosion that is otherwise common for the slow forming soils of arid environments (Pointing and Belnap, 2012). In arid environments, vascular plant coverage is limited and BSCs are thus an important source of fixed C and N (Belnap, 2003). BSCs can fix over 2.6 Pg of C from atmospheric carbon dioxide (CO_2) globally per year and have been shown to contribute largely to N fixation, nitrification, and denitrification in arid environments (Castillo-Monroy *et al.*, 2010; Elbert *et al.*, 2012).

However, in some desert environments temperature extremes and low water availability impede the formation of surface BSCs. In such environmental conditions, cryptic biofilms similar to BSCs are able to form on the ventral surfaces of translucent rocks (hypoliths) and inside the spaces of porous stones (endoliths) (Makhalanyane *et al.*, 2015).

1.3.2 Cryptic microbial communities

Gravel plains are a major geomorphological feature of desert surfaces and provide niche environments where cryptic microbial communities are able to thrive (Laity, 2009). The underside of translucent rocks (such as quartz and marble) found on these plains are often colonized by 'hypolithic' communities at the soil-rock interface (Warren-Rhodes *et al.*, 2006). The rocks provide a stable substrate for growth while trapping water and protecting the communities from harmful UV radiation. Limestone, sandstone, and weathered granite provide similar protection for endolithic community colonization in the cracks, porous spaces, and fissures of these stones (Pointing and Belnap, 2012). Hot desert hypolithic and endolithic communities are dominated by cyanobacteria, and the genera *Chroococcidiopsis* is particularly well represented (Warren-Rhodes *et al.*, 2006; Tracy *et al.*, 2010; Bahl *et al.*, 2011; Lacap *et al.*, 2011; Azua-Bustos *et al.*, 2012; Makhalanyane *et al.*, 2013). The cyanobacterial members present in hypolithic communities possess the genetic capability to mediate key nutrient cycling processes (Chan *et al.*, 2012). For example, the N_2 fixing capacity of *Gloeothece* and *Nostoc* may contribute significantly to soil N budgets in arid environments (Makhalanyane *et al.*, 2015). These photoautotrophic, hypolithic taxa are thought to support heterotrophic bacteria or fungi members as C and N sources (Pointing *et al.*,

2009). In hyperarid systems, hypoliths are a major source of biomass and are often the primary producers for the region (Cary *et al.*, 2010). Hypolithic microbial communities share a significant degree of community diversity with the open soil communities surrounding them, as the edaphic communities likely act as a reservoir from which hypolithic communities recruit (Makhalanyane *et al.*, 2013).

Recently described 'hypoendolithic' microbial communities (Wierzchos *et al.*, 2012) have been found inhabiting gypsum (hydrous calcium sulfate; $CaSO_4 \cdot 2H_2O$) and halite (NaCl) crusts in desert regions too dry to support hypolithic communities (Warren-Rhodes *et al.*, 2006; Davila *et al.*, 2010). Hypoendolithic microbial communities may survive on water made available by the deliquescence of the hygroscopic minerals they inhabit (Davila *et al.*, 2010; Robinson *et al.*, 2015). These extreme microbial communities are of particular interest in the field of astrobiology as gypsum and other hygroscopic minerals are known to occur on the surface of Mars (Davila *et al.*, 2010; Schopf *et al.*, 2012). Hypoendolithic microbial communities may exist close to the dry limit of life on Earth, and hygroscopic minerals are capable of deliquescence under the present day climatic conditions of Mars (Davila *et al.*, 2010). Cryptic microbial communities represent a wide spectrum of habitability in extreme environments.

1.3.3 Open soil microbial communities

BSCs and cryptic microbial communities have been studied extensity in desert systems (Wynn-Williams, 2002; Warren-Rhodes *et al.*, 2006; Pointing *et al.*, 2009; Cary *et al.*, 2010; Wong *et al.*, 2010). Over 3 000 publications examining the biology, ecology, and ecophysiology of BSCs alone are currently available (Belnap, 2003). However, soil as a biological system is complex and dynamic, and comparably little is known about the desert open soil microbial communities that surround BSCs and other cryptic refuge niches (Nannipieri *et al.*, 2003). Analyses that have been conducted on desert soil around the world typically reveal similar phyla, including Actinobacteria, Bacteroidetes and Proteobacteria (Chanal *et al.*, 2006; Connon *et al.*, 2007; Lester *et al.*, 2007; Fierer *et al.*, 2009; Makhalanyane *et al.*, 2015). Actinobacteria often dominate phylogenetic surveys in arid environments (Liu *et al.*, 2009; Makhalanyane *et al.*, 2013; Goswami *et al.*, 2014; Makhalanyane *et al.*, 2015), which may be unsurprising given their ability for sporulation, UV

damage repair, and extensive metabolic capacities (Ensign, 1978; McCarthy and Williams, 1992; Chater and Chandra, 2006; Gao and Garcia-Pichel, 2011; Makhalanyane *et al.*, 2015). Interestingly, many Actinobacteria isolated from arid soils appear to be novel species, highlighting the need for further research in these regions (Li *et al.*, 2005; Li *et al.*, 2006; Mayilraj *et al.*, 2006; Lester *et al.*, 2007; Luo *et al.*, 2012). A better understanding of open soil microbial communities in desert environments is critical, and this study focuses on open soil microbial communities in the Namib Desert.

1.3.4 Microbial communities in the Namib Desert

As with other studies conducted on deserts soils, phylogenetic surveys in the Namib Desert have shown open soil samples to be dominated by Actinobacteria (accounting for up to 44% of phyla found) (Makhalanyane *et al.*, 2015). The Actinobacteria in the Namib Desert have high sequence homology to *Arthrobacter*, *Rubrobacter*, *Streptomyces*, and *Thermopolyspora* spp. (Drees *et al.*, 2006; Makhalanyane *et al.*, 2013; Santhanam *et al.*, 2013). Namib Desert Actinobacteria are well suited for survival for the arid environment as they are UV resistant, capable of sporulation, and have shown plasticity in carbon and energy utilization (Lynch *et al.*, 2014). Proteobacteria and Firmicutes (specifically of the genus *Bacillus*) are also found in high numbers in Namib Desert soils (Prestel *et al.*, 2008; Makhalanyane *et al.*, 2013). Other phyla found in the Namib Desert include Acidobacteria, Bacteroidetes, Chloroflexi, and Planctomycetes, all of which are commonly found in desert soils worldwide (Prestel *et al.*, 2008; Makhalanyane *et al.*, 2013). The Namib Desert soil communities are generally similar in composition to those of other hot hyperarid deserts (Dunbar *et al.*, 2002; Chanal *et al.*, 2006; Fierer and Jackson, 2006; Jones *et al.*, 2009; Lauber *et al.*, 2009; Makhalanyane *et al.*, 2013). However, a recent phylogenetic study indicated that up to 94% of the bacterial community analyzed may be of novel taxa (Makhalanyane *et al.*, 2013). This is consistent with findings from other desert soils, where many isolates were found to be novel species (Li *et al.*, 2005; Li *et al.*, 2006; Mayilraj *et al.*, 2006; Lester *et al.*, 2007; Luo *et al.*, 2012).

Open soil microbial communities may act as biological reservoirs from which hypolithic communities are ‘seeded’ (Makhalanyane *et al.*, 2013). Makhalanyane *et al.*, 2013 found that 88% of sequenced operational taxonomic units (OTUs) from hypolithic community samples in the

Namib Desert were also found in open soil. The increased water availability found beneath hypolithic rocks may allow desiccation sensitive species found in low abundance in the open soil to thrive and proliferate (Cockell and Stokes, 2004; Wood *et al.*, 2008a; Cowan *et al.*, 2010; Khan *et al.*, 2011). The actual mechanisms of this assembly are still unknown, but the growth of the hypolithic communities may be in the time scale of decades (Warren-Rhodes *et al.*, 2006).

Hypolith communities in the Namib have been shown to be dominated by Cyanobacteria (85%) and may act as reservoirs for cyanobacterial diversity (Makhalanyane *et al.*, 2013; Stomeo *et al.*, 2013). Some samples show high homology to unknown cyanobacteria, but many are part of the *Chroococcidiopsis* genus (Makhalanyane *et al.*, 2015). Members of the *Chroococcidiopsis* genus are a common primary producer found in hot and cold deserts, and are resistant to desiccation and ionizing-radiation (Billi *et al.*, 2000; Tracy *et al.*, 2010; Caruso *et al.*, 2011; Lacap *et al.*, 2011). Acidobacteria, Actinobacteria, and Proteobacteria phyla are also present, though found in much lower proportions (less than 3% of the total bacterial community) (Makhalanyane *et al.*, 2013). *Methylobacterium* spp. are also found in Namib Desert hypolithons (Makhalanyane *et al.*, 2013). *Methylobacterium* are facultative methylotrophs, indicating the utilization of one-carbon compounds such as methanol or methane as a possible adaptation of Namib hypolithons (Green, 2006; Makhalanyane *et al.*, 2015).

The assembly of the hypolithic and open soil communities in the Namib Desert appears to be shaped primarily by the deterministic effects of soil salinity, with stochastic processes playing a lesser role (Stomeo *et al.*, 2013). This is not uncommon in harsh environments, where niche-selective environmental forces appear to have a greater impact on community composition (Chase, 2007, 2010). Water availability and source specifically play a critical role in determining the abundance and composition of hypolithic communities in the Namib (Warren-Rhodes *et al.*, 2006; Makhalanyane *et al.*, 2013; Stomeo *et al.*, 2013). Supplemented by fog moisture near the coast, high hypolithic abundance was observed at landscape scales (1 to 10 km) with quartz rock colonization rates above 95% (Warren-Rhodes *et al.*, 2006). In contrast, total quartz rock colonization rates in the hyperarid core of the Atacama Desert were as low as 0.0008% (Lacap *et al.*, 2011). Fog moisture also contributed to the colonization of 98% of small quartz rocks

(5 to 7.5 cm diameter), in contrast to the 3% colonization rate observed in other hyperarid deserts (Warren-Rhodes *et al.*, 2006). Namib hypolithic community diversity also differed significantly based on water source (fog or rainfall), and the hypolithic communities found in the rainfall dominated zone contained more unique OTUs than those found in the fog dominated zones (Stomeo *et al.*, 2013). This variation in community structure based on climatic regime was not observed in the open soil communities. However, both open soil and hypolithic microbial communities showed differences in composition based on the sodium content of the soil, and increased sodium content resulted in decreased bacterial richness (Stomeo *et al.*, 2013). Soil texture and sand content has also been shown to affect microbial communities in the Namib, as low microbial biomass was found in soil with increased sand content (Wichern and Joergensen, 2009). This was not surprising, as high sand content limits the water holding capacity of soil, and salts decrease biological water availability by reducing water activity (a_w) (Austin *et al.*, 2004; Cowan, 2009). No other geochemical variables measured (soil pH, C, N, calcium, magnesium, or potassium content) had an effect on open soil or hypolithic communities, highlighting the importance of water availability in this system (Stomeo *et al.*, 2013).

Analysis of the bacterial communities present in the Namib Sand Sea indicated the deterministic effects of habitat filtering were shaping the bacterial communities present (Ronca *et al.*, 2015). Similarly to open soil microbial communities of the Namib Desert, the dune sands were dominated by Proteobacteria, Actinobacteria, and Bacteroidetes (Makhalanyane *et al.*, 2015; Ronca *et al.*, 2015). This phylogenetic profile on the Namib Sand Sea was similar to the dune systems of the Gobi and Taklamaken deserts (of Mongolia and China, respectively) (An *et al.*, 2013). Further investigation into this system is warranted, as the Namib Sand Sea covers over 41% of the Namib Desert's land surface (Seely, 2012).

Another little explored driver of microbial community structure and function in the Namib Desert is the presence of viruses. The biogeochemical cycles in desert environments are thought to be primarily microbially driven, and viruses are expected to have a significant role in these processes (Makhalanyane *et al.*, 2015). In the Namib Desert, high numbers of phage-like morphotypes of the families *Myoviridae* and *Siphoviridae* have been found (Prestel *et al.*, 2008; Adriaenssens *et al.*,

2014). The high diversity of *Myoviridae*-type bacteriophages was surprising, as their complex contractile tails and fragile caudal fibers were not anticipated to be able to be able to survive in desert conditions (Prestel *et al.*, 2008; Makhalanyane *et al.*, 2015).

1.4 Strategies for examining soil microbial communities

Although up to 10^9 bacterial cells are found per gram of soil, it is estimated that 99% of environmental prokaryotes cannot be recovered through culturing (Amann *et al.*, 1990). Culture-independent methods have therefore evolved and allowed further investigation of microbial communities. Based on the work of Carl Woese (Woese, 1987), the genetic sequence of the small ribosomal RNA subunit (rRNA) is used to compare the phylogenetic relationships of prokaryotes. Norm Pace and his colleagues expanded on the work of Carl Woese (Lane *et al.*, 1985; Stahl *et al.*, 1985; Pace *et al.*, 1986) and used nucleic acids isolated directly from environmental samples to describe the diversity of microorganisms present by direct amplification and analysis of the 5S and 16S rRNA genetic sequences.

1.4.1 Community fingerprinting

Molecular community fingerprinting techniques that have been developed to assess microbial diversity include: denaturing gradient gel electrophoresis (DGGE) (Muyzer *et al.*, 1993), amplified rDNA restriction analysis (ARDRA) (Vaneechoutte *et al.*, 1992), automated amplified ribosomal intergenic spacer analysis (ARISA) (Fisher and Triplett, 1999), and terminal restriction fragment length polymorphism analysis (T-RFLP) (Liu *et al.*, 1997).

T-RFLP analysis is a robust, reproducible, and relatively high throughput molecular method (Osborn *et al.*, 2000). The technique is capable of distinguishing closely related OTUs yielding high-quality microbial community fingerprints (Osborn *et al.*, 2000). Unique terminal restriction fragments (T-RFs) are generated for each OTU present in an environmental sample through the restriction digestion of fluorescently labeled amplicons. The precise lengths of T-RFs are determined by high-resolution gel electrophoresis using an automated DNA sequencer. The sequence polymorphism within species creates different sized T-RFs, revealing overall abundance and diversity of OTUs, and

allowing for phylogenetic resolution between populations (Liu *et al.*, 1997). The data obtained is amenable to statistical analyses such as hierarchical clustering algorithms, principal component analysis, self-organizing maps, and similarity indices (Forney *et al.*, 2004). T-RFLP analysis affords greater sensitivity in distinguishing similar species within microbial communities than other fingerprinting techniques, providing a 'snapshot' of microbial diversity within a sample (Osborn *et al.*, 2000; Blackwood *et al.*, 2003; Mardis, 2008). For higher resolution of microbial communities next-generation sequencing (NGS) technologies such as 454-pyrosequencing can be utilized (Petrosino *et al.*, 2009).

1.4.2 Functional analysis

It is a widespread ecological paradigm that community structure determines function, although the relationship between microbial community structure and function is largely unknown (Nannipieri and Smalla, 2006). Linking community structure with function may be facilitated by the study of desert systems because nutrient cycling rates are lower in depauperate habitats than in more mesic environments, reducing complexity (Fierer *et al.*, 2007; Fierer *et al.*, 2012b; Manzoni *et al.*, 2012; Paul, 2014; Makhalanyane *et al.*, 2015). Because ribosome content and metabolic activities are only weakly correlated (Klappenbach *et al.*, 2000), it is difficult to obtain information on the functional role of taxa detected using the 16S rRNA genes used in community profiling (Forney *et al.*, 2004). However, other genes related to the functional processes of microbial communities can be utilized to assess functional potential, such as genes for nitrogen fixation (*nifH*), nitrification (*amoA*), and denitrification (*nirK*, *nirS*, and *nosZ*).

Alternately, as extracellular enzymes are released by microorganisms into the soil to extract substrates from the environment for nutrient acquisition, direct analysis of these enzymes through enzyme assays provides a way of determining the actual rates of functional metabolic processes (Nannipieri *et al.*, 2003; Bell *et al.*, 2013). Extracellular enzymes released by soil microbial communities are essential to nutrient cycling and energy transformation (Nannipieri and Smalla, 2006). Enzyme assays are able to measure the rates of C mineralization, chitin degradation, protein degradation, phosphate mineralization, and lignin degradation by targeting enzymes specific to these processes, such as ß-glucosidase (BG), ß-N-acetylglucosaminidase (NAG),

leucine aminopeptidase (LAP), alkaline phosphatase (AP), and phenol oxidase (PO). Enzymes assays targeting these specific enzymes are frequently used to connect soil microbial metabolic rates with biogeochemical processes, as well as to indicate microbial nutrient demand (Sinsabaugh *et al.*, 2009; Frossard *et al.*, 2012). Specifically, BG is involved in C biogeochemical cycling by cellulose degradation through the hydrolysis of cellobiose ß1 — 4 bonds (Bell *et al.*, 2009). NAG plays an important role in both C and N biogeochemical cycling through the degradation of chitin, a component of insect exoskeletons and fungal cell walls and one of the most abundant polysaccharides found in nature (Ekenler and Tabatabai, 2002). NAG hydrolyzes chitin into its constituent amino-sugars, which are a major source of mineralizable N in soils (Ekenler and Tabatabai, 2002). LAP plays an essential role in N biogeochemical cycling through protein degradation, specifically by hydrolyzing leucine and other hydrophobic amino acids from the N-terminus of proteins and peptides (Aukerman *et al.*, 1991; Matsui *et al.*, 2006). AP plays an important role in P biogeochemical cycling by hydrolyzing phosphodiester bonds under alkaline conditions (Nannipieri *et al.*, 2011). PO is involved in C, N, and P acquisition through the oxidation of the phenolic humics and lignin that comprise up to one-third of plant cell wall material (Vinardell *et al.*, 2008; Burns *et al.*, 2013). PO has a multitude of other functions, including the detoxification of reactive metals, pigment production, morphogenesis, and defense (Sinsabaugh, 2010).

In addition, the activity measurement of the non-specific esterases, proteases, and lipases involved in the decomposition of organic matter in soils can provide a proxy for overall microbial activity as over 90% of the energy flow in a soil system goes through microbial decomposers (Paul, 2014). This is commonly done through fluorescein diacetate (FDA) hydrolysis assays, which colorimetrically measures the hydrolytic cleavage of the colorless FDA into the yellow tinted fluorescein (Nannipieri *et al.*, 2003; Green *et al.*, 2006).

It is important to note that the enzymes measured using enzyme activity assays may be intracellular, extracellular, or bound to the surrounding microhabitat and enzyme activity assays are often conducted at optimal catalytic conditions (Nannipieri *et al.*, 2012). As such, enzyme assay measurements should be viewed as *potential* enzyme activities (Nannipieri *et al.*, 2012).

1.5 Research objectives

Deserts are the largest terrestrial ecosystem (Laity, 2009). Of the 5.2 billion hectares of desert lands that are used for agriculture around the world, it is estimated that 69% are either degraded or undergoing desertification as a consequence of climatic variation or intensive human activity (UNEP, 1992; Souvignet *et al.*, 2012). Due to the limited range of higher plants and animals, soil microbial communities are likely the most productive component of desert systems and the dominant drivers of the biogeochemical processes that are critical for overall soil quality (Friedmann and Ocampo, 1976; Makhalanyane *et al.*, 2015). As recent climate change models have predicted that variability of rainfall events will intensify in desert regions, understanding how microbial communities respond to varying degrees of moisture input and xeric stress is important for the development of sustainable agriculture practices and resource management, as well as for predicting the impacts of global climate change on terrestrial systems (Faramarzi *et al.*, 2013; Paul, 2014).

This study utilized an environmental transect in the Namib Desert to investigate microbial community structure and function across varying intensities of xeric stress due to fog and rainfall (Eckardt *et al.*, 2013b). We hypothesize that moisture regime is a dominant driver of microbial community structure and function in the Namib Desert.

The specific objectives of this study were:

i) To investigate differences in bacterial community composition using T-RFLP community fingerprinting analyses.

ii) Examine the possible mechanisms of community assembly.

iii) Evaluate microbial community function using extracellular enzyme activity assays.

iv) Explore the abiotic drivers of microbial community structure and function.

Chapter 2: Materials and methods

2.1 Sampling sites and soil collection

Desert soil samples were collected across a 190 km west to east transect from the coastal town of Walvis Bay (Namibia) inland along the C14 – C26 roads in April of 2013 (Figure 12). The transect traversed the two overlapping water availability gradients formed by rainfall and fog (Figure 6; Figure 9).

Twenty sampling sites were established at 10 km intervals along the transect (Figure 12). At each of the 20 sampling sites, four replicate samples were collected (Figure 13a). Approximately 1 kg of surface soil (0 to 5 cm) was collected aseptically at each replicate site from within a 1 m^2 area (Figure 13b). A total of 80 samples were collected, and each site's GPS coordinates were recorded (Appendix A). Vegetation and rocks larger than 1 cm were avoided during the sample collection. Disturbed areas such as dry riverbeds and footprints were also avoided. Each replicate sample was collected in separate sterile Whirl-Pak® plastic bag (Nasco, Fort Atkinson, U.S.A.) and homogenized.

Each sampling site was instrumented with an iButton® data logger (model DS1923: temperature sensor operating range -10°C to +65°C with ±0.5°C accuracy; and relative humidity (RH) sensor operating range 0 to 100% RH with ±0.6% accuracy) (Maxim Integrated Products, San Jose, U.S.A). The data loggers were placed at replicate sampling site 'A' at a depth of 1 cm (iButton® location marked with rocks; Figure 13b). Data loggers recorded RH and temperature data at 4 h intervals for 12 months.

Two sub-samples were taken from each replicate sample within 12 h of collection; 4 g for the determination of soil moisture content and 15 g for enzymatic assays (stored at -20 °C).

Each sample was kept at room temperature until returned to the Centre for Microbial Ecology and Genomics (CMEG) laboratory at the University of Pretoria. At CMEG, a 6 g sub-sample was taken from each replicate sample for DNA extraction and stored at -80 °C. The remaining sample was then placed in storage at 4 °C.

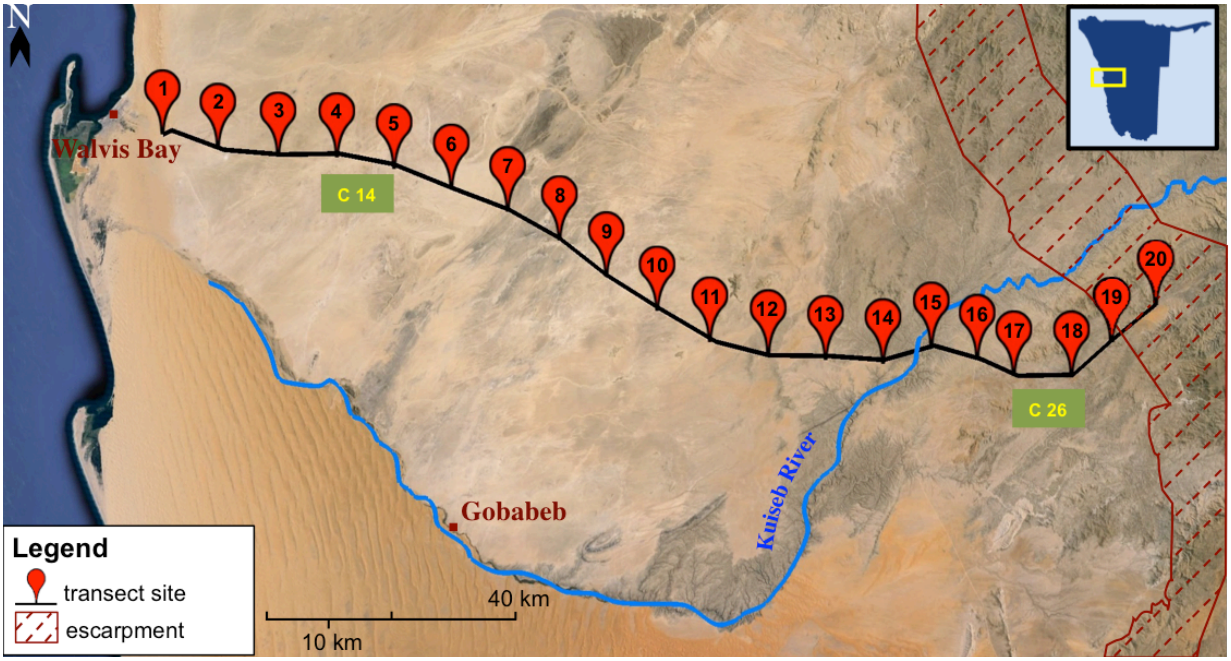

Figure 12: Transect sampling sites in the Namib Desert. A sampling site was established every 10 km along the C14 – C26 roads from Walvis Bay, Namibia toward the inland capital of Windhoek (not pictured) (Figure adapted by author from Google Earth, 2013).

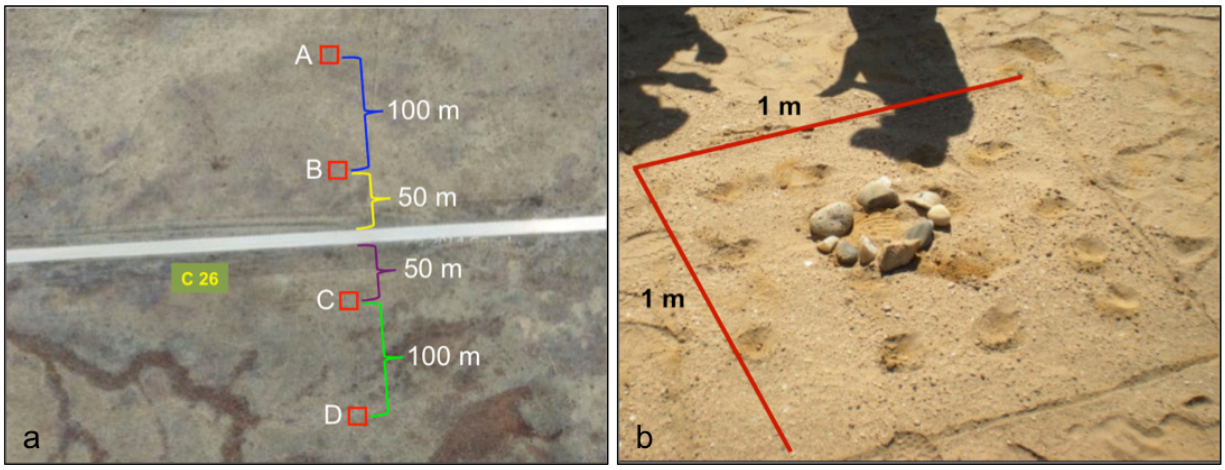

Figure 13: At each sampling site, a) four replicate samples were taken at distances of 50 and 150 meters from the north and south sides of the road (marked as A, B, C, and D) b) from a 1 meter square area. An iButton® data logger was placed at replicate site 'A' at each sampling site (Figure adapted by author from Google Earth, 2013).

2.2 Molecular biology techniques

2.2.1 Soil metagenomic DNA extraction

Metagenomic DNA was extracted using the PowerSoil® DNA Isolation Kit (MO BIO, Carlsbad, U.S.A.), with minor modifications to the manufacturer's protocol (MO BIO Laboratories, 2013). Soil (0.5 g) was added to the 2 mL PowerBead Tubes provided, which contained 750 µL of buffer and lysis

beads. This was combined with 60 µL of Solution C1, which contained sodium dodecyl sulfate (SDS) and assisted in complete cell lysis. The PowerBead Tubes were placed in a PowerLyzer® 24 bench top bead-based homogenizer (MO BIO, Carlsbad, U.S.A.) at 2 000 rpm for 5 min to mechanically lyse the cells. After centrifugation at 10 000 x g for 30 s at room temperature, the supernatant was transferred to a 2 mL microcentrifuge tube. To precipitate non-DNA organic and inorganic material, 250 µL of Solution C2 was added. This was incubated at 4°C for 5 min. After centrifugation at 10 000 x g for 1 min at room temperature, 600 µL of supernatant was transferred to a new 2 mL microcentrifuge tube. To precipitate additional non-DNA organic and inorganic material, 200 µL of Solution C3 was added. This was incubated at 4°C for 5 min. After centrifugation at 10 000 x g for 1 min at room temperature, 750 µL of supernatant was transferred to a new 2 mL microcentrifuge tube. To enable the DNA to bind the silica spin columns provided, 1 200 µL of Solution C4 (a high concentration salt solution) was added to the 2 mL microcentrifuge tube. Approximately 700 µL was then loaded onto the silica spin column and centrifuged at 10 000 x g for 1 min at room temperature. This was repeated until the entire sample had passed through the column. The column was then washed with 500 µL of ethanolic Solution C5.

DNA was eluted from the column by adding 55 µL of the Solution C6 elution buffer and centrifugation at room temperature for 30 s at 10 000 x g. Eluted DNA was stored at -80 °C.

2.2.2 High solute/low biomass metagenomic DNA extraction

Environmental samples within 60 km of the coast (sample sites 1 to 6) contained high concentrations of calcium (which is inhibitory to downstream applications) and low biomass. To remove solutes, the soil was washed three times with TE buffer (10 mM Tris-EDTA, pH 5.0) (Emmerich *et al.*, 2012). The slurry then underwent centrifugation for 10 min at 7 200 x g, and the supernatant was removed.

To obtain sufficient DNA from each of the low biomass samples, a series of 6 successive DNA extractions was performed for each replicate sample using TE buffer washed soil and the MoBio PowerSoil kit with a modified elution step: the eluate from the first spin column in the series was collected and used as the eluent for the next spin column. This was repeated for each extraction in

the series, combining 6 extractions onto a single spin column that was incubated for 5 minutes at room temperature before centrifugation (Fierer *et al.*, 2012a). Eluted DNA was stored at -80 °C.

2.2.3 Polymerase chain reaction (PCR) amplification and verification

PCR amplification targeting the bacterial 16S rRNA gene was performed using a T100 Thermo Cycler (Bio-Rad, Hercules, U.S.A.) in 96 well PCR microplates (Axygen, Union City, U.S.A.). A standard 50 µL reaction volume was used that combined: 0.75% formamide, 0.1 mg/mL bovine serum albumin (BSA), 1 X DreamTaq™ buffer (Thermo Scientific, Waltham, U.S.A.), 0.2 mM of each dNTP, 0.5 µM of forward primer 341F (Ishii and Fukui, 2001) (5′ - CCTACGGGAGGCAGCAG - 3′), 0.5 µM of reverse primer 908R (Lane *et al.*, 1985) (5′ - CCGTCAATTCCTTTRAG-TTT - 3′), 0.005 U/µL DreamTaq™ DNA polymerase (Thermo Scientific, Waltham, U.S.A.), and 1 µL of metagenomic DNA as template. Thermocycler conditions consisted of an initial denaturation step of 5 min at 95°C; 20 amplification cycles of 95°C for 30 s, 55°C for 30 s, and 72°C for 90 s; and a final extension step at 72°C for 10 min.

PCR amplification of the high solute/low biomass samples (sites 1 to 6) were performed using nested PCR. Nested PCR improves the sensitivity of PCR amplification through two successive PCR amplification runs (Kemp *et al.*, 1989). The product of the first PCR is used as the template for the second PCR. The second primer set targeted the 16S rRNA gene. The first round of PCR amplification used a 50 µL reaction that combined: 5% dimethyl sulfoxide (DMSO), 1 X KAPA2G Buffer A (Kapa Biosystems, Wilmington, MA), 1 X KAPA Enhancer 1 (Kapa Biosystems, Wilmington, U.S.A.), 0.2 mM of each dNTP, 0.25 µM of forward primer E9F (Farrelly *et al.*, 1995) (5′ - GAGTTTGATCCTGGCTAG - 3′), 0.25 µM of reverse primer U151OR (Reysenbach *et al.*, 1995) (5′ - GGTTACCTTGTTACGACTT - 3′), 0.04 U/µL KAPA2G Robust DNA Polymerase (Kapa Biosystems, Wilmington, U.S.A.), and 3 µL of metagenomic DNA extracted using the high solute/low biomass DNA extraction procedure described in Section 2.2.2 as template. Thermocycler run conditions consisted of an initial denaturation step of 4 min at 94°C; 20 amplification cycles of 94°C for 30 s, 52°C for 30 s, and 72°C for 105 s; and a final extension step at 72°C for 10 min. The second round of nested PCR amplification used a 50 µL reaction that combined: 0.75% formamide, 0.2 mg/mL BSA, 1 X DreamTaq™ buffer (Thermo Scientific, Waltham, U.S.A.), 0.2 mM of each dNTP, 0.2 µM of

forward primer 341F (Ishii and Fukui, 2001) (5′ - CCTACGGGAGGCAGCAG - 3′), 0.2 µM of reverse primer 908R (Lane *et al.*, 1985) (5′ - CCGTCAATTCCTTTRAG-TTT - 3′), 0.005 U/µL DreamTaq™ DNA polymerase (Thermo Scientific, Waltham, U.S.A.), and 1 µL of the amplified PCR product from the first round of nested PCR amplification. Thermocycler run conditions consisted of an initial denaturation step of 3 min at 95°C; 17 amplification cycles of 95°C for 30 s, 55°C for 30 s, and 72°C for 90 s; and a final extension step at 72°C for 10 min.

PCR amplification product sizes were verified by gel electrophoresis on 1% to 2% agarose gels prepared in 0.5 X TAE buffer. Loading buffer combined with 2 X GelRed™ (Biotium, Hayward, CA) was added to the PCR product to visualize the amplicons. Electrophoresis was performed at 120 V in 0.5 X TAE buffer with the KAPA™ Express molecular weight marker (sizes: 100, 200, 400, 800, 1600, 4000, and 8000 bp) (KAPA Biosystems, Wilmington, U.S.A.). The amplicons were visualized and photographed with ultraviolet light using the Molecular Imager® Gel Doc™ XR+ imaging system (Bio Rad, Hercules, U.S.A.).

The concentration of the amplicons was determined using the Image Lab™ image acquisition and analysis software (Bio Rad, Hercules, U.S.A.). Band intensity of the amplicons was compared to the known concentration of the KAPA™ Express molecular weight marker (KAPA Biosystems, Wilmington, U.S.A.) (Figure 14).

2.2.4 PCR product purification

In order to recover a sufficient quantity of DNA for terminal restriction fragment length polymorphism (T-RFLP) analysis (Section 2.2.5), 400 ng of PCR product was obtained from each sample. This required the pooling of 5 to 15 replicate PCR reactions. Pooled replicated PCR reactions were purified using the NucleoSpin® Gel and PCR Clean-up kit (Macherey-Nagel, Duren, Germany) in accordance with the manufacturer's protocol (Macherey-Nagel, 2012). Briefly, DNA was bound to the silica membrane of the spin column by the addition of chaotropic salt in buffer NTI. The membrane was then washed with ethanolic Wash Buffer NT3 and dried to remove all residual ethanol. The DNA was then eluted from the column with 20 µL of sterile, ultra-pure

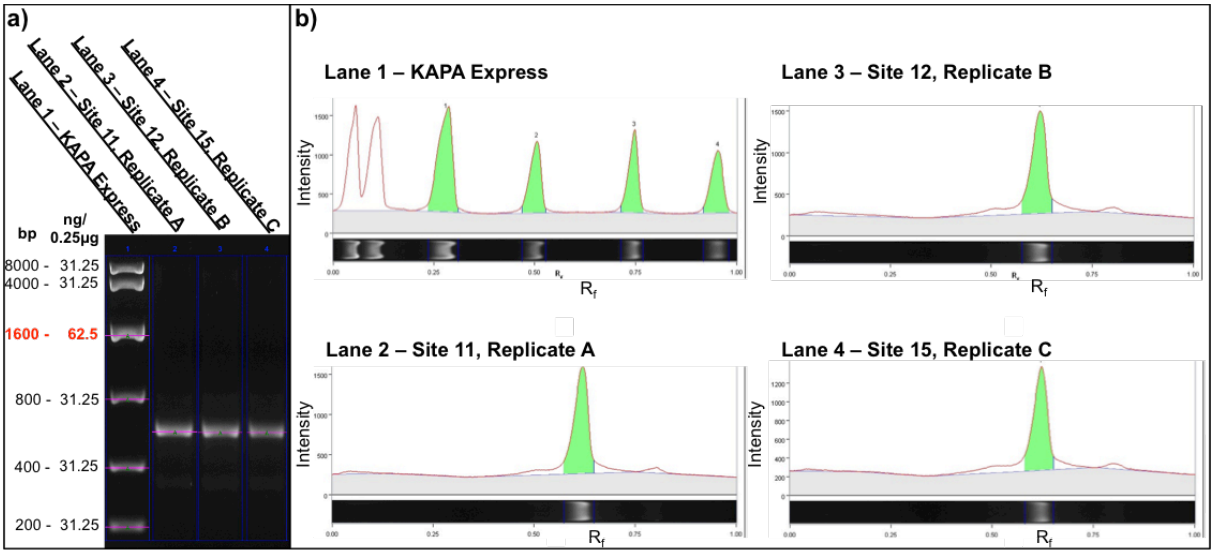

Figure 14: Gel quantification by the Image Lab™ image acquisition and analysis software (Bio Rad, Hercules, U.S.A.). a) Image of gel with the KAPA™ Express molecular weight marker in lane 1 and metagenomic DNA extract from sampling sites 11, 12, and 15 in lanes 2, 3, and 4 (respectively). b) Peak inference from the image analysis software, comparing the peak intensities the molecular weight marker to determine the concentration of the DNA extracts.

water prepared by the Milli-Q Integral Water Purification System (Milli-Q water) (Merck, Darmstadt, Germany) (Macherey-Nagel, 2012).

2.2.5 Terminal restriction fragment length polymorphism (T-RFLP)

Bacterial 16S rRNA genes were amplified as described in section 2.2.3 using forward primer 341F labeled at the 5' end with 6-carboxyfluorescein. Purified PCR amplicons were digested according to the manufacturer's specifications using the FastDigest® *Msp*I restriction endonuclease (recognition site C^CGG) (Thermo Scientific, Waltham, U.S.A.). Briefly, a 40 µL reaction mix was prepared with 400 ng of purified PCR product, 1 X FastDigest® buffer, and 4 µL FastDigest® *Msp*I. The reaction mix was incubated for 15 min at 37°C (Thermo Scientific, 2012a; Thermo Scientific, 2012b). Digested products were purified using the NucleoSpin® Gel and PCR Clean-up kit as outlined in Section 2.2.4 and eluted in 10 µL of sterile MilliQ water.

After purification, 7.5 µL digested PCR product was combined with 6.75 µL formamide in a MicroAmp® Optical 96-Well Reaction Plate (Life Technologies, Carlsbad, U.S.A.). A volume of 0.25 µL GeneScan™ – 600 LIZ® size standard was then added to each well (sizes: 20, 40, 60, 80, 100, 114, 120, 140, 160, 180, 200, 214, 220, 240, 250, 260, 280, 300, 314, 320, 340, 360, 380, 400, 414,

420, 440, 460, 480, 500, 514, 520, 540, 560, 580 and 600; Life Technologies, Carlsbad, U.S.A.). The reaction mix was heated for 5 min at 95°C to denature the DNA. The plates were sent to the DNA Sequencing Facility at the University of Pretoria (South Africa) and underwent capillary electrophoresis using an ABI 3500 XL Genetic Analyzer (Applied Biosystems, Foster City, U.S.A.).

2.3 Physicochemical soil analysis

Physicochemical analyses were performed on all soil samples. Unless otherwise specified, all samples were ground by mortar and pestle, sieved (2.0 mm), and dried at 40°C overnight. This preparation is hereafter referred to as "*prepared soil*".

2.3.1 Organic carbon

Total organic carbon (TOC) in all samples was determined using the Walkley–Black acid digestion method (Walkley, 1947) as described in the AgriLASA Soil Handbook (ALASA, 2004), with minor modifications. Between 1 to 2 g of *prepared soil* was combined with 10 mL of 0.167 M potassium dichromate solution ($K_2Cr_2O_7$). The carbon in the sample was oxidized by the dichromate ($Cr_2O_7^{2-}$) portion of the $K_2Cr_2O_7$. The $Cr_2O_7^{2-}$ that remains was measured titrimetrically and used in calculating the TOC. To further oxidize the carbon, 20 mL of concentrated sulfuric acid (98% H_2SO_4) was added, creating an exothermic reaction. The mix was allowed to sit until cooled to room temperature (10 to 30 min). The oxidation was halted by the addition of 150 mL of deionized water, and 10 mL of concentrated phosphoric acid (85%) was added to prevent ferric iron from interfering with the titration endpoint (Schumacher, 2002). A volume of 1 mL of 63.1 M barium diphenylamine sulphonate was also added as an indicator solution. The excess dichromate ions were back-titrated with ferrous ions, using 0.5 M Iron (II) ammonium sulphate ($(NH_4)_2Fe(SO_4)_2$) until the endpoint of the reaction was reached (indicated by color change from orange to green).

The volume of 0.5 M $(NH_4)_2Fe(SO_4)_2$ titrated was inversely related to the amount of carbon in the sample. To account for oxidation of $(NH_4)_2Fe(SO_4)_2$ upon exposure to air, the above procedure was then repeated with a blank sample (no soil added). The average recovery rate of organic carbon using this method is 76% due to incomplete carbon oxidation (Walkley and Black, 1934). A

correction factor of 1.33 was used to adjust the organic carbon recovery (Schumacher, 2002). The following formula was used to calculate TOC:

$$TOC\ (\%) = \frac{\left[mL\ (NH_4)_2Fe(SO_4)_{2\text{blank}} - mL\ (NH_4)_2Fe(SO_4)_{2\ sample}\right] * \left[\frac{(vol\ K_2Cr_2O_7) * M * v)}{mL(NH_4)_2Fe(SO_4)_{2\text{blank}}}\right] * mEq(C) * f * 100}{mass\ soil\ (g)}$$

Where:

$M = concentration\ of\ K_2Cr_2O_7 = 0.167\ M$

$v = valence\ of\ K_2Cr_2O_7 = 6$

$mEq(C) =$ The milliequivalent mass of carbon in g $= 0.003$

$f = correction\ factor = 1.33$

2.3.2 Inorganic nitrogen

The total extractable inorganic nitrogen was determined for each sample using the steam distillation method (Technicon, 1977), as described in the AgriLASA Soil Handbook (ALASA, 2004).

An equilibrium extraction was performed with 50 mL of 1 M potassium chloride solution (KCl) and 5 g of *prepared soil*. This soil slurry was placed on a shaker for 30 min at 220 rpm during which the ammonium (NH_4^+), nitrate (NO_3^-), and nitrite (NO_2^-) was extracted from the sample. The soil slurry was then filtered using Whatman no. 2 filter paper (Sigma-Aldrich, St. Louis, U.S.A.). Approximately 0.2 g of magnesium oxide (MgO) was combined with 40 mL of the filtered soil extract. This solution was steam distilled using a Büchi 321 steam distillation unit (Flawil, Switzerland). A volume of 50 mL of the distillate was combined with 10 mL indicator solution (boric acid, bromocresol green, and methyl red) (ALASA, 2004), then titrated with 0.0025 M H_2SO_4 until the endpoint of the reaction was reached, indicated by color change from green to violet. A titration volume of 1 mL 0.0025 M H_2SO_4 equals 35 µg of nitrogen, and the following formula was used to calculate the NH_4^+ concentration in the sample:

$$\mu g\ N/_{g\ soil} = \frac{vol\ (mL)H_2SO_4 * vol\ (mL)KCl * 35}{vol\ of\ extract\ distilled\ (mL) * mass\ soil\ (g)}$$

After the removal of NH_4^+ from the filtered soil extract as described above, approximately 0.2 g of Devarda alloy (50% copper, 45% aluminum, and 5% zinc) was added to the extract and placed on the steam distillation unit. NO_3^- and NO_2^- were reduced to NH_4^+ by the Devarda alloy, which was then volatilized by reacting with the MgO. The distillation and titration procedure described above was then repeated, and the same formula was used to calculate the combined NO_3^- and NO_2^- concentration in the sample.

2.3.3 Extractable phosphorus

The concentration of extractable phosphorus was determined using the Bray-1 method (Bray and Kurtz, 1945). *Prepared soil* (4 g) was mixed for 1 min with 30 mL Bray-1 solution. The soil slurry was then filtered through Whatman no. 2 filter paper (Sigma-Aldrich, St. Louis, U.S.A.). Phosphorus concentration was determined by inductively coupled plasma optical emission spectrometry (ICP-OES) with a SPECTRO Genesis ICP-OES spectrometer (Ametek, Kleve, Germany) at the Soil Sciences Laboratory of the University of Pretoria, South Africa.

2.3.4 Extractable ions

Extractable ions (potassium, calcium, magnesium, and sodium) as well as sulfur concentrations were determined by the method described in 'Handbook of Standard Soil Testing Methods for Advisory Purposes' (Non-Affiliated Soil Analysis Work Committee, 1990), with minor modifications. To extract the ions from the samples, 25 mL of 1 M Ammonium acetate solution ($NH_4C_2H_3O_2$) was combined with 5 g *prepared soil*. The soil slurry was placed on a shaker at 220 rpm for 60 min and then allowed to settle overnight. The slurry was then centrifuged for 10 min at 2 500 rpm and the supernatant filtered through Whatman no. 42 filter paper (Sigma-Aldrich, St. Louis, U.S.A.). A second ion extraction step was performed by adding 25 mL of 1 M ammonium acetate to the soil pellet and placing it on a shaker for 10 min at 220 rpm. The slurry was then centrifuged for 10 min at 2 500 rpm. The supernatant was filtered through Whatman no. 42 filter paper and combined with the previous filtrate. Extractable ion concentration was determined by ICP-OES at the Soil Sciences Laboratory of the University of Pretoria, South Africa.

2.3.5 Cation exchange capacity (CEC)

The soils ability to retain NH_4^+ was used for determination of the cation exchange capacity (CEC). The soil pellet used to determine the extractable ion concentration (section 2.3.4) was combined with 25 mL of 0.1 M ammonium acetate. The soil pellet and ammonium acetate solution were placed on a shaker for 30 min at 220 rpm to allow the soil to absorb NH_4^+. The soil slurry was then centrifuged for 10 min at 2 500 rpm. The supernatant was collected and the mass of the soil pellet determined. The NH_4^+ concentration of the supernatant was determined by steam distillation and the formula outlined in Section 2.3.2.

To extract the absorbed NH_4^+, 25 mL of 1 M KCl was then added to the remaining soil pellet, shaken for 30 min at 220 rpm, centrifuged for 10 min at 2 500 rpm, and the supernatant collected. This process was repeated and the supernatants combined. The NH_4^+ concentration was determined by the steam distillation method and the calculation outlined in Section 2.3.2. The following formula was used to determine the CEC:

$$CEC = (T_1 * 20) - [(X_2 - X_1) * T_2 * cmol(+)/kg * 0.2]$$

$Where$:

$T_1 = titration\ value\ for\ KCl\ solution\ (mL)$

$T_2 = titration\ value\ for\ NH_4C_2H_3O_2\ solution\ (mL)$

$X_1 = mass\ soil\ (g)$

$X_2 =$ mass soil plus occluded $NH_4C_2H_3O_2\ solution\ (mL)$

2.3.6 Soil pH

Soil pH was determined using the slurry method described in the AgriLASA Soil Handbook (ALASA, 2004). A 1:2.5 soil to water ratio was prepared using 10 g of *prepared soil* and 25 mL Milli-Q water. The slurry was thoroughly mixed and allowed to settle for 50 min. The slurry was then mixed again and allowed to settle for another 10 min. The pH of the liquid phase was recorded with a benchtop pH meter (Crison Basic +20, Crison, Barcelona, Spain). The pH meter was recalibrated every two readings.

2.3.7 Soil moisture content

Soil moisture content was determined using a modified gravimetric method (Black and Dinauer, 1969). Soil sub-samples sealed *in situ* (section 2.1) were used for this analysis. Between 1.5 – 3.5 g of soil was placed on a 3 cm^2 aluminum foil sheet. The mass of the soil was recorded, then placed in an oven at 105°C and left overnight. Samples were removed, allowed to cool in a desiccator, and the mass of the soil after drying was recorded. The difference in measurements after drying was used to determine the percentage soil moisture content.

2.3.8 Particle size distribution

Soil particle size distribution was determined using a modified version of the Bouyoucos protocol (Bouyoucos, 1962). A dispersing solution was prepared by combining 35.7 g of sodium hexametaphosphate and 7.94 g sodium carbonate in 1 L deionized water. In a temperature controlled room (26°C), 50 g of *prepared soil* was combined with 10 mL dispersing solution and brought up to a volume of 150 mL with deionized water. The dispersing solution and soil were mixed for 5 min with an electric mixer and passed through a 0.053 mm sieve. The filtrate, which contained the silt and clay fraction of the sample, was collected and brought up to a volume of 1 L with deionized water. A hydrometer reading of the suspension was taken after 6.5 h and used to determine the silt and clay fraction of the soil.

The soil remaining on the 0.053 mm sieve was used to determine the sand fraction of the soil samples according the American Society for Testing and Materials sieving procedure (ASTM D, 2007). The sand fraction was placed in an oven and allowed to dry overnight at 105°C. The dried sand was then passed through a column of sieves (2 mm; 0.5 mm, 0.25 mm, 0.053 mm). The mass of aggregate retained on each sieve was recorded (coarse sand ≤ 2 mm, medium sand ≤ 0.5 mm, and fine sand ≤ 0.25 mm).

2.4 Microbial enzyme activity assays

2.4.1 Fluorescein diacetate (FDA) hydrolysis

Total microbial community activity was estimated using the Fluorescein diacetate (FDA) hydrolysis assay protocol described by Green *et al.*, (2006), with minor modifications. To avoid analytic bias, sample order was randomized and all assays performed in triplicate. For each sample, 0.5 g of soil (stored at -20°C after sampling) was combined with 12.5 mL of 1 X PBS (pH 7.4) and 0.25 mL of 4.9 mM FDA then placed on a shaking incubator set to 120 rpm at 43°C (the average daytime soil temperature of the sampling site on collection days). After 2 h, FDA hydrolysis was halted by adding 40 µL of acetone to 1 ml of the soil slurry. Samples were then centrifuged at 8 800 × g for 5 min at room temperature. After centrifugation, the sample was transferred to a glass tube and the fluorescence was measured with a portable fluorometer (Quantifluor™, Promega, Madison, U.S.A.) and read in triplicate. Control volumes for autofluorescence (triplicate samples prepared without FDA) and background fluorescence (triplicate samples prepared without soil) were subtracted from the readings.

2.4.2 Enzyme activity assays

Extracellular enzyme activity was determined using the colorimetric protocol described by Allison and Vitousek (2004), with minor modifications. Substrates for ß-glucosidase (BG), ß-N-acetylglucosaminidase (NAG), leucine aminopeptidase (LAP), alkaline phosphatase (AP), and phenol oxidase (PO) were used (Table 4).

Table 4: Potential activity and biogeochemical function of the target extracellular enzymes (Frossard *et al.*, 2012).

Target Enzyme		Substrate analog	Microbial process and function
ß-glucosidase	BG	p-Nitrophenyl-ß-D-glucopyranoside	Cellulose degradation; C acquisition
ß-N-acetylglucosaminidase	NAG	p-Nitrophenyl-N-acetyl-ß-D-glucosaminide	ß-1,4 glucosamine (chitin) degradation; C and N acquisition
Leucine aminopeptidase	LAP	L-Leucine-p-nitroanilide	Peptide degradation; N acquisition
Alkaline phosphatase	AP	p-Nitrophenyl Phosphate	Phosphomonoester degradation; P acquisition
Phenol oxidase	PO	L-3,4-dihydroxyphenylalanine (L-DOPA)	Lignin degradation and phenol oxidation; C, N, and P acquisition

To perform the assays, 10 g of soil stored at -20°C after sampling and 300 mL 50 mM Tris-HCl buffer was combined and mixed on a magnetic stirrer. Seven 96-well flat bottom plates were prepared (6 plates for each substrate analog, and 1 plate as a control) (Greiner Bio-One, Frickenhausen, Germany). While under agitation, 100 µL of slurry and 100 µL of substrate analog were transferred to 4 wells on each 96-well plate. The control plate received 100 µL Tris-HCl buffer in place of the substrate analog. Each plate was protected from light and incubated at 43°C. After 4 h, 10 µl of 0.5 M NaOH was added to each well. The color change was measured using a Multiskan™ GO Microplate spectrophotometer (Thermo Scientific, Waltham, U.S.A.).

The extinction coefficient (EC) of p-nitroanilide (pNP) and L-DOPA was determined by making 2-fold dilution series of each in 50 mM Tris-HCl buffer. A volume of 100 µL of each dilution was added to a 96 well flat bottom plate, protected from light, and incubated at 43°C. After 4 h, 10 µl of 0.5 M NaOH was added. The color change was measured using the spectrophotometer. The slope of absorbance vs. concentration indicated the EC for each substrate. The enzyme activity was calculated using the following calculation:

$$Activity\ (\mu mol/g * h) =$$

$$\frac{(final\ OD)}{EC * vol\ assay(mL) * vol\ homogenate\ per\ assay(mL) * time(h) * \frac{mass\ sample(\mathrm{g})}{vol\ homogenate(mL)}}$$

2.5 Statistical Analysis

Overall pairwise differences between data sets were assessed by Permutational Multivariate Analysis of Variance (PERMANOVA) using the ADONIS function of the 'vegan' package in the statistical computing software R (Oksanen *et al.*, 2007; RCD Team, 2013). Analysis of Variance (ANOVA) was used to determine if individual data set differed significantly using R (Oksanen *et al.*, 2007; RCD Team, 2013). Betadisper was used to determine the degree of group homogeneity, and the Tukey's Honest Significant Difference (HSD) method was used to identify significant differences in variance (Oksanen *et al.*, 2007).

2.5.1 Environmental statistical analysis

The values for the 17 environmental descriptors recorded (Table 5; Appendix A) were normalized in PRIMER 6 (PRIMER-E Ltd, Devon, UK) (Clarke and Warwick, 2001). This was done in order to account for the complex mixture of measurement scales used in recording environmental data. In order to visualize the dominant environmental gradients present on the transect, a correlation-based principal component analysis (PCA) was created in PRIMER 6 using transformed data. A correlation based PCA is a mathematical algorithm that takes a multivariate data set (where each variable can be defined as a dimension) and lowers its dimensionality while preserving much of the data's variation (Ringnér, 2008; Borcard *et al.*, 2011). This data set is then projected onto a set of normalized axes so they have a comparable, dimensionless scale. The correlation based PCA is an unconstrained ordination method that preserves Euclidean distances between samples and is preferred when plotting environmental data (Clarke and Warwick, 2001).

2.5.2 Microbial community function statistical analysis

Functional data for all samples underwent Hellinger-transformation (Legendre and Gallagher, 2001) and was visualized using non-metric multidimensional scaling (NMDS) using Bray-Curtis dissimilarity matrices (Bray and Curtis, 1957) in PRIMER 6. NMDS provides a visual representation of similarity patterns by fitting data nonlinearly onto low-dimensional ordination space calculated by the ranking of the distances between the data points (Ramette, 2009). The quality of the fit is designated by a stress value between 0 and 1, where stress values closer to 0 indicate a better fit and a stress value >0.2 as unreliable (Clarke and Ainsworth, 1993).

2.5.3 T-RFLP statistical analysis

The T-RFLP electropherograms were analyzed using Gene Mapper® software (Applied Biosystems, Foster City, U.S.A.). Terminal restriction fragments smaller than 50 base pairs (bp) and greater than 600 bp were eliminated, and a baseline threshold of 20 fluorescence units was used to delineate background noise. Data peaks were then binned into Operational Taxonomic Units (OTU's) with custom scripts (standard deviation 1.5) using R (Abdo *et al.*, 2006; RCD Team, 2013). OTU data for all samples then underwent Hellinger-transformation (Legendre and Gallagher, 2001) and were visualized using NMDS with Bray-Curtis dissimilarity matrices (Bray and Curtis, 1957) in

PRIMER 6. Community assembly mechanisms were explored using a Raup-Crick dissimilarity metric (Raup and Crick, 1979), which indicates community assembly dissimilar from that produced under the neutral model (Hubbell, 2001). The neutral model was generated using 999 randomizations with the *raupcrick* function of the 'vegan' package in R (Oksanen *et al.*, 2007; RCD Team, 2013).

The effect of the measured environmental parameters on the overall potential microbial activity and community structures was assessed using the *envfit* function of the 'vegan' package in R (Oksanen *et al.*, 2007). Significant environmental parameters were calculated by *envfit* ($p < 0.05$; 999 permutations) and fitted as vectors on the respective NMDS plots. The direction and length of the vectors on the NMDS plot showed where the individual parameters were the greatest, as well as indicating the strength of correlation with the overall potential microbial activity.

Chapter 3: Environmental transect in the Namib Desert

3.1 Results

3.1.1 Geology and vegetation cover

Soil samples were collected across an environmental transect in the Namib Desert that began 10 km from the coast and terminated 200 km inland (Figure 12). The first 14 transect sites were predominately comprised of soils with secondary accumulations of soluble salts and non-saline carbonates (Figure 15) (Directorate of Environmental Affairs, 2002). The remainder of the transect contained thin soils with coarse fragmentation. Specifically, sites 1 to 6 contained indurated gypsisols; sites 7 and 8 were comprised of rock outcrops; and sites 9 to 14 were dominated by cemented calcisols. Site 14 was at a junction between gypsisols, calcisols, and regosols (Figure 15). Sites 15 to 20 were dominated by leptosols, with the exception of site 17 (an area of weakly developed and unconsolidated regosols; Figure 15).

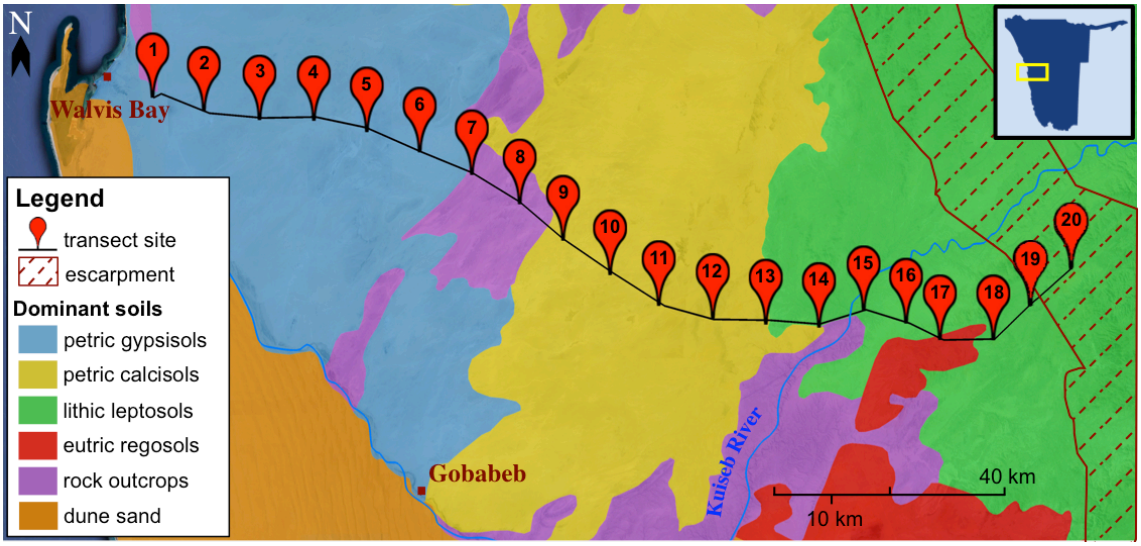

Figure 15: Dominant soil types across the transect (Figure adapted by author from Directorate of Environmental Affairs, 2002; Google Earth, 2013).

Vegetation coverage on the transect was extremely low from the coastal plain (site 1; Figure 16a; Figure 16b) to the Kuiseb River (site 14; Figure 16c). West of the Kuiseb River the landscape was dominated by grasslands of low green vegetation biomass (GVB) (sites 1 to 14; Figure 16a), transitioning to sparse shrublands east of the Kuiseb River (site 15; Figure 16a; Figure 16d) as the vegetation coverage steadily increased with elevation (Figure 17; Appendix B).

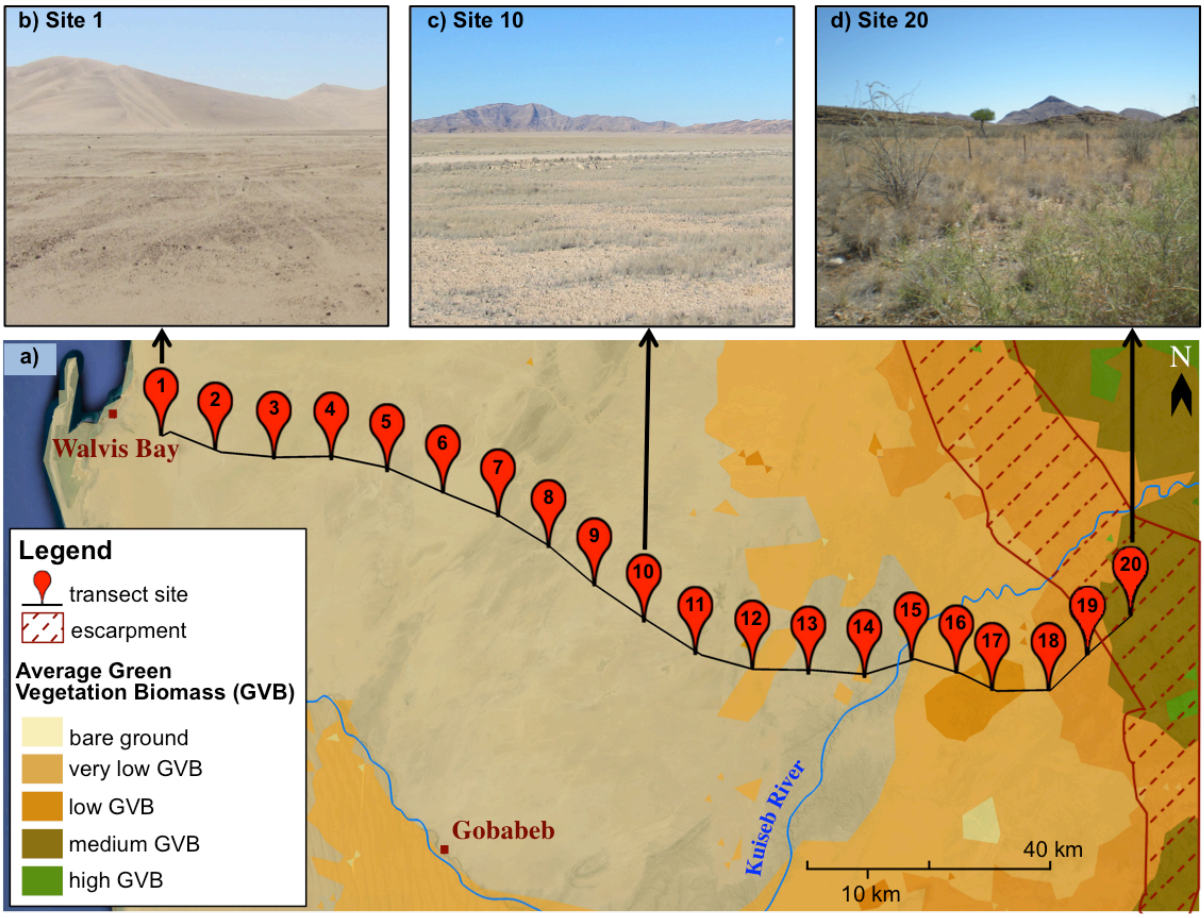

Figure 16: a) Average green vegetation biomass (GVB) of the transect. GVB gradually increased across the transect as the vegetation structure transitioned from b) bare ground at site 1, to c) grasslands on the gravel plains, and d) sparse shrublands with high GVB east of the Kuiseb River (See Appendix B for the full transition across all transect sites) (Figure adapted by author from Directorate of Environmental Affairs, 2002; Google Earth, 2013).

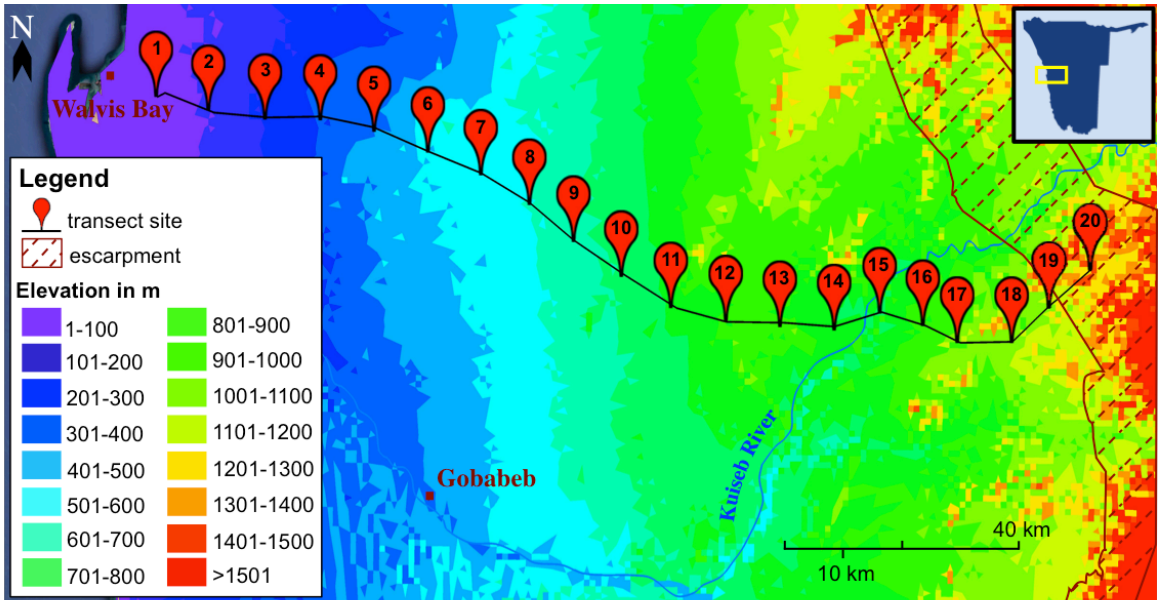

Figure 17: Elevation increased from 21 m at sampling site 1 to 1 255 m at sampling site 20 (Figure adapted by author from Directorate of Environmental Affairs, 2002; Google Earth, 2013).

3.1.2 Climate

The transect spanned a 1 200 m elevation gain (Figure 17), and annual rainfall increased with elevation (from the coast inland; Figure 18). Annual rainfall averaged 15 mm at Walvis Bay and 184 mm near Kos (175 km inland at an elevation of 1 200 m; combined climatic data of Lancaster, 1984 and Eckardt et al., 2013b; Figure 18; Appendix C; Appendix D). Near the coast, fog events supplanted rainfall as the dominant form of available moisture, reaching as far inland as 75 km up to 100 days per year (Figure 19). The transect traversed these two overlapping water availability gradients of rain and fog (Figure 18; Figure 19).

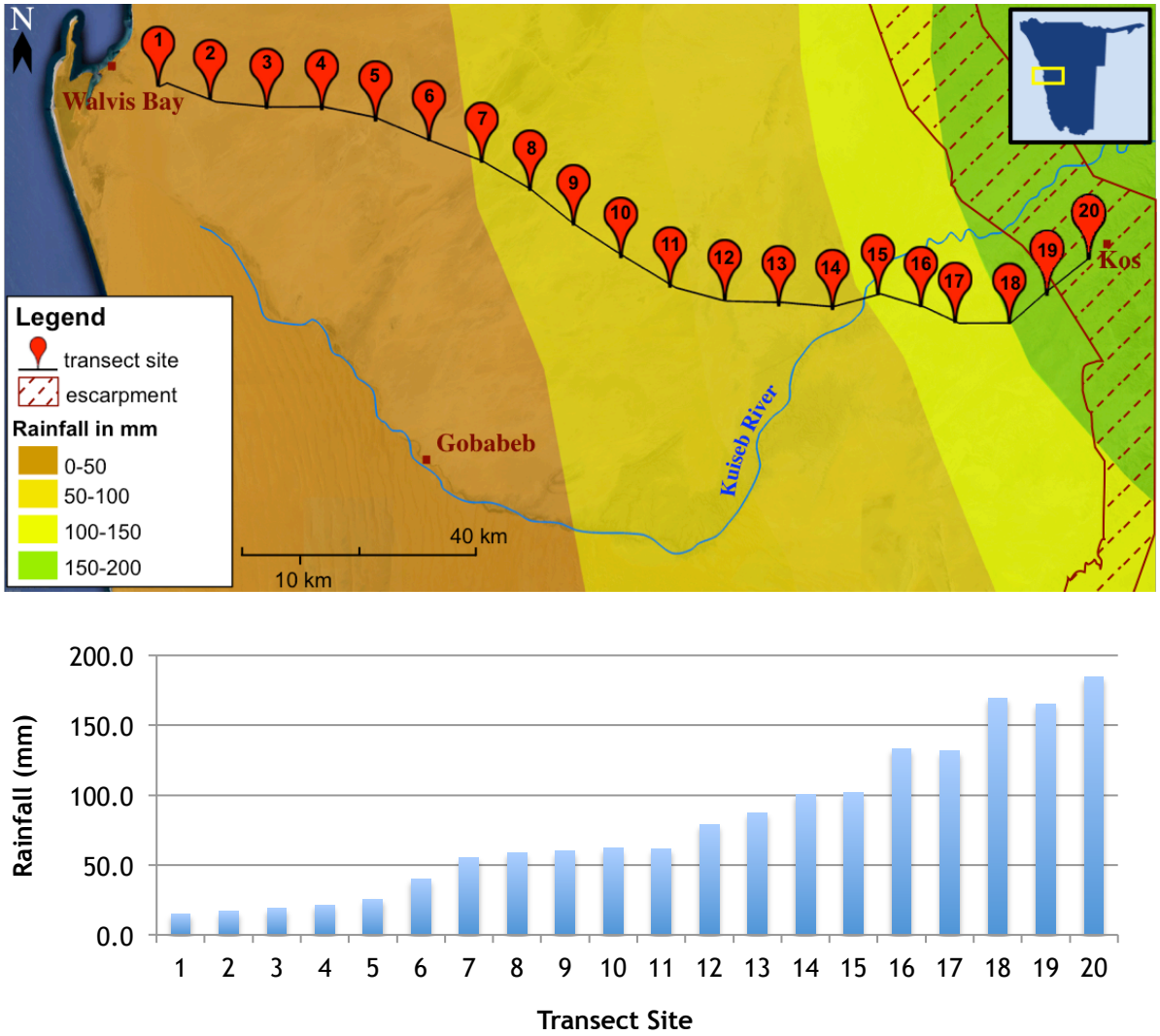

Figure 18: Average annual rainfall across the transect (see Appendix C and Appendix D) (Figure adapted by author from Lancaster and Seely, 1984; Directorate of Environmental Affairs, 2002; Eckardt *et al.*, 2013c; Google Earth, 2013).

Three zones of differing xeric stress were defined along the transect based on long-term climatic data (Lancaster and Seely, 1984; Directorate of Environmental Affairs, 2002; Eckardt *et al.*, 2013c) (Figure 18; Figure 19; Appendix C; Appendix D). The first zone contained sites 1 to 6, and was the region of the transect most affected by fog events (Figure 19) (Directorate of Environmental Affairs, 2002). The second zone extended from the edge of this 'Fog Zone' to the Kuiseb River (site 14). In this 'Dry Zone' of sites 7 to 14, moisture availability was extremely low due to the infrequent rainfall received in the area (50 to 100 mm mean per year; Figure 18; Appendix C; Appendix D) (Lancaster and Seely, 1984; Directorate of Environmental Affairs, 2002; Eckardt *et al.*,

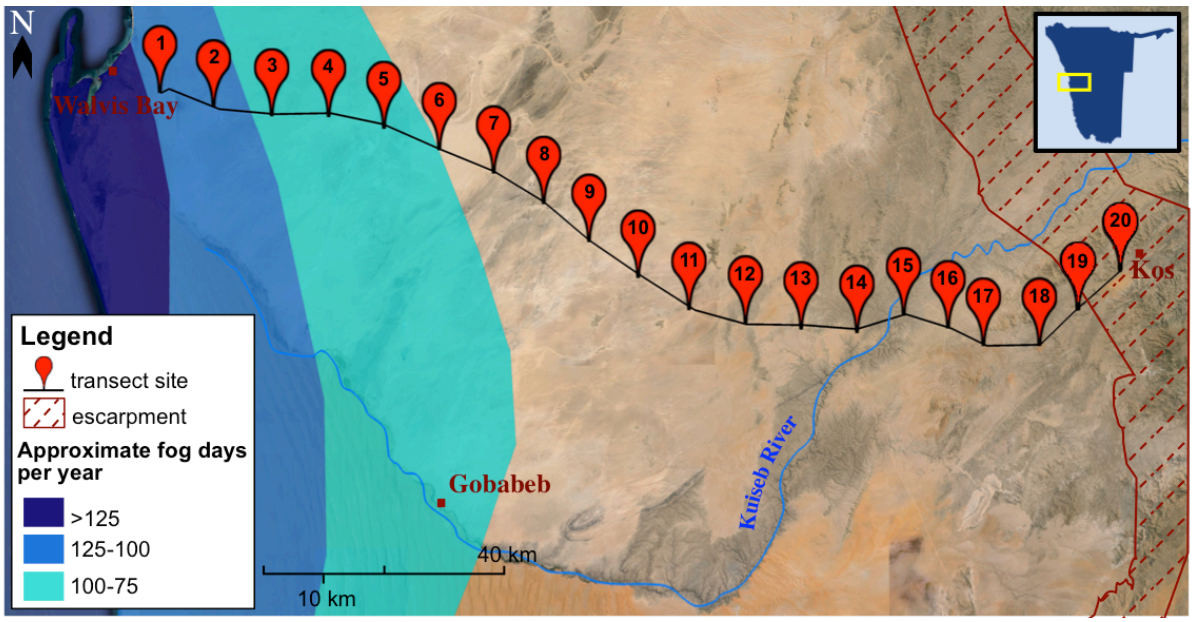

Figure 19: Approximate fog days per year (Figure adapted by author from Directorate of Environmental Affairs, 2002; Google Earth, 2013).

2013b, 2013c). The third zone, the 'Rain Zone', contained sites 15 to 20. In the 'Rain Zone', the elevation rose from 880 m to 1 250 m with a mean annual rainfall of up to 200 mm per year (Figure 17; Figure 18; Appendix C; Appendix D) (Lancaster and Seely, 1984; Directorate of Environmental Affairs, 2002; Eckardt *et al.*, 2013c).

3.1.3 Soil physicochemical properties

Physicochemical characterization of the transect's soils utilized 17 environmental descriptors (Table 5; Appendix A). Soil organic matter content increased across the transect with elevation, and differed significantly between all three *a priori* defined xeric zones; i.e., the 'Fog Zone' (sites 1 to 6), the 'Dry Zone' (sites 7 to 14), and the 'Rain Zone' (sites 15 to 20) (ANOVA $p = 0.001$; Table 6; Figure 20). Soil organic matter, Ca^{+}, K^{+}, and S concentrations also differed significantly between the three zones (ANOVA $p < 0.05$; Table 6). Additionally, Ca^{+}, K^{+}, Mg^{+}, Na^{+}, NO_3^{-}, and S concentrations showed large within group variation in the 'Fog Zone', and pH and P showed large within group variation in the 'Rain Zone' (Figure 21).

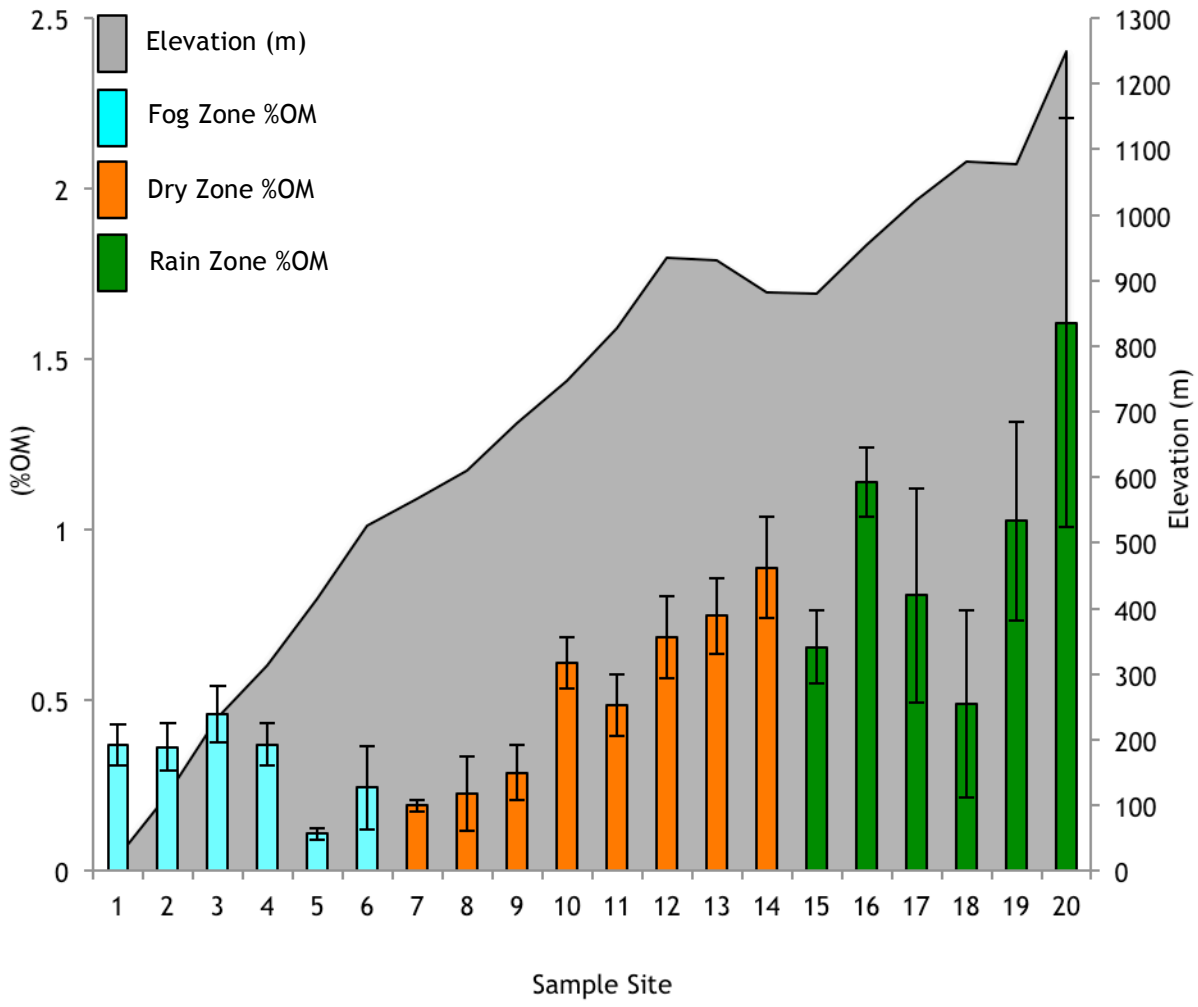

Figure 20: Percentage of organic matter found in the soil across the sampling transect, increasing with elevation (n = 4, error bars = SD).

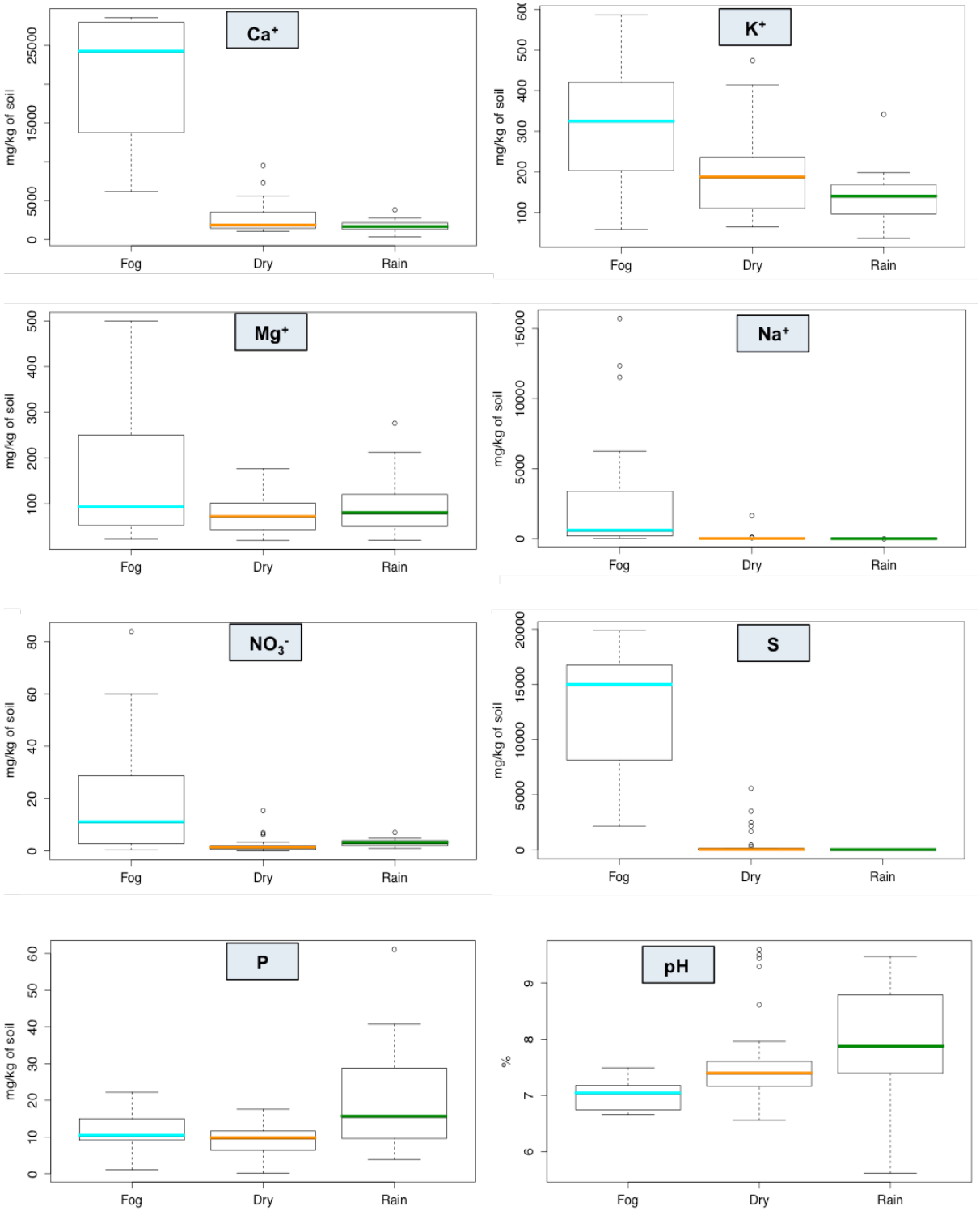

Figure 21: Boxplots of soil physicochemical parameters with significant within-group variation. (Ca^+ = calcium, K^+ = potassium, Mg^+ = magnesium, Na^+ = sodium, NO_3^- = nitrate, S = sulfur, P = phosphorus, and pH = soil pH)

Table 5a: Soil physicochemical properties of the transect sampling sites.

(Elev. = elevation, Org. matter = organic matter content, C = carbon, NH_4^+ = ammonium, NO_3^- = nitrate, P = phosphorus, pH = soil pH, CEC = cation exchange capacity, Ca^+ = calcium, and K^+ = potassium; n = 4, mean ± SD)

Site	Elev. (m)	Org. Matter (%OM)	C (%)	NH_4^+ ($mg \cdot kg^{-1}$)	NO_3^- ($mg \cdot kg^{-1}$)	P ($mg \cdot kg^{-1}$)	pH	CEC ($cmol(+) \cdot kg^{-1}$)	Ca^+ ($mg \cdot kg^{-1}$)	K^+ ($mg \cdot kg^{-1}$)
1	21	0.37 (±0.06)	0.25 (±0.07)	11.3 (±2.6)	54.1 (±20.2)	12.4 (±4.57)	6.7 (±0.0)	5.1 (±0.2)	18525.6 (±6174.4)	522.9 (±61.3)
2	117	0.36 (±0.07)	0.06 (±0.01)	5.2 (±1.2)	9.1 (±4.9)	17.6 (±2.77)	7.1 (±0.3)	5.9 (±0.2)	26497.2 (±2253.0)	299.7 (±57.5)
3	237	0.46 (±0.08)	0.21 (±0.04)	3.9 (±0.6)	10.9 (±7.2)	10.4 (±6.28)	7.2 (±0.1)	6.6 (±1.0)	27419.9 (±1032.0)	332.5 (±94.4)
4	311	0.37 (±0.06)	0.07 (±0.02)	3.1 (±0.7)	28.6 (±13.8)	6.7 (±3.37)	7.2 (±0.2)	7.2 (±0.6)	25573.1 (±1803.7)	339.3 (±54.8)
5	416	0.11 (±0.02)	0.05 (±0.04)	3.1 (±0.6)	6.9 (±11.0)	9.8 (±1.89)	6.9 (±0.2)	4.7 (±0.5)	9834.0 (±3263.8)	181.9 (±177.0)
6	525	0.25 (±0.12)	0.05 (±0.06)	4.4 (±0.9)	5.1 (±6.3)	10.7 (±2.57)	6.9 (±0.1)	4.7 (±0.6)	19092.4 (±7560.3)	163.6 (±56.3)
7	568	0.19 (±0.02)	0.03 (±0.01)	4.0 (±0.2)	0.3 (±0.0)	12.9 (±2.02)	7.6 (±1.2)	4.1 (±0.3)	4734.6 (±3084.5)	80.8 (±13.4)
8	613	0.23 (±0.11)	0.08 (±0.02)	3.3 (±0.3)	4.0 (±6.6)	10.0 (±2.71)	7.0 (±0.2)	3.8 (±0.3)	4511.4 (±2048.7)	130.1 (±73.1)
9	686	0.29 (±0.08)	0.08 (±0.03)	3.5 (±0.2)	1.3 (±0.2)	10.6 (±3.05)	7.8 (±1.0)	5.2 (±0.8)	2013.4 (±453.8)	130.0 (±37.5)
10	749	0.61 (±0.08)	0.28 (±0.03)	3.5 (±0.3)	1.1 (±0.6)	5.7 (±1.87)	8.1 (±0.9)	7.6 (±0.3)	4427.4 (±73.6)	232.9 (±22.3)
11	828	0.49 (±0.09)	0.09 (±0.05)	4.5 (±0.6)	1.4 (±0.5)	11.3 (±4.4)	7.5 (±0.1)	6.2 (±0.9)	1658.1 (±345.1)	209.6 (±78.4)
12	938	0.69 (±0.12)	0.21 (±0.08)	4.9 (±1.7)	1.5 (±0.5)	3.0 (±2.67)	7.9 (±0.8)	6.8 (±1.2)	1291.1 (±158.7)	244.2 (±134.3)
13	931	0.75 (±0.11)	0.24 (±0.06)	4.5 (±0.7)	3.3 (±1.9)	10.2 (±2.3)	7.4 (±0.7)	7.2 (±0.6)	1308.5 (±173.0)	284.5 (±83.5)
14	884	0.89 (±0.15)	0.35 (±0.07)	5.2 (±1.5)	4.2 (±2.7)	9.0 (±3.01)	7.5 (±0.3)	5.7 (±1.0)	1823.5 (±80.8)	215.2 (±25.3)
15	881	0.66 (±0.11)	0.27 (±0.12)	4.3 (±0.9)	2.1 (±0.6)	14.1 (±3.37)	8.0 (±0.7)	5.6 (±1.1)	2051.3 (±92.8)	143.8 (±24.6)
16	962	1.14 (±0.1)	0.51 (±0.05)	5.8 (±0.8)	2.7 (±1.1)	10.1 (±4.57)	7.7 (±1.5)	7.8 (±0.8)	1952.3 (±565.1)	152.0 (±15.3)
17	1023	0.81 (±0.31)	0.3 (±0.16)	6.7 (±2.0)	3.8 (±1.0)	14.5 (±8.68)	7.9 (±0.5)	6.6 (±0.7)	2231.0 (±335.0)	176.4 (±15.9)
18	1085	0.49 (±0.28)	0.18 (±0.13)	4.4 (±1.2)	2.6 (±0.7)	27.5 (±20.72)	8.5 (±0.8)	5.1 (±1.4)	745.5 (±297.4)	70.3 (±27.4)
19	1078	1.03 (±0.29)	0.58 (±0.47)	2.9 (±0.5)	2.1 (±1.2)	29.7 (±6.15)	8.8 (±0.2)	6.8 (±0.7)	1318.9 (±281.2)	89.7 (±23.1)
20	1255	1.61 (±0.6)	0.71 (±0.28)	3.8 (±0.5)	4.4 (±1.8)	23.4 (±12.2)	7.5 (±0.3)	8.2 (±1.5)	2235.7 (±980.6)	192.5 (±90.3)

Table 5b: Soil physicochemical properties of the transect sampling sites.
(Mg^+ = magnesium, Na^+ = sodium, S = sulfur, Coarse sand = coarse sand content, Med. sand =medium sand content, Fine sand = fine sand content, Silt = silt content, and Clay = clay content; n = 4, mean ± SD)

Site	Mg^+ ($mg \cdot kg^{-1}$)	Na^+ ($mg \cdot kg^{-1}$)	S ($mg \cdot kg^{-1}$)	Coarse sand (<2 mm; %)	Med. sand (<500 µm; %)	Fine sand (<250 µm; %)	Silt (<53 µm; %)	Clay (<2 µm; %)
1	459.6 (±39.9)	11357.7 (±3546.2)	12278.6 (±5300.08)	16.5 (±4.4)	9.0 (±1.6)	59.8 (±7.2)	8.3 (±2.0)	6.5 (±0.9)
2	102.3 (±42.2)	1465.2 (±1577.1)	16101.9 (±1115.61)	19.5 (±3.2)	10.4 (±0.8)	53.7 (±2.1)	12.5 (±3.2)	4.0 (±1.4)
3	165.6 (±86.3)	1060.4 (±903.3)	16436.1 (±535.93)	18.4 (±4.3)	14.1 (±3.1)	45.6 (±5.0)	17.3 (±2.6)	4.5 (±0.9)
4	168.8 (±92.5)	621.8 (±172.2)	15270.5 (±1111.82)	11.7 (±0.8)	14.2 (±0.5)	52.5 (±2.9)	14.6 (±1.6)	7.0 (±2.2)
5	67.6 (±65.4)	1589.2 (±2690.9)	5637.2 (±2632.51)	20.2 (±2.3)	23.0 (±2.7)	47.3 (±2.3)	4.0 (±1.6)	5.5 (±1.7)
6	40.5 (±18.1)	151.3 (±152.74	11454.1 (±5137.1)	23.7 (±4.1)	15.5 (±1.5)	46.5 (±3.4)	8.8 (±4.0)	5.5 (±1.7)
7	23.7 (±3.2)	23.2 (±2.3)	2375.5 (±2005.35)	8.2 (±1.4)	12.9 (±1.5)	68.0 (±2.4)	5.3 (±1.6)	5.5 (±1.7)
8	65.1 (±63.8)	437.2 (±699.5)	1646.9 (±1420.41)	10.6 (±2.3)	14.3 (±1.6)	64.5 (±2.9)	6.6 (±1.3)	4.0 (±0.0)
9	49.3 (±8.3)	31.0 (±8.1)	141.0 (±104.44)	7.7 (±2.8)	15.1 (±4.5)	64.0 (±4.6)	9.1 (±3.6)	4.0 (±0.0)
10	76.0 (±8.1)	19.6 (±4.2)	10.9 (±3.36)	12.6 (±1.5)	11.8 (±1.5)	49.8 (±3.3)	18.9 (±3.1)	7.0 (±1.0)
11	83.2 (±14.2)	27.9 (±2.5)	62.7 (±22.66)	8.2 (±2.3)	18.7 (±4.8)	53.1 (±2.8)	15.1 (±4.5)	5.0 (±1.7)
12	70.9 (±14.5)	36.8 (±22.1)	72.0 (±24.96)	14.5 (±5.7)	7.5 (±0.9)	58.1 (±5.7)	14.4 (±8.4)	5.5 (±1.7)
13	101.7 (±7.2)	35.3 (±8.7)	45.3 (±10.13)	12.2 (±2.7)	6.9 (±1.1)	56.6 (±5.7)	17.3 (±1.9)	7.0 (±1.7)
14	155.3 (±13.8)	48.9 (±34.4)	50.3 (±29.87)	16.3 (±7.0)	12.1 (±1.3)	54.5 (±5.6)	12.6 (±2.5)	4.5 (±0.9)
15	114.4 (±6.8)	22.0 (±3.3)	30.6 (±6.12)	14.0 (±4.1)	9.6 (±0.6)	57.9 (±3.6)	14.1 (±3.4)	4.5 (±0.9)
16	199.6 (±52.7)	23.9 (±2.2)	19.6 (±8.18)	16.1 (±5.9)	9.3 (±2.8)	45.5 (±4.2)	24.5 (±5.6)	4.5 (±0.9)
17	82.2 (±13.4)	23.3 (±2.6)	11.3 (±2.36)	9.4 (±2.5)	13.3 (±3.5)	65.4 (±5.1)	7.8 (±6.1)	4.0 (±0.0)
18	41.2 (±19.3)	18.8 (±1.4)	2.5 (±1.09)	6.9 (±0.8)	28.7 (±12.2)	49.7 (±2.7)	9.7 (±9.4)	5.0 (±1.0)
19	55.0 (±13.6)	14.6 (±1.9)	2.7 (±2.68)	6.4 (±1.5)	10.3 (±1.6)	60.3 (±2.5)	16.5 (±4.0)	6.5 (±0.9)
20	83.1 (±35.3)	2.6 (±0.5)	0.1 (±0.11)	9.7 (±4.3)	11.9 (±1.5)	56.8 (±5.8)	15.2 (±2.0)	6.5 (±0.9)

Table 6: ANOVA analyses showing differences in the climatic and soil physicochemical properties overall, and between the three defined environmental zones. Significant values ($p < 0.05$) are designated by an asterisk.

(Df = degree of freedom, F = F value, and p = P value; Rain = mean annual rainfall, Org. matter = organic matter content, C = carbon, NH_4^+ = ammonium, NO_3^- = nitrate, Phos. = phosphorus, pH = soil pH, CEC = cation exchange capacity, Ca^+ = calcium, K^+ = potassium, Mg^+ = magnesium, Na^+ = sodium, S = sulfur, Coarse sand = coarse sand content, Med. sand = medium sand content, Fine sand = fine sand content, Silt = silt content, and Clay = clay content)

	Df	Org. Matter		C		NH_4^+		NO_3^-		Phos.		pH	
		F	p	F	p	F	p	F	p	F	p	F	p
Overall	2,77	23.04	**<0.001***	17.12	**<0.001***	1.50	0.23	16.31	**<0.001***	11.47	**<0.001***	12.20	**<0.001***
Fog - Dry	1,54	9.98	**0.003***	3.40	0.071	2.61	0.11	19.51	**<0.001***	3.06	0.09	11.83	**0.001***
Fog - Rain	1,46	34.79	**<0.001***	20.90	**<0.001***	0.57	0.45	13.46	**<0.001***	8.49	**0.006***	28.81	**<0.001***
Dry - Rain	1,54	18.02	**<0.001***	17.06	**<0.001***	1.25	0.27	1.51	0.23	18.24	**<0.001***	3.70	0.060

	Df	CEC		Ca^+		K^+		Mg^+		Na^+		S	
		F	p	F	p	F	p	F	p	F	p	F	p
Overall	2,77	3.49	**0.035***	153.1	**<0.001***	14.95	**<0.001***	6.36	**0.003***	9.90	**<0.001***	159.47	**<0.001***
Fog - Dry	1,54	0.082	0.78	168.83	**<0.001***	11.75	**0.001***	9.51	**0.003***	11.09	**0.002***	175.65	**<0.001***
Fog - Rain	1,46	6.19	**0.016***	150.42	**<0.001***	24.67	**<0.001***	4.39	**0.042***	8.73	**0.005***	154.25	**<0.001***
Dry - Rain	1,54	4.38	**0.041***	5.06	**0.029***	5.56	**0.022***	1.60	0.21	1.23	0.27	4.48	**0.039***

	Df	Coarse and		Med. Sand		Fine Sand		Silt		Clay	
		F	p	F	p	F	p	F	p	F	p
Overall	2,77	18.31	**<0.001***	0.76	0.47	7.52	**0.001***	1.97	0.15	2.41	0.79
Fog - Dry	1,54	27.29	**<0.001***	2.37	0.13	15.97	**<0.001***	0.89	0.35	0.15	0.70
Fog - Rain	1,46	28.04	**<0.001***	0.06	0.81	5.68	**0.021***	3.66	0.06	0.51	0.48
Dry - Rain	1,54	0.43	0.51	0.64	0.43	1.64	0.21	1.39	0.24	0.12	0.73

The values recorded for the 17 environmental descriptors (Table 5) were used to create a correlation-based principal component analysis (PCA) (Figure 22). The first two axes of the PCA accounted for 53.3% of the environmental variability among sampling sites. Axis 1 accounted for 30.6% of the variability and was strongly correlated with Ca^+, S, Na^+, and NO_3^- (Figure 22b; Figure 22c). Axis 2 accounted for 22.6% of the variability and was strongly correlated with soil particle size, C, and soil organic matter (Figure 22b; Figure 22c). The PCA showed some degree of overlap between the 'Dry' and 'Rain' zone samples; however, permutational multivariate analysis of variance (PERMANOVA) confirmed an overall significant separation between all three *a priori* defined environmental zones (i.e., 'Fog', 'Dry', and 'Rain' zones; PERMANOVA p = 0.001; Table 7).

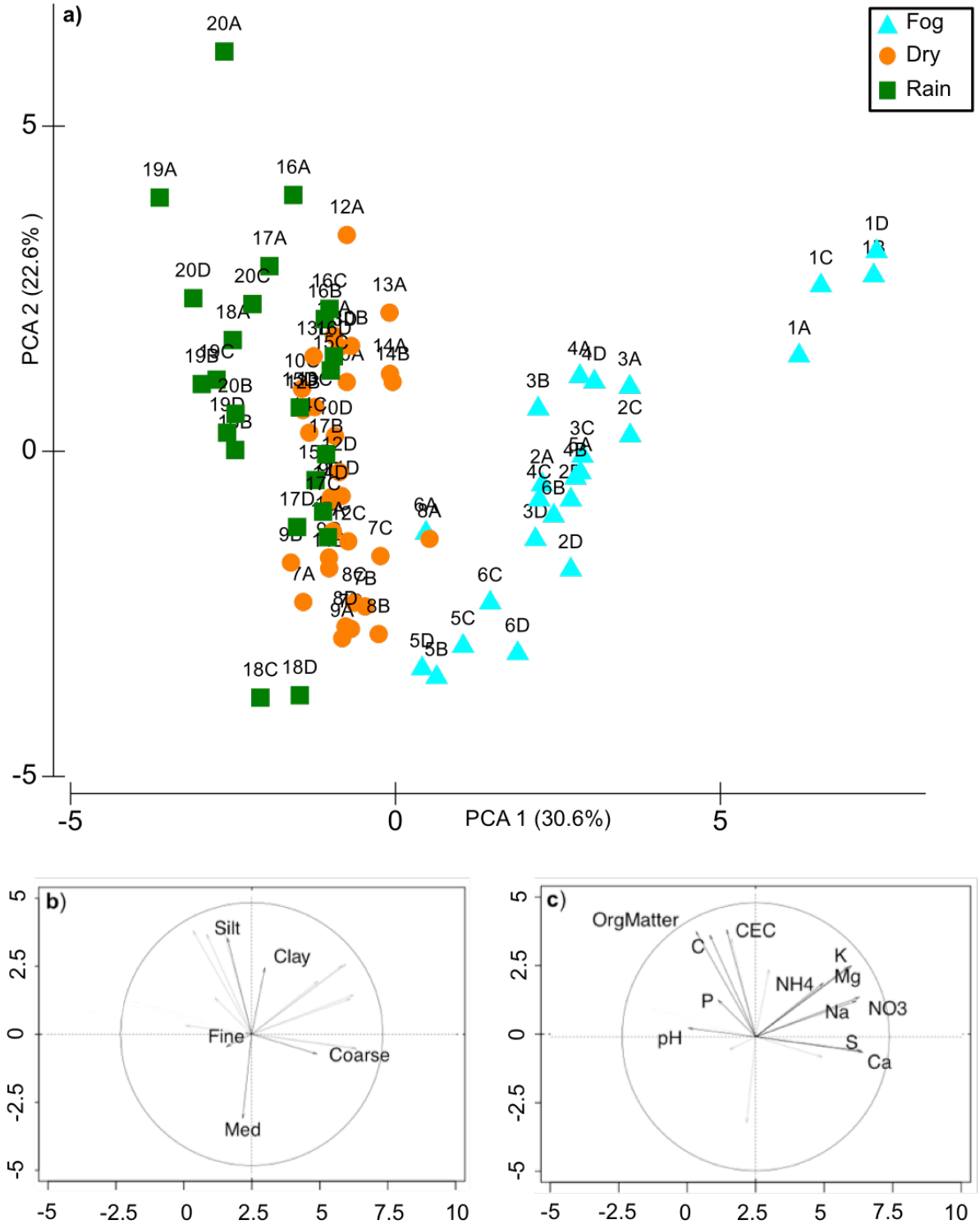

Figure 22: a) Correlation-based principal component analysis (PCA) using the 17 environmental descriptors recorded. Correlation circles (separated on two maps for clarity) show the relationships between b) soil particle size and c) soil chemical descriptors with the first two axes of the PCA plot.

(Coarse = coarse sand content, Med = medium sand content, Fine = fine sand content, Silt = silt content, Clay = clay content, C = carbon, CEC = cation exchange capacity, Ca^{+} = calcium, K^{+} = potassium, Mg^{+} = magnesium, Na^{+} = sodium, NH_4^{+} = ammonium, NO_3^{-} = nitrate, OrgMatter = organic matter content, Phos. = phosphorus, pH = soil pH, and S = sulfur)

Post-hoc Tukey's Honest Significant Difference (HSD) and betadisper tests indicated large within-group variation in the overall physicochemical profile of the 'Fog Zone' (Table 7), and betadisper tests revealed data outliers in the 'Fog Zone' sample (1.5 times the interquartile range [IQR] of the boxplot; Figure 23). These results corresponded to the large observed variation in Na^+, Ca^+, S, Mg^+, and NO_3^- soil content in the 'Fog Zone' (Table 5; Figure 21).

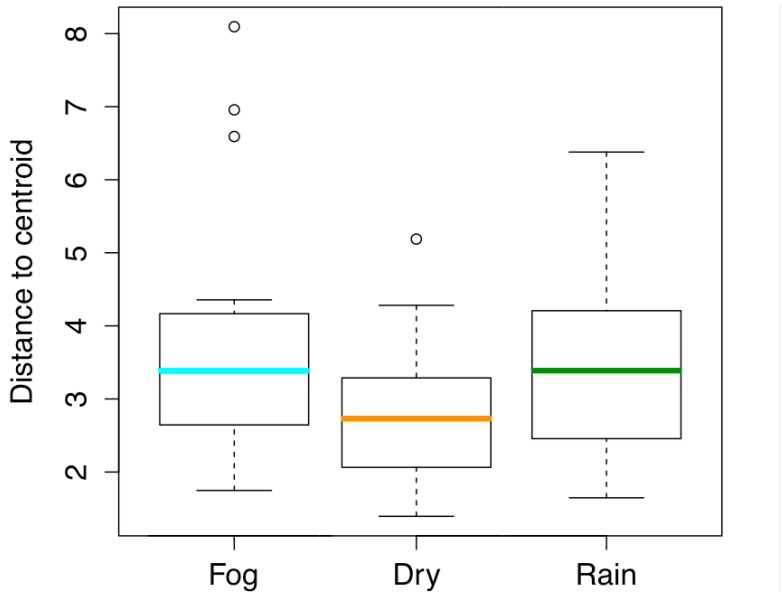

Figure 23: Boxplots of the betadisper analyses of the three environmental zones. The degree of homogeneity of group variances is shown as the distance to the centroid.

The large within-group variation in the 'Fog Zone' was primarily due to the physicochemical properties of the sampling site 1. Site 1 was approximately 10 km from the ocean and contained Na^+ in excess of 11 000 $mg \cdot kg^{-1}$, over 3 000% higher than the rest of the sampling sites (Table 5; Appendix A). The levels of NH_4^+, NO_3^-, Mg^+, and K^+ were also all significantly higher than all other transect sampling sites (ANOVA $p = 0.001$; Table 5; Table 6; Appendix A). In addition, site 1 had the lowest pH of the transect ($pH = 6.7 \pm 0.03$; Table 5). The distinct physicochemical profile of site 1 was observed in the PCA of Figure 22a, as the four replicates of site 1 separated from the other 'Fog Zone' samples along PCA axis 1. Based on these results, sampling site 1 was separated into a fourth 'Coastal Zone' due to the proximal oceanic effects. The PCA in Figure 24 shows the four environmental zones, and PERMANOVA confirmed an overall statistically significant separation

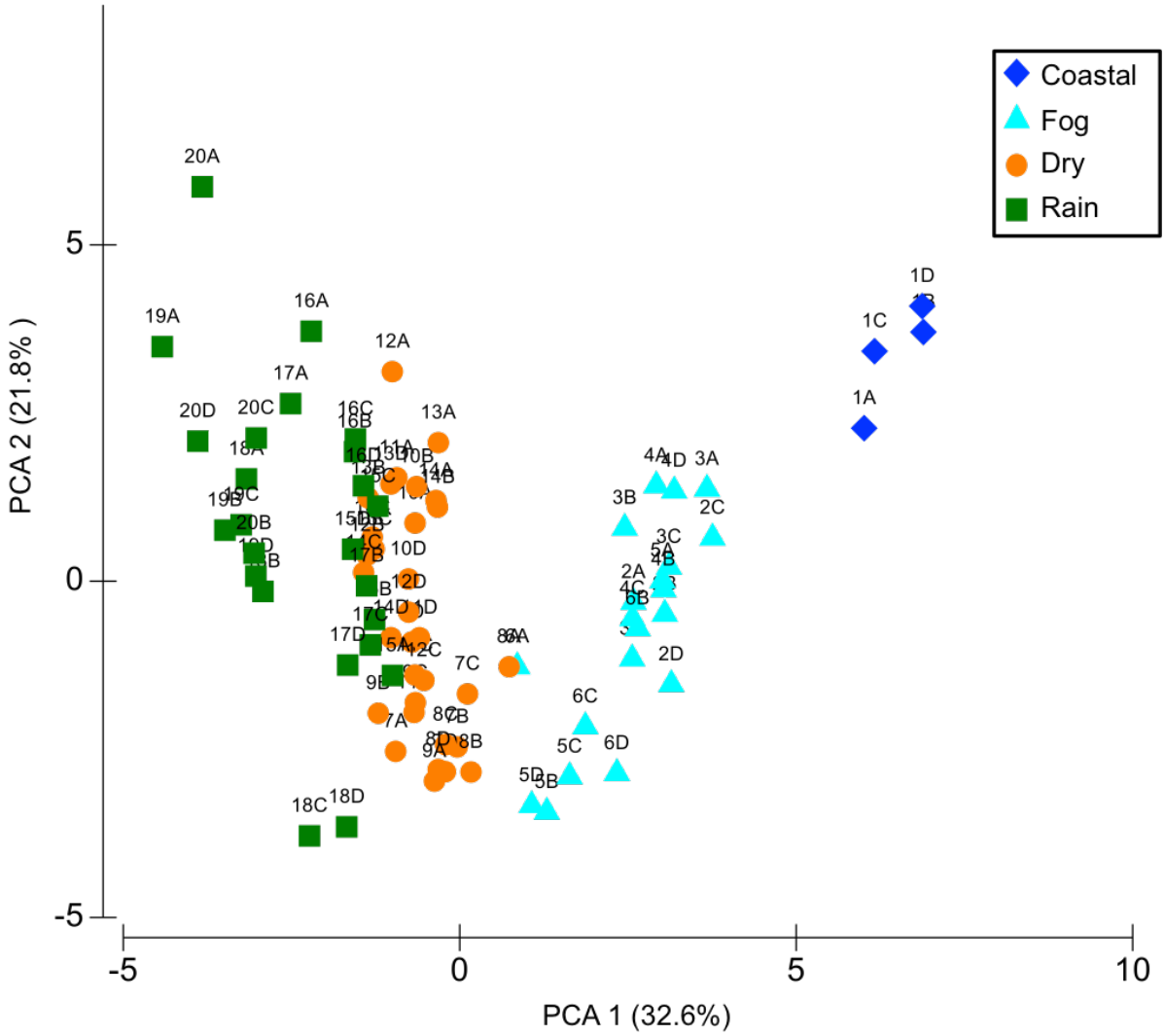

Figure 24: Correlation-based principal component analysis (PCA) using the 17 environmental descriptors recorded. Sample clusters separated into 4 environmental zones, 'Coastal', 'Fog', 'Dry', and 'Rain'.

between them (PERMANOVA $p = 0.001$; Table 7; Figure 24). Further PERMANOVA analysis showed statistically significant separation between all pairwise groupings (Table 7). However, post-hoc analysis using betadisper and the Tukey HSD tests did not show homogeneity of dispersion within the 'Rain Zone', and indicated large within-group variation (Tukey $p < 0.05$; Table 7; Figure 25).

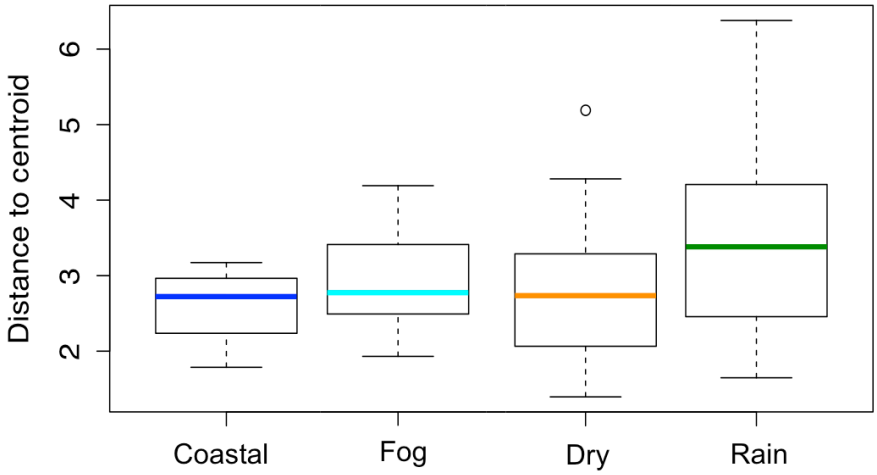

Figure 25: Boxplots of the betadisper analyses of the four environmental zones. These boxplots indicate the degree of homogeneity of group variances as the distance to the centroid and show homogeneity within each group.

Table 7: PERMANOVA results showing differences in environmental characteristics between the xeric zones. The adjusted p value of the Tukey test shows differences in the homogeneity of group dispersion (Tukey p < 0.05 indicates significant within group variation). Significant values (p < 0.05) are designated by an asterisk (Df = degree of freedom, F = F value, and p = p value).

Environments	PERMANOVA Df	PERMANOVA F	PERMANOVA p	Tukey p
4 Zones (Coastal, Fog, Dry, and Rain)				
Overall	3,76	18.570	**0.001***	
Pairwise				
Coastal - Fog	1,22	9.085	**0.001***	0.996
Coastal - Dry	1,34	20.364	**0.001***	0.995
Coastal - Rain	1,26	19.950	**0.001***	0.663
Fog - Dry	1,50	16.995	**0.001***	0.817
Fog - Rain	1,42	19.446	**0.001***	0.356
Dry - Rain	1,54	7.567	**0.001***	**0.034***
3 Zones (Fog, Dry, and Rain)				
Overall	2,77	17.52	**0.001***	
Pairwise				
Fog - Dry	1,54	18.57	**0.001***	**0.024***
Fog - Rain	1,46	21.35	**0.001***	0.831
Dry - Rain	1,54	7.57	**0.001***	0.095

The PCA in Figure 24 suggested the large within-group variation in the 'Rain Zone' may be due to sampling points 18C and 18D. The soil structure of sampling points 18C and 18D was highly dissimilar to the other sampling points of site 18 (Figure 26; Appendix B). Furthermore, sampling

points 18C and 18D had the highest sand content and lowest Ca^{+} and K^{+} of all sampling points on the transect (18C sand content: 95.6%; 18D sand content: 95.7%; 18C Ca^{+}: 555.9 $mg \cdot kg^{-1}$; 18D Ca^{+}: 377.2 $mg \cdot kg^{-1}$; 18C K^{+}: 36.9 $mg \cdot kg^{-1}$; 18D K^{+}: 51.3 $mg \cdot kg^{-1}$; Appendix A), and also the lowest soil organic matter, CEC, and Mg^{+} concentrations of the 'Rain Zone' (18C organic matter: 0.24%; 18D organic matter: 0.31%; 18C CEC: 3.9 $cmol(+) \cdot kg^{-1}$; 18D CEC: 3.5 $cmol(+) \cdot kg^{-1}$; 18C Mg^{+}: 19.9 $mg \cdot kg^{-1}$; 18D Mg^{+}: 26.4 $mg \cdot kg^{-1}$; Appendix A). Sampling point 20A was also outside the 'Rain Zone' cluster and differed from the other sampling points on the transect (Appendix A; Appendix B). Sampling point 20A had the highest soil organic matter of any sampling point (2.9 %OM, 195% greater than the average 'Rain Zone' sample; Appendix A), and the highest CEC (10.6 $cmol(+) \cdot kg^{-1}$, 110% greater than any other sample; Appendix A). If sampling points 18C, 18D, or 20A were removed from the data set, betadisper and the Tukey HSD tests indicated homogeneity of dispersion within the 'Rain Zone' (Tukey $p > 0.05$).

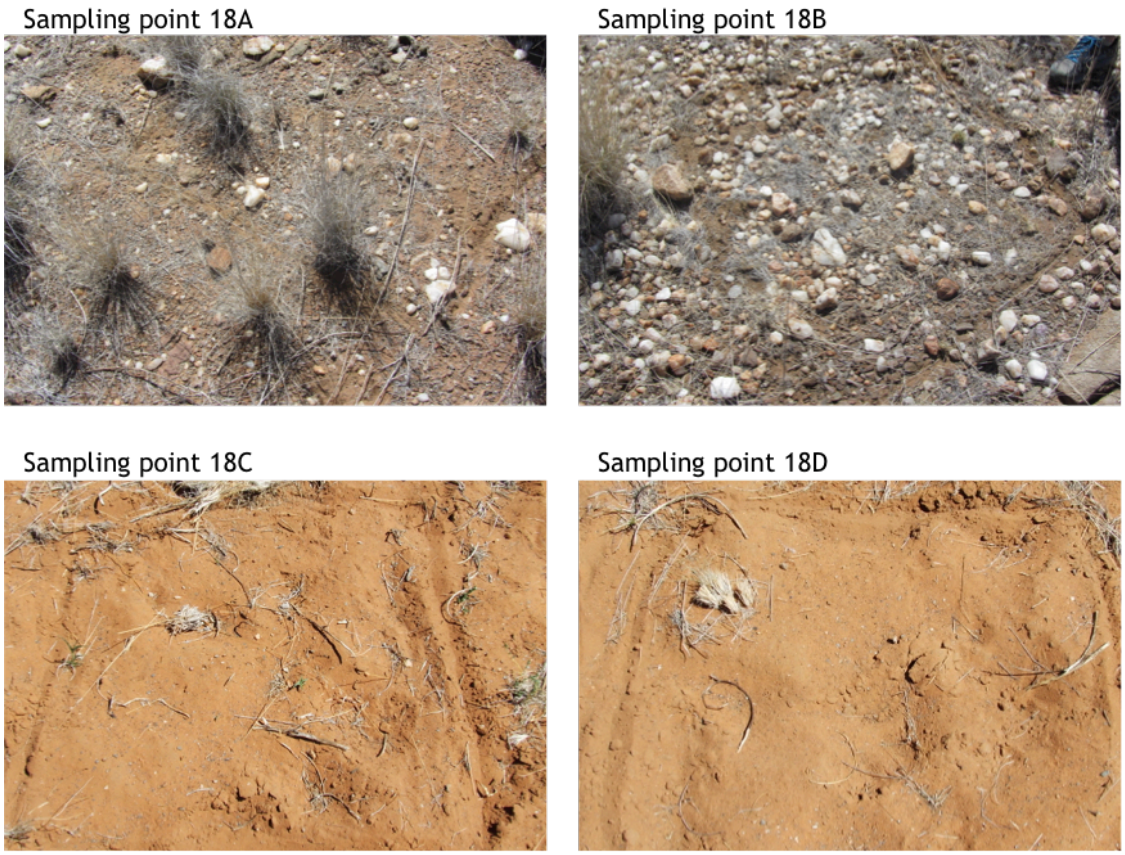

Figure 26: Photos of sampling points 18A, B, C, and D.

The separation of site 1 into a 'Coastal Zone' reduced the within group variation in the 'Fog Zone' and also removed the environmental data outliers in the 'Fog Zone' (Figure 23; Figure 24; Figure 25). The 'Fog Zone' (sites 2 to 6) had a significantly higher percentage of coarse sand (1 mm - 2 mm) than the rest of the sampling sites (ANOVA $p < 0.05$, Table 5). The concentration of organic matter in the 'Fog Zone' was also significantly lower than the rest of the transect (ANOVA $p < 0.05$; Table 5; Figure 20). However, significantly elevated levels of Ca^{+} and S occurred in both the 'Coastal Zone' and the 'Fog Zone' samples due to the secondary accumulation of gypsum (hydrous calcium sulfate; $CaSO_4 \cdot 2H_2O$) found in the gypsisols in this portion of the transect (ANOVA $p < 0.05$; Figure 15; Figure 27) (Eckardt *et al.*, 2001; Directorate of Environmental Affairs, 2002).

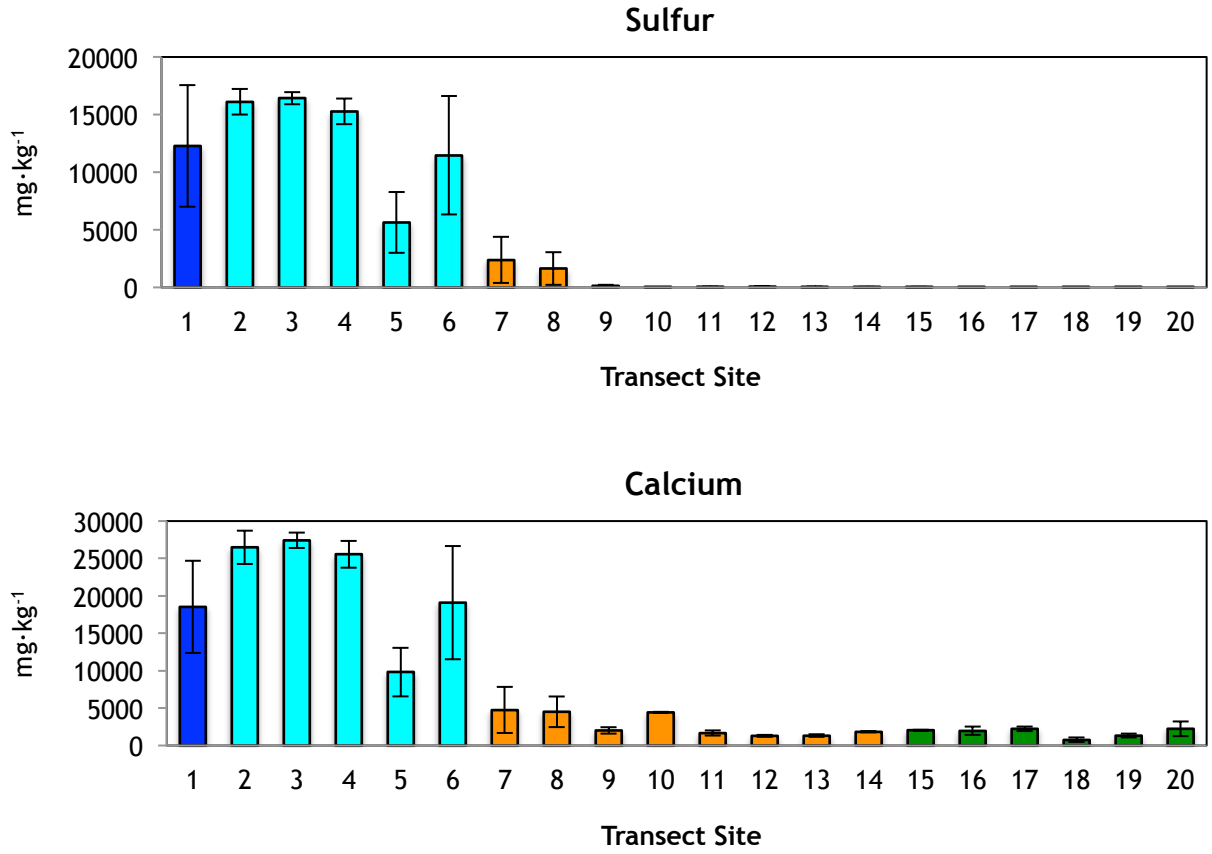

Figure 27: Calcium and sulfur concentrations along the transect.

The 'Dry Zone' (sites 7 to 14) contained a significantly higher percentage of fine sand (250 µm to 53 µm; ANOVA $p < 0.05$; Table 5) from the rest of the transect. The concentration of

organic matter in the 'Dry Zone' also differed significantly from the rest of the transect (ANOVA $p < 0.05$; Table 5), gradually increasing with elevation (Figure 20).

The 'Rain Zone' (sites 15 to 20) contained the highest sampling points of the transect (up to 1 255 m at site 20; Table 5; Figure 17; Appendix A). Sampling site 20 was located on the Great Escarpment, the eastern border of the Namib Desert (Figure 2; Figure 17). Organic matter, C, and P were all significantly higher in the 'Rain Zone' than the rest of the transect (ANOVA $p < 0.05$; Table 5), while coarse sand content was lower (ANOVA $p < 0.05$; Table 5). The CEC and pH also differed significantly from the rest of the transect in the 'Rain Zone' and showed a large degree of variation (ANOVA $p < 0.05$; Table 5; Figure 21).

To conclude, soil structure, pH, and soil salt and cation concentrations were globally shown to be significant determinants in the environmental groupings of this transect. Geology appears to play an important role in the shaping of these environments.

Chapter 4: Microbial community function in The Namib Desert

4.1 Introduction

Potential extracellular enzyme activity assays targeting the following five enzymes were used to characterize microbial community function across the studied transect in the Namib Desert: ß-glucosidase (BG), ß-N-acetylglucosaminidase (NAG), leucine aminopeptidase (LAP), alkaline phosphatase (AP), and phenol oxidase (PO) (Table 4). The total potential microbial activity of the community was estimated using a fluorescein diacetate (FDA) hydrolysis assay.

Potential extracellular enzyme activities were calculated both 'per g dry soil' (gDS) and 'per g organic matter' (gOM). Expressing potential enzyme activity per gDS reflects an ecosystem-level measure of activity and allows for direct comparison of activity between samples (Boerner *et al.*, 2005; Cunha *et al.*, 2010). Potential enzyme activity expressed per gOM (also called 'specific activity') normalizes activity to organic matter content, as differences in potential enzyme activity may be indistinguishable from concurrent changes in organic matter input (Waldrop *et al.*, 2000). This normalization allows for a comparison of potential enzyme activity at the community level (Boerner *et al.*, 2005). Describing potential enzyme activity either per gDS or per gOM is common for enzymatic studies (Acosta-Martínez *et al.*, 2007; Bell *et al.*, 2009; Sinsabaugh *et al.*, 2009). In this study, no substantial differences were observed between activity per gDS and activity per gOM, with the exception of potential PO activity. Thus, all potential enzyme activities will be expressed per gDS with the exception of potential PO activity, which will be presented both per gDS and per gOM.

4.2 Results

4.2.1 Fluorescein diacetate (FDA) hydrolysis enzyme activity assay

Total soil microbial activity, as estimated by FDA hydrolysis, increased across the transect from the coast inland (Figure 28a; Appendix A). FDA hydrolysis activity was greatest in the 'Rain Zone' (12.4 µmol h^{-1} gDS^{-1}; Figure 28a; Appendix A) and was positively correlated with soil organic matter content (the target substrate for microbial decomposers) (Spearman's r_s $|>|$ 0.40; $p < 0.001$;

Table 9; Figure 29a). FDA hydrolysis activity was also positively correlated with C, pH, CEC, and silt content (Spearman's r_s |>| 0.40; $p < 0.001$; Table 9; Figure 30a; Figure 31a). Soil organic matter content, CEC, and silt content were positively correlated with potential enzyme activity across all enzyme assays, as shown in Figures 28, 29, and 30 (Spearman's r_s |>| 0.30; $p < 0.05$), a result consistent with enzymatic studies of soil microbial communities worldwide (Burns and Dick, 2002; Grandy *et al.*, 2008; Sinsabaugh, 2010; Legg *et al.*, 2012). Mean FDA hydrolysis activity was extremely low in the 'Fog Zone' (0.74 µmol h^{-1} gDS^{-1}; Figure 28a; Appendix A) and was negatively correlated with Ca^{+}, Na^{+}, S, and coarse sand content (Spearman's r_s |>| 0.40; $p < 0.001$; Table 9). ANOVA showed an overall significant separation of FDA hydrolysis activity between the three *a priori* defined xeric zones (i.e., 'Fog', 'Dry', and 'Rain' zones) (ANOVA $p < 0.001$; Table 8). However, pairwise ANOVA comparison did not indicate a significant separation in activity between the 'Dry' and 'Rain' zones (Table 8). This was despite the fact that soil organic matter content in the 'Dry' and 'Rain' zones was shown to be significantly differentiated (ANOVA $p < 0.05$; Table 6), indicating a complex relationship between substrate availability and soil microbial activity overall.

Table 8: ANOVA results showing differences in overall potential microbial activity and between xeric zones. Significant values ($p < 0.05$) are designated by an asterisk.

(Df = degree of freedom, F = F value, and p = p value; FDA = fluorescein diacetate hydrolysis, BG = ß-glucosidase, NAG = ß-N-acetylglucosaminidase, LAP = leucine aminopeptidase, AP = alkaline phosphatase, and PO = phenol oxidase

		FDA		BG		NAG		LAP		AP		PO	
	Df	F	p	F	p	F	p	F	p	F	p	F	p
Overall	2,77	41.85	**<0.001***	12.93	**<0.001***	3.67	**0.030***	12.51	**<0.001***	16.28	**<0.001***	2.43	0.095
Fog - Dry	1,54	69.15	**<0.001***	13.26	**<0.001***	1.22	0.27	4.62	**0.036***	0.06	0.81	0.42	0.52
Fog - Rain	1,46	92.90	**<0.001***	26.26	**<0.001***	2.31	0.14	25.51	**<0.001***	21.61	**<0.001***	2.25	0.14
Dry - Rain	1,54	0.97	0.33	4.06	**0.049***	7.05	**0.01***	9.98	**0.003***	20.75	**<0.001***	4.45	**0.040***

4.2.2 ß-glucosidase (BG) extracellular enzyme activity

BG activity increased across the transect from the coast inland (Figure 28b; Appendix A), and ANOVA showed a significant separation in BG activity overall and between all pairwise combinations of the three xeric zones (ANOVA $p < 0.001$; Table 8). BG activity was positively correlated with C, organic matter content, silt, and CEC (Spearman's r_s |>| 0.30; $p < 0.001$; Table 9; Figure 29b, Figure 30b; Figure 31b), and mean BG activity was highest in the 'Rain Zone' (12.4 µmol h^{-1} gDS^{-1}; Figure 28b; Appendix A). This corresponded to the observed change in vegetation structure at the

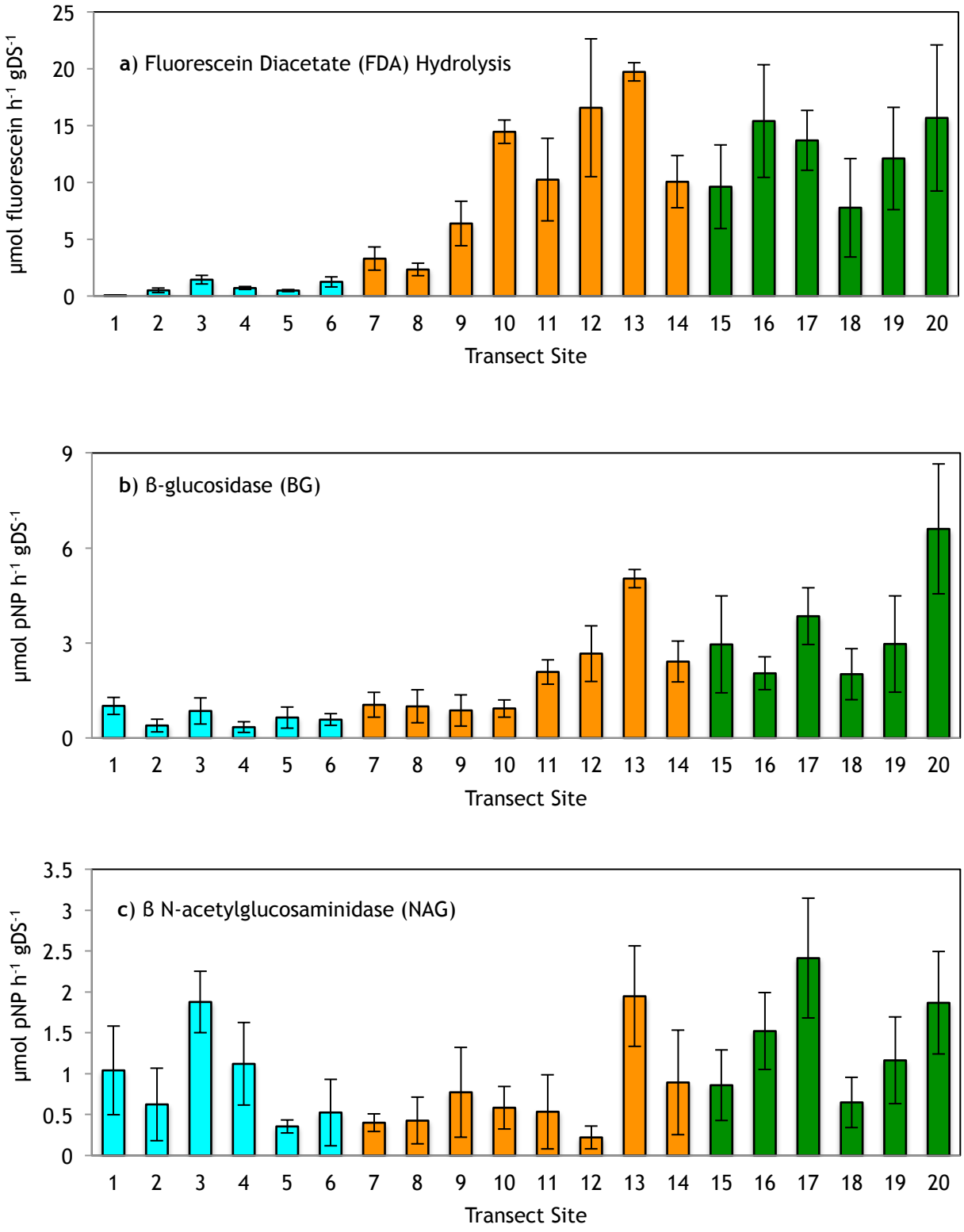

Figure 28: Soil microbial activity assessed across the transect by a) fluorescein diacetate (FDA) hydrolysis, b) potential ß-glucosidase (BG) activity, and c) potential ß-N-acetylglucosaminidase (NAG) activity.
(At each transect site n = 4 and error bars = SE)

= 'Fog Zone' activity, = 'Dry Zone' activity, and = 'Rain Zone' activity.

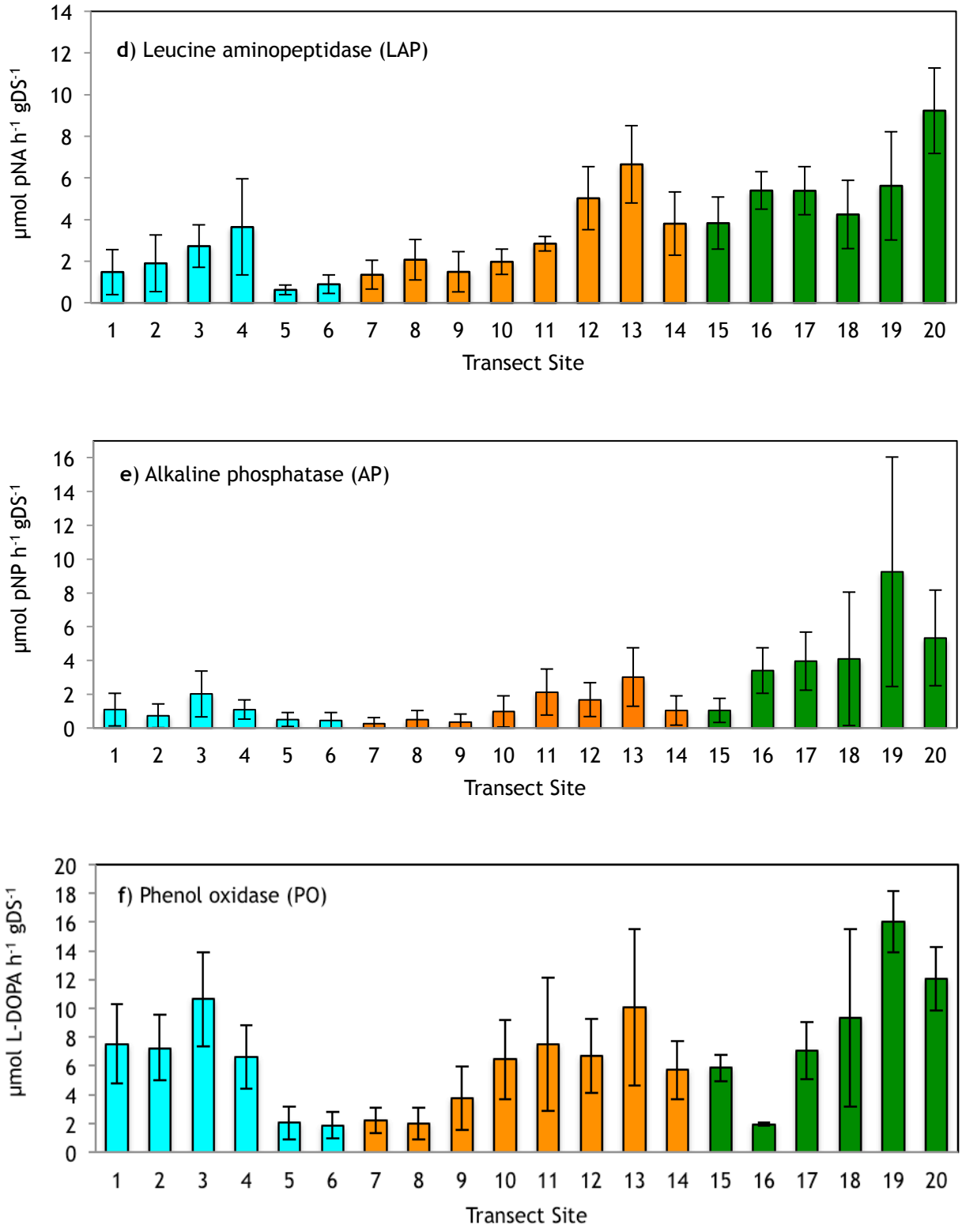

Figure 28: d) Potential leucine aminopeptidase (LAP) activity, e) alkaline phosphatase (AP) activity, and f) phenol oxidase (PO) activity across the transect.
(At each transect site n = 4 and error bars = SE)

= 'Fog Zone' activity, = 'Dry Zone' activity, and = 'Rain Zone' activity.

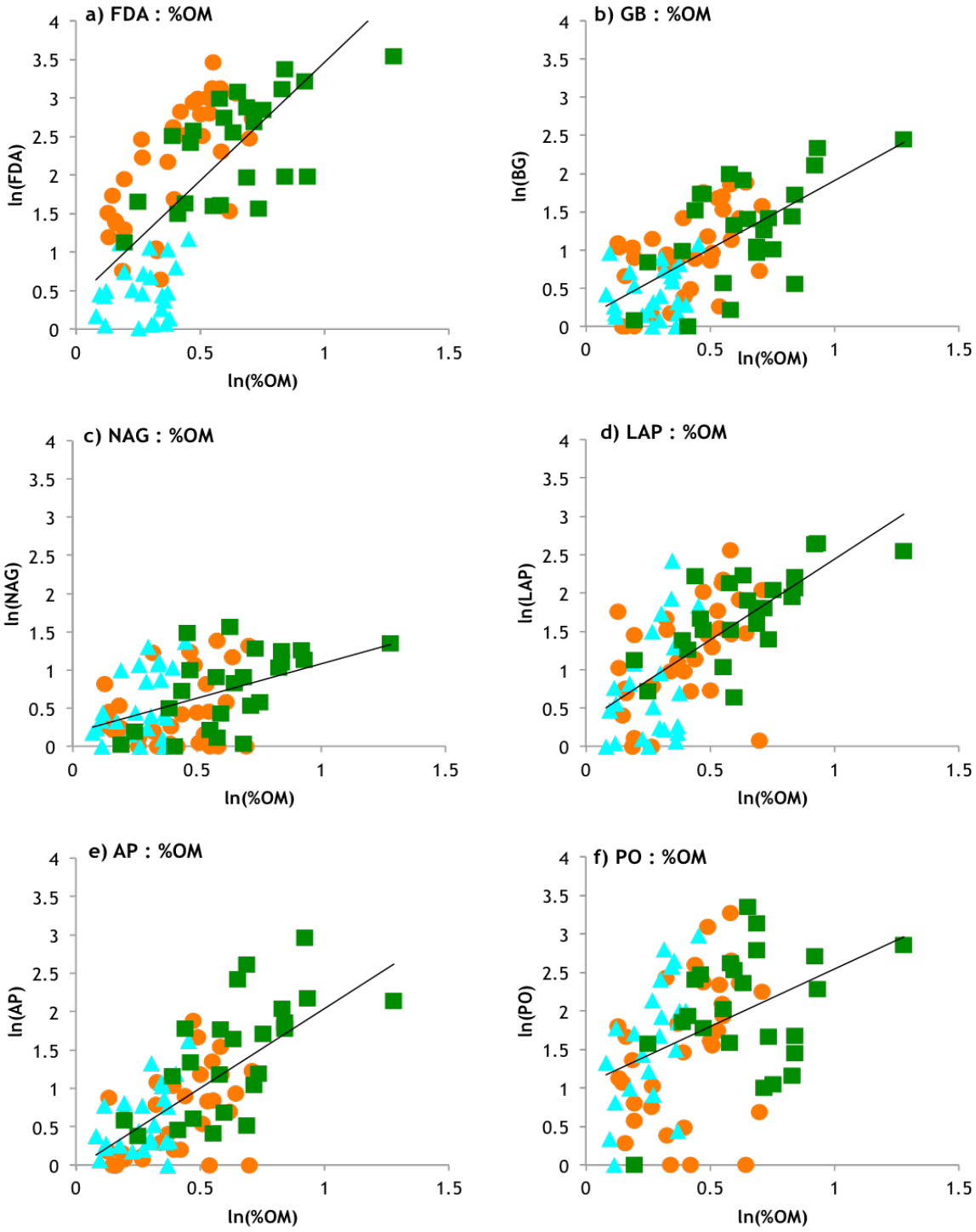

Figure 29: Natural logarithm of potential enzyme activity in relation to organic matter content (n = 80). The regression slopes (marked by the black line) are: FDA = 3.0, BG = 1.8, NAG = 0.9, LAP = 2.1, AP = 2.1, and PO = 1.5. The correlation between soil organic matter and all enzyme assays was statistically significant (Spearman's $p < 0.05$). R_s values are: FDA = 0.7, BG = 0.6, NAG = 0.4, LAP = 0.7, AP = 0.6, and PO = 0.4 (Table 9).

(%OM = soil organic matter content; FDA = fluorescein diacetate hydrolysis, BG = ß-glucosidase, NAG = ß-N-acetylglucosaminidase, LAP = leucine aminopeptidase, AP = alkaline phosphatase, and PO = phenol oxidase)

▲ = 'Fog Zone' activity, ● = 'Dry Zone' activity, and ■ = 'Rain Zone' activity.

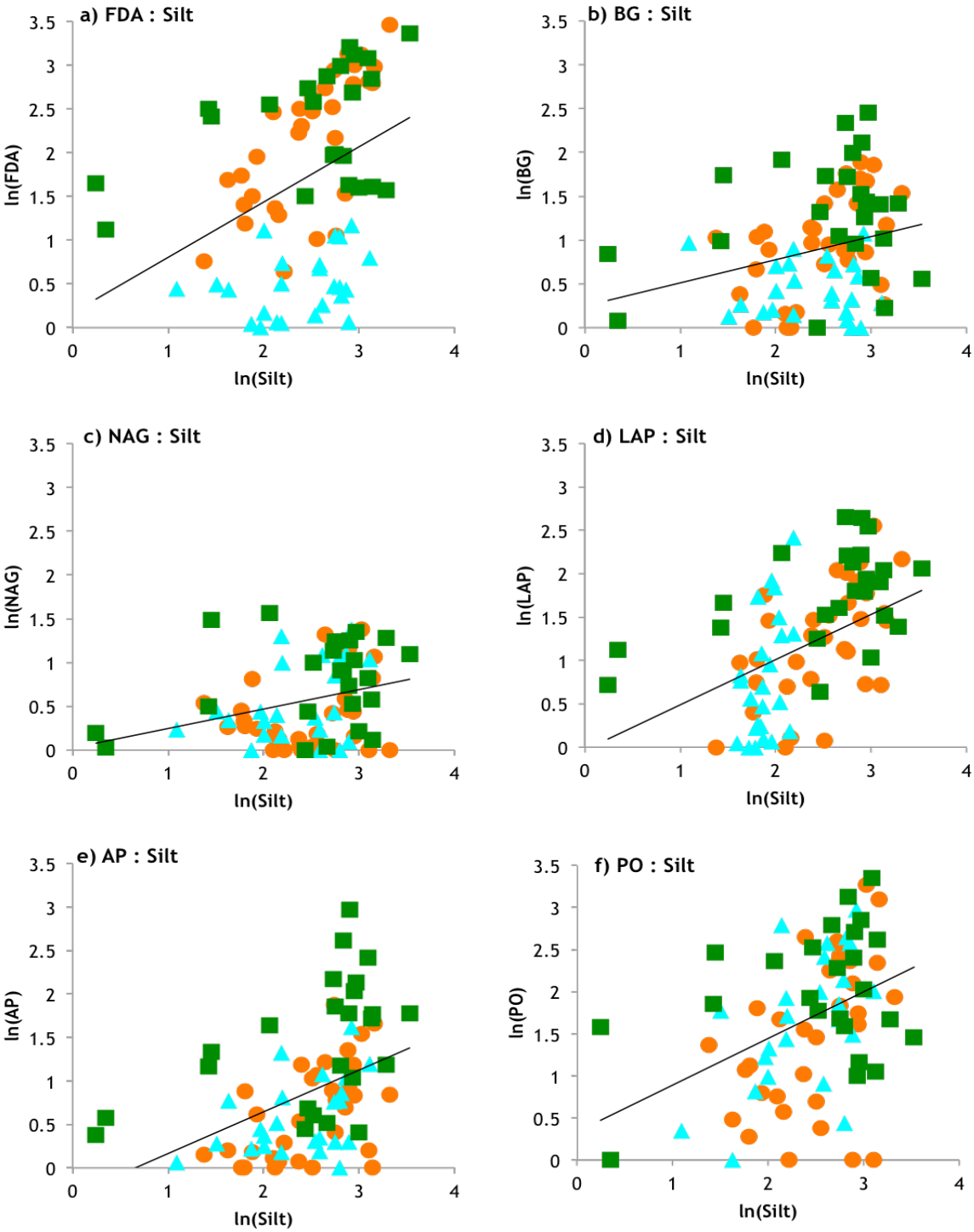

Figure 30: Natural logarithm of potential enzyme activity in relation to silt content in soil (n = 80). The regression slopes (marked by the black line) are: FDA = 0.6, BG = 0.3, NAG = 0.2, LAP = 0.5, AP = 0.5, and PO = 0.6. The correlation between silt and all enzyme assays was statistically significant (Spearman's $p < 0.05$). R_s values are: FDA = 0.5, BG = 0.3, NAG = 0.3, LAP = 0.5, AP = 0.5, and PO = 0.4 (Table 9).

(Silt = soil silt content; FDA = fluorescein diacetate hydrolysis, BG = ß-glucosidase, NAG = ß-N-acetylglucosaminidase, LAP = leucine aminopeptidase, AP = alkaline phosphatase, and PO = phenol oxidase)

▲ = 'Fog Zone' activity, ● = 'Dry Zone' activity, and ■ = 'Rain Zone' activity.

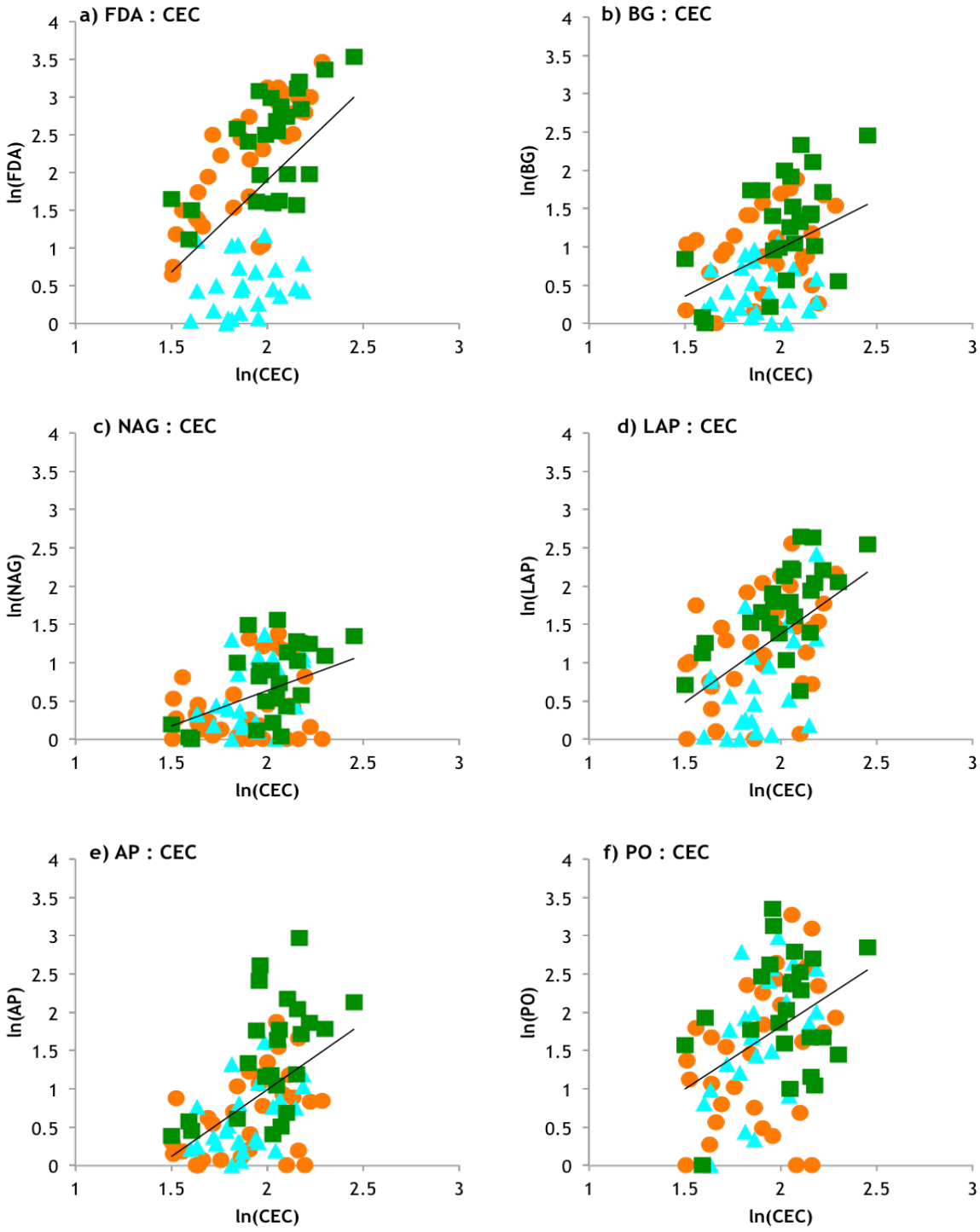

Figure 31: Natural logarithm of potential enzyme activity in relation to CEC (n = 80). The regression slopes (marked by the black line) are: FDA = 2.4 , BG = 1.3, NAG = 1.0, LAP = 1.8, AP = 1.8, and PO = 1.7. The correlation between silt and all enzyme assays was statistically significant (Spearman's $p < 0.05$). R_s values are: FDA = 0.5, BG = 0.4, NAG = 0.4, LAP = 0.5, AP = 0.6, and PO = 0.4 (Table 9).

(CEC= cation exchange capacity; FDA = fluorescein diacetate hydrolysis, BG = ß-glucosidase, NAG = ß-N-acetylglucosaminidase, LAP = leucine aminopeptidase, AP = alkaline phosphatase, and PO = phenol oxidase)

▲ = 'Fog Zone' activity, ● = 'Dry Zone' activity, and ■ = 'Rain Zone' activity.

Table 9: Spearman's correlation matrix between potential enzyme activities per gDS and soil environmental parameters.

Site	FDA		BG		NAG		LAP		AP		PO	
	r_s	p	r_s	p	r_s	p	r_s	p	r_s	p	r_s	p
Mean Ann. Rain	**0.75**	<0.001*	**0.57**	<0.001*	0.18	0.118	**0.53**	<0.001*	**0.42**	<0.001*	0.18	0.103
C	**0.59**	<0.001*	**0.55**	<0.001*	**0.38**	<0.001*	**0.53**	<0.001*	**0.54**	<0.001*	**0.34**	0.002*
Organic matter	**0.71**	<0.001*	**0.62**	<0.001*	**0.37**	<0.001*	**0.66**	<0.001*	**0.63**	<0.001*	**0.43**	<0.001*
NH_4^+	0.11	0.317	**0.25**	0.026*	0.19	0.091	0.12	0.301	0.11	0.312	-0.02	0.894
NO_3^-	-0.22	0.053	-0.01	0.935	0.24	0.034*	0.12	0.277	**0.25**	0.026*	0.19	0.096
P	0.03	0.771	0.14	0.222	**0.30**	0.008*	0.15	0.193	0.18	0.107	0.21	0.062
pH	**0.52**	<0.001*	0.23	0.037*	-0.06	0.580	**0.27**	0.016*	0.20	0.068	0.11	0.311
Coarse Sand	**-0.36**	<0.001*	**-0.26**	0.021*	0.01	0.953	-0.23	0.043*	**-0.25**	0.023*	-0.17	0.121
Med. Sand	**-0.35**	<0.001*	**-0.25**	0.023*	-0.20	0.070	**-0.32**	<0.001*	**-0.27**	0.015*	**-0.25**	0.025*
Fine Sand	0.08	0.487	0.15	0.172	-0.03	0.802	-0.02	0.859	-0.09	0.446	0.02	0.835
Silt	**0.46**	<0.001*	**0.28**	0.012*	**0.28**	0.012*	**0.52**	<0.001*	**0.51**	<0.001*	**0.40**	<0.001*
Clay	0.17	0.125	0.19	0.089	0.21	0.067	0.21	0.063	**0.34**	0.002*	**0.30**	0.007*
CEC	**0.52**	<0.001*	**0.40**	<0.001*	**0.37**	<0.001*	**0.53**	<0.001*	**0.58**	<0.001*	**0.40**	<0.001*
Na^+	**-0.59**	<0.001*	**-0.31**	0.006	-0.01	0.938	**-0.29**	<0.001*	-0.18	0.115	-0.06	0.605
Ca^+	**-0.67**	<0.001*	**-0.55**	<0.001*	-0.06	0.605	**-0.45**	<0.001*	**-0.42**	<0.001*	-0.12	0.276
S	**-0.72**	<0.001*	**-0.49**	<0.001*	-0.13	0.260	**-0.46**	<0.001*	**-0.41**	<0.001*	-0.22	0.053
K^+	-0.13	0.257	0.02	0.892	0.20	0.069	0.09	0.428	0.20	0.075	**0.26**	0.019*
Mg^+	0.02	0.894	0.20	0.080	**0.30**	0.007*	**0.26**	0.019*	**0.31**	0.005*	**0.27**	0.017*

Spearman's correlation matrix indicates microbial community functional correlations to environmental variables across the transect; n = 80. Values in this matrix can range from −1.0 to 1.0, where 1.0 indicates completely correlated variables, and −1.0 indicates completely negative correlated variables. Correlations greater than 0.3 are indicated in bold, and significant p values ($p \leq 0.05$) are indicated in with an asterisk.

FDA = fluorescein diacetate hydrolysis, BG = ß-glucosidase, NAG = ß-N-acetylglucosaminidase, LAP = leucine aminopeptidase, AP = alkaline phosphatase, and PO = phenol oxidase.

start of the 'Rain Zone' (site 15), where the grasslands transitioned to sparse shrublands with increased concentrations of cellulosic biomass (the target substrate of BG) (Figure 16; Appendix B). In the 'Fog Zone', an area effectively devoid of cellulosic biomass, BG activity was predictably low and negatively correlated with the Ca^{+}, Na^{+}, and S found high concentrations there (Spearman's r_s |>| 0.30; $p < 0.001$; Table 5; Table 9; Figure 16; Appendix B).

4.2.3 ß-N-acetylglucosaminidase (NAG) extracellular enzyme activity

NAG activity showed a high degree of variability across the transect (Figure 28c). While ANOVA showed a significant separation in NAG activity overall, pairwise comparison indicated that only the 'Dry' and 'Rain' zones were significantly differentiated from one another (ANOVA $p < 0.001$; Table 8). Mean NAG activity was highest in the 'Rain Zone' (1.4 µmol h^{-1} gDS^{-1}), and lowest in the 'Dry Zone' (0.72 µmol h^{-1} gDS^{-1}) (Figure 28c; Appendix A). As NAG degrades the chitin found in fungal cell walls, the relatively high mean NAG activity in the 'Fog Zone' (0.92 µmol h^{-1} gDS^{-1}) may indicate a larger fungal community in this region as compared to the 'Dry Zone' (Figure 28c; Appendix A) (Burns and Dick, 2002). NAG activity showed positive correlations with soil C, organic matter content, CEC, and silt, and was the only enzyme assay to show any significant correlation with soil P content (Spearman's r_s |>| 0.30; $p < 0.001$; Table 9; Figure 29c; Figure 30c; Figure 31c). NAG activity showed no significant negative correlations with any measured environmental parameter (Table 9).

4.2.4 Leucine aminopeptidase (LAP) extracellular enzyme activity

LAP activity levels differed in each xeric zone, generally increasing across the transect from the coast inland (Figure 28d). ANOVA confirmed a significant separation in LAP activity overall, and between all pairwise combinations of xeric zones (ANOVA $p < 0.001$; Table 8). LAP activity was positively correlated with C, soil organic matter, silt, and CEC (Spearman's r_s |>| 0.50; $p < 0.001$; Table 9; Figure 29d; Figure 30d; Figure 31d), and mean LAP activity was highest in the 'Rain Zone' (5.6 µmol h^{-1} gDS^{-1}; Figure 28d; Appendix A) where these positively correlated environmental parameters were found in the greatest concentrations (Table 5). LAP activity was negatively correlated with Ca^{+}, Na^{+}, and S (Spearman's r_s |>| 0.30; $p < 0.001$; Table 9), and mean LAP activity

was lowest in the 'Fog Zone' (1.9 µmol h^{-1} gDS^{-1}; Figure 28d; Appendix A) where these environmental parameters were found in the greatest concentrations (Table 5).

4.2.5 Alkaline phosphatase (AP) extracellular enzyme activity

AP activity increased across the transect from the coast inland (Figure 28e; Appendix A). ANOVA showed a significant separation in AP activity overall (ANOVA $p < 0.001$; Table 8); however, pairwise analysis indicated the separation between the 'Fog' and 'Dry' zone samples was not significant (ANOVA $p = 0.8$; Table 8). Mean AP activity was highest in the 'Rain Zone' (4.51 µmol h^{-1} gDS^{-1}) and lowest in the 'Fog Zone' (1.26 µmol h^{-1} gDS^{-1}) (Figure 28e; Appendix A). As with FDA, BG, and LAP, AP activity was positively correlated with C, soil organic matter, CEC, and silt and negatively correlated with Ca^{+}, Na^{+}, and S (Spearman's r_s |>| 0.30; $p < 0.001$; Table 9; Figure 29e; Figure 30e; Figure 31e). However, AP activity showed no significant correlation with soil P content (Table 9). This was unexpected as phosphatase activity has repeatedly been shown to be negatively correlated with soil P concentration (McGill and Cole, 1981; Olander and Vitousek, 2000; Allison and Vitousek, 2005; Bell *et al.*, 2014).

4.2.6 Phenol oxidase (PO) extracellular enzyme activity

PO activity showed a high degree of variability across the transect (Figure 28f), and ANOVA indicated there was no significant overall separation in PO activity (ANOVA $p = 0.1$; Table 8). Mean PO activity was highest in the 'Rain Zone' (5.5 µmol h^{-1} gDS^{-1}) and lowest in the 'Dry Zone' (8.6 µmol h^{-1} gDS^{-1}) (Figure 28f; Appendix A). PO activity showed positive correlations with C, soil organic matter content, CEC, and silt (Spearman's r_s |>| 0.30; $p < 0.001$; Table 9; Figure 29f; Figure 30f; Figure 31f), and no significant negative correlations with any measured environmental parameter.

When PO activity was calculated per gOM, it displayed a greater degree of consistency across the transect (Figure 32). PO activity per gOM increased across the transect from the coast inland (Figure 32) and, unlike PO activity expressed per gDS, ANOVA indicated a significant separation in overall activity per gOM between the three xeric zones (ANOVA $p < 0.05$; Table 10). Pairwise analysis showed a significant separation between the 'Fog' and 'Rain' zones, as well as between

the 'Fog' and 'Dry' zones (ANOVA $p < 0.05$; Table 10). This differentiation between activity per gDS and per gOM may be due to the functions of PO that are beyond nutrient acquisition and unrelated to organic matter content, such as defense and the detoxification of toxic compounds (Sinsabaugh, 2010).

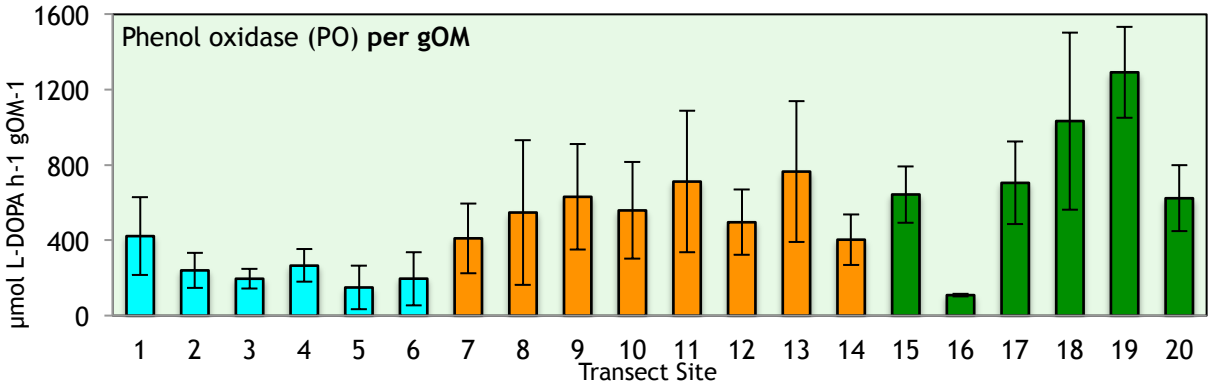

Figure 32: Potential phenol oxidase (PO) activity per gOM (At each transect site n = 4 and error bars = SE).

= 'Fog Zone' activity per gOM, = 'Dry Zone' activity per gOM, and = 'Rain Zone' activity per gOM

Table 10: ANOVA results showing differences in potential PO activity per gDS and per gOM both overall and between xeric zones. Significant values ($p < 0.05$) are designated by an asterisk.

(Df = degree of freedom, F = F value, and p = p value, PO = phenol oxidase, gDS = g dry soil, gOM = g organic matter)

	Df	PO per gDS F	PO per gDS p	PO per gOM F	PO per gOM p
Overall	2,77	2.43	0.095	6.31	**0.003***
Fog - Dry	1,54	0.42	0.52	6.09	**0.017***
Fog - Rain	1,46	2.25	0.14	14.86	**<0.001***
Dry - Rain	1,54	4.45	**0.040***	1.51	0.22

4.2.7 Overall functional community fingerprint of Namib Desert soil

To determine the overall trend in the potential microbial activity across the transect, all enzyme assays were analyzed together using non-metric multidimensional scaling (NMDS) (Figure 33). The NMDS plot showed a separation between all three *a priori* defined xeric zones, although a large degree of overlap is evident between the 'Dry' and 'Rain' zone samples (Figure 33). Despite the observed overlap, PERMANOVA confirmed a statically significant separation between all xeric zones overall, as well as between all pairwise combinations (PERMANOVA, $p < 0.05$; Table 11). Unlike the

soil physicochemical properties, the positioning of sampling site 1 into a separate 'Coastal Zone' was not observed for the functional community fingerprint (Figure 24; Figure 33). PERMANOVA confirmed that sampling site 1 was not significantly different from the rest of the 'Fog Zone' samples (PERMANOVA, p = 0.10).

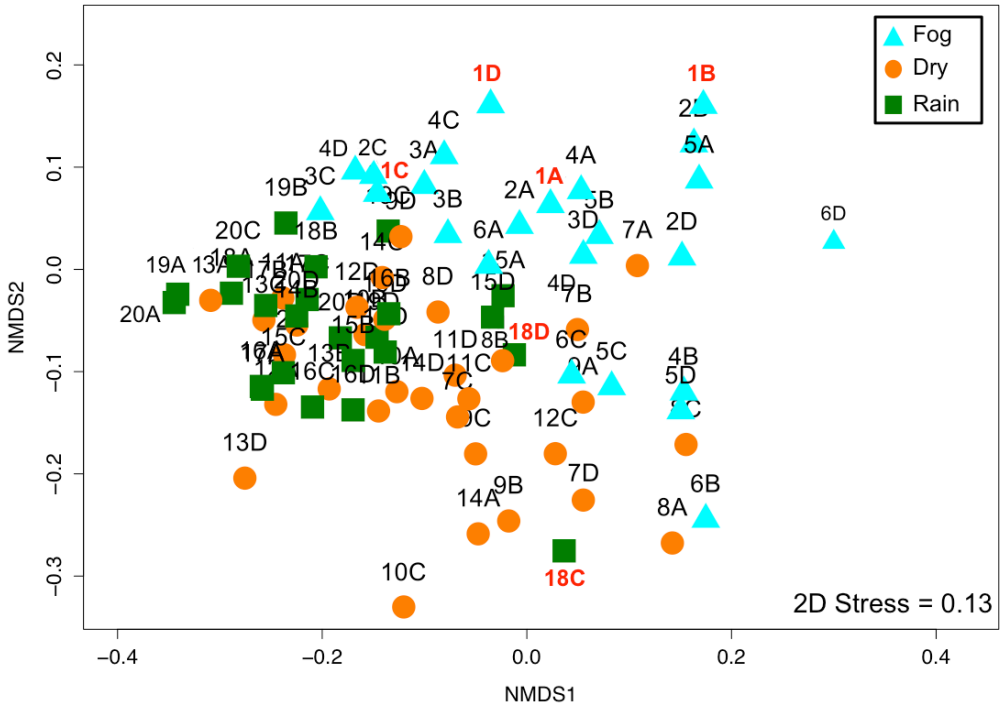

Figure 33: Non-metric multidimensional scaling (NMDS) plot of the overall potential enzyme activity across the transect. Sampling sites referred to specifically in this chapter have been labeled in red; site 1 (A, B, C, and D) and 18C and D (Bray-Curtis dissimilarities, Hellinger transformed, n = 80).

The clustering of the 'Rain Zone' samples in the NMDS plot indicated they share a greater similarity to one another than the more dispersed 'Fog' and 'Dry' zone samples (Figure 33). The level of dispersion and within-group variability in the 'Fog' and 'Dry' zone samples is also evident from betadisper analyses (Figure 34). However, post hoc Tukey's HSD and betadisper tests signified the within-group variations in the 'Fog' and 'Dry' zones were not significantly dissimilar (Tukey $p > 0.05$; Table 11).

Of the 'Rain Zone' samples, sampling point 18C was positioned outside the general 'Rain Zone' cluster (Figure 33). Sampling point 18C had the lowest mean enzyme activity in the 'Rain Zone' (0.7 µmol h^{-1} gDS^{-1}), which may be explained by the high sand content (96%, the highest of all sampling points) and low organic matter content (0.24%, the lowest in the 'Rain Zone') found at

sampling point 18C (Figure 26) (Appendix A). The physicochemical composition of sampling point 18D was similar to 18C (Figure 26), which may explain why the mean enzyme activity of sampling point 18D was the second lowest in the 'Rain Zone' (7.3 µmol h^{-1} gDS^{-1}), although sampling point 18D was positioned closer to the general cluster of 'Rain Zone' samples (Figure 33) (Appendix A).

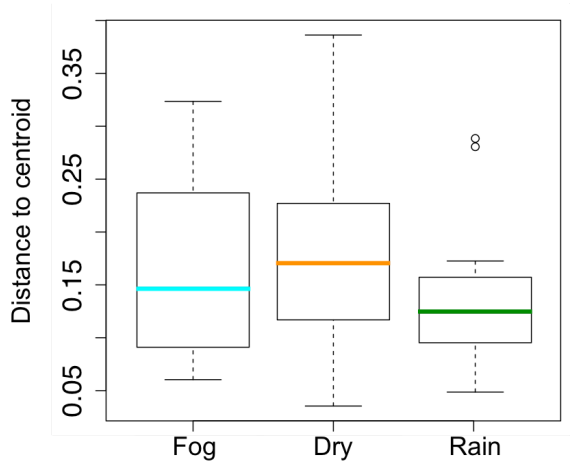

Figure 34: Boxplots of the betadisper analyses for the overall functional community fingerprint. Boxplots indicate the degree of homogeneity of group variances as the distance to the centroid.

Table 11: PERMANOVA results showing differences in overall potential microbial activity and between the xeric zones. The adjusted p value of the Tukey test shows differences in the homogeneity of group dispersion (Tukey p < 0.05 indicates significant within group variation). Significant values (p < 0.05) are designated by an asterisk.

(Df = degree of freedom, F = F value, and p = p value

	PERMANOVA Df	PERMANOVA F	PERMANOVA p	Tukey p
Overall Pairwise	2,77	13.547	**0.001***	
Fog - Dry	1,54	22.113	**0.001***	0.875
Fog - Rain	1,46	12.89	**0.001***	0.129
Dry - Rain	1,54	3.225	**0.022 ***	0.250

4.2.8 Environmental drivers of community function in Namib Desert soil

Soil organic matter content, Ca^{+}, K^{+}, Mg^{+}, Na^{+}, NO_3^{-}, pH, and S were identified as significantly contributing to the functional community fingerprint of the transect, accounting for 10.7% of the total variation observed (envfit p < 0.05; Table 12; Figure 35). Of these eight environmental parameters, six were of soil physicochemical properties found at their high concentrations in the 'Fog Zone' (NO_3^{-}, Ca^{+}, Na^{+}, Mg^{+}, K^{+}, and S; Table 5; Table 12).

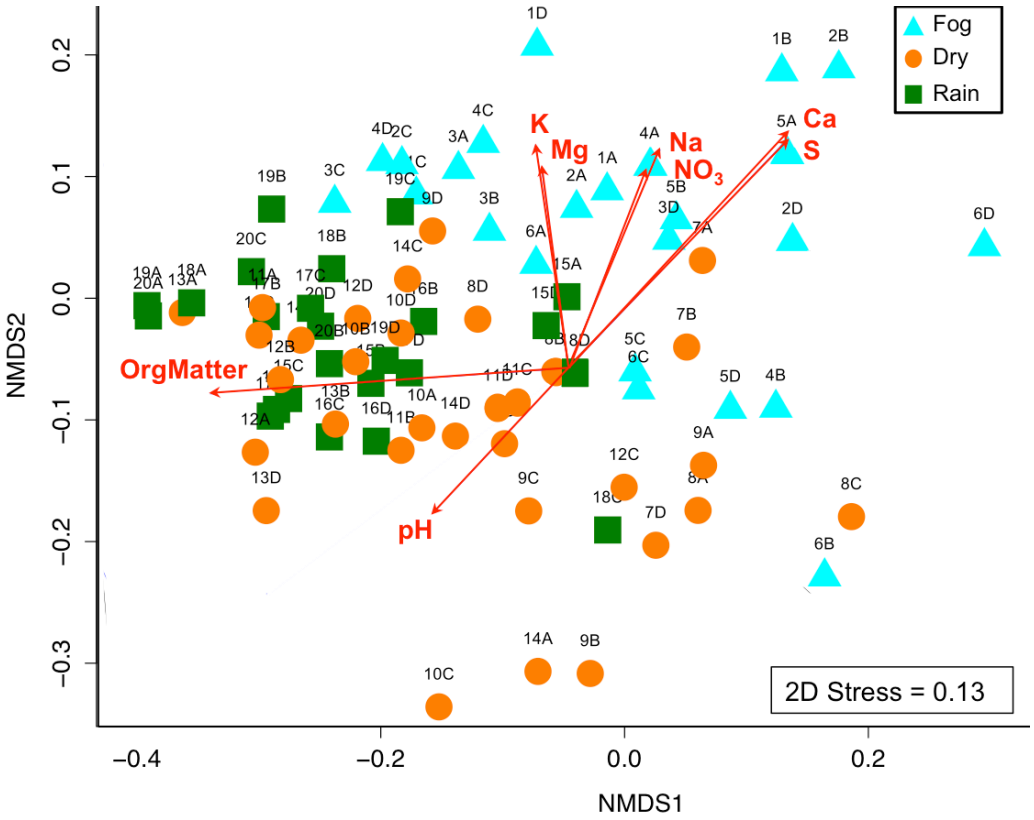

Figure 35: Non-metric multidimensional scaling (NMDS) plot of the overall potential enzyme activity across the transect. Arrows indicate significant correlations (envfit $p < 0.05$) with the overall potential enzyme activity (Bray-Curtis dissimilarities, Hellinger transformed, n = 80).

(Ca = calcium, K = potassium, Mg = magnesium, NO_3 = nitrate, OrgMatter= organic matter content, ph = soil pH, and S = sulfur)

The overlapping functional community fingerprint of the 'Dry' and 'Rain' zone samples separated from the 'Fog Zone' along the second axis (Figure 35). Soil pH and soil organic matter content, both of which increased across the transect from the coast inland, were indicated as significant contributors to this separation (envfit $p < 0.05$; Table 5; Table 12; Figure 20; Figure 35). The observed separation between the 'Dry' and 'Rain' zone samples along the first axis is primarily due to soil organic matter content, which was found in greater concentrations in the 'Rain Zone' (Table 5; Table 12; Figure 20).

Despite a majority of the soil physicochemical parameters between the 'Dry' and 'Rain' zones showing no significant differentiation (NH_4^+, NO_3^-, pH, Mg^+, Na^+, coarse sand, medium sand, fine sand, silt, and clay; ANOVA $p > 0.05$; Table 5; Table 6), the 'Dry' and 'Rain' zone functional community fingerprints were significantly different (PERMANOVA $p < 0.05$; Table 11), highlighting the importance of water availability to enzyme activity in the Namib Desert.

Table 12: Correlations (r^2) of environmental parameters with the NMDS plot of overall potential enzyme activity. Significant correlations based on the envfit function ($p < 0.05$; 999 permutations) are denoted with an asterisk.

Parameter	r^2	p
Org. matter	0.075	**0.049***
C	0.059	0.096
NH_4^+	0.041	0.199
NO_3^-	0.199	**0.001***
P	0.026	0.357
pH	0.128	**0.003***
CEC	0.023	0.431
Ca^+	0.361	**0.001***
K^+	0.190	**0.002***
Mg^+	0.165	**0.001***
Na^+	0.238	**0.001***
S	0.370	**0.001***
Coarse sand	0.071	0.067
Med. sand	0.013	0.606
Fine Sand	0.017	0.507
Silt	0.009	0.726
Clay	0.025	0.431

(n=80; Org. matter = organic matter content, C = carbon, NH_4^+ = ammonium, NO_3 = nitrate, P = phosphorus, pH = soil pH, CEC = cation exchange capacity, Ca^+ = calcium, K^+ = potassium, Mg^+ = magnesium, Na^+ = sodium, S = sulfur, Coarse sand = coarse sand content, Med. sand =medium sand content, Fine sand = fine sand content, Silt = silt content, and Clay = clay content)

4.2.9 Enzyme stoichiometry

Enzyme stoichiometry, expressed as the ratio between potential enzyme activities, is a useful metric to analyze relative shifts in potential microbial nutrient demand through changing environmental conditions (Bell *et al.*, 2013). The ratio of C:N, C:P, and N:P nutrient acquisition was calculated across the transect (Figure 36). In order to normalize variance and conform to the conventions of published stoichiometric analyses, all potential enzyme activities were calculated per gOM and log transformed (ln[x + 1]) prior to analysis (Sterner and Elser, 2002; Sinsabaugh and Shah, 2011). C:N enzyme activity was calculated as the ratio of potential BG activity to the combined potential activity of NAG and LAP (BG:[NAG + LAP]). C:P enzyme activity was calculated as the ratio of potential BG activity to potential AP activity (BG:AP). N:P enzyme activity was calculated as the combined potential activity of NAG and LAP to potential AP activity ([NAG + LAP]:AP). Additionally, the relationship between hydrolytic and oxidative C, N, and P acquisition was calculated by the ratios of BG:PO, (NAG + LAP):PO, and AP:PO potential activities, respectively (Figure 37).

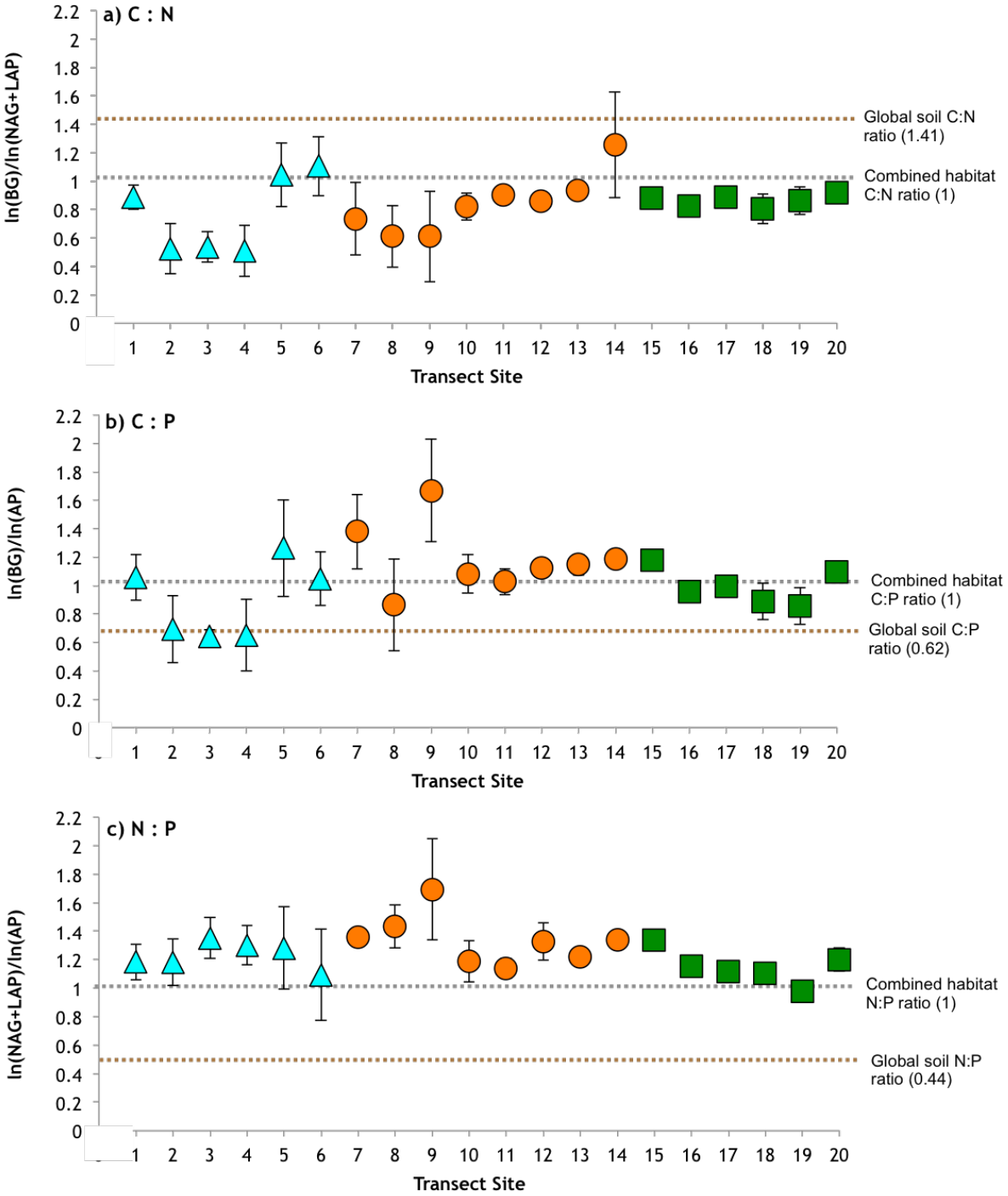

Figure 36: a) Potential C:N microbial nutrient demand estimated by the ratio of BG activity to the combined activities of NAG and LAP (BG:[NAG+LAP]); b) potential C:P microbial nutrient demand estimated by the ratio of BG activity to AP activity (BG:AP); and c) potential N:P microbial nutrient demand estimated by the combined activities of NAG and LAP to AP activity ([NAG+LAP]:AP). The ratio of activities across 40 soil environments is denoted by the brown dashed line, and the ratio of activities across terrestrial soil, wetland sediments, and river sediments is denoted with the gray dashed line (as measured by Sinsabaugh *et al.*, 2009).

▲ = 'Fog Zone' activity, ● = 'Dry Zone' activity, and ■ = 'Rain Zone' activity.

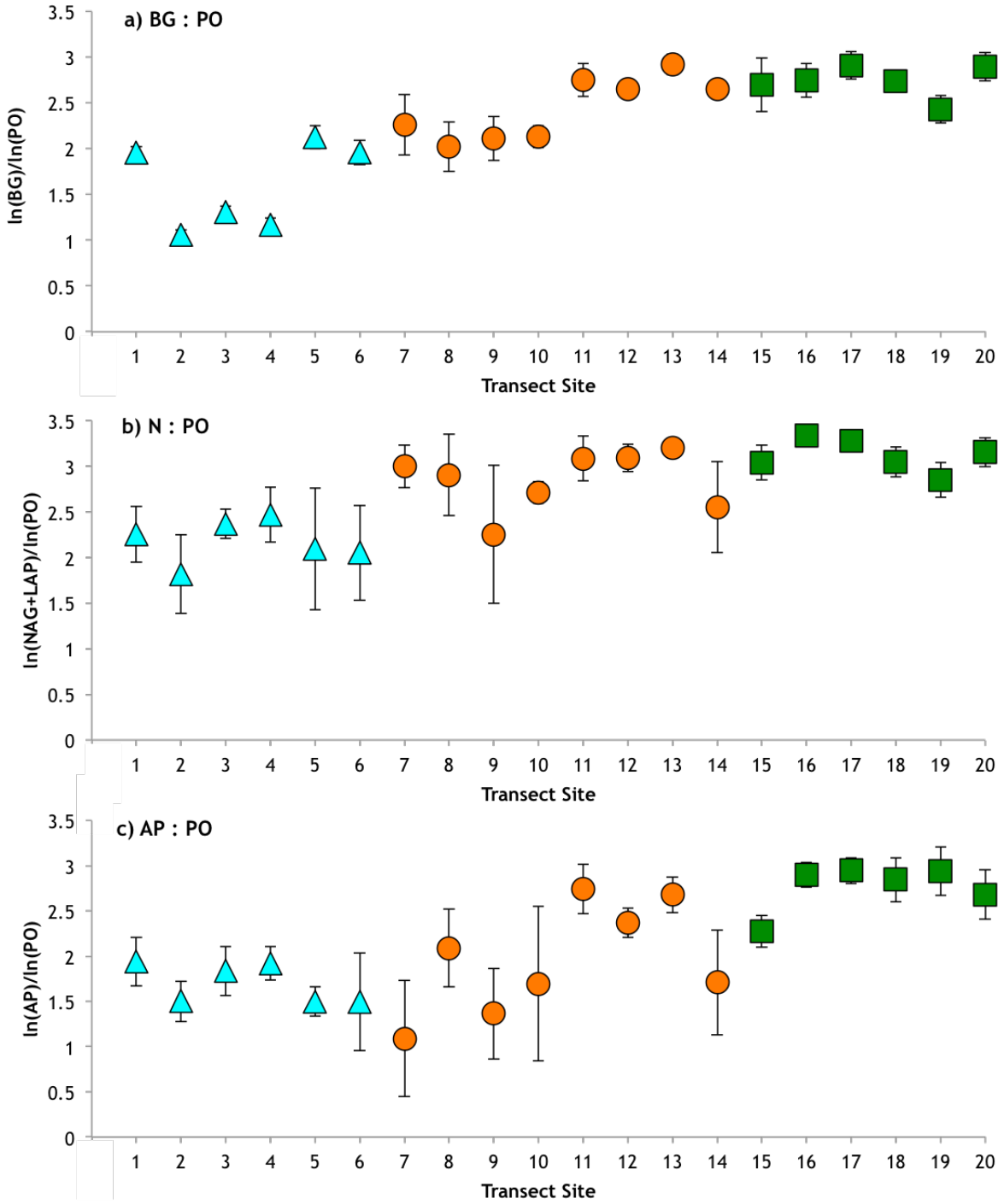

Figure 37: The relationship between hydrolytic and oxidative C, N, and P acquisition, calculated by the ratios of a) of BG:PO, b) (NAG + LAP):PO, and c) AP:PO potential activities, respectively.

▲= 'Fog Zone' activity, ● = 'Dry Zone' activity, and ■ = 'Rain Zone' activity.

Combined global analysis of terrestrial soil, wetland (lentic) sediment, and river (lotic) sediment show the mean worldwide ratio of C:N:P enzyme activities approaches 1:1:1 (Sinsabaugh *et al.*, 2009). The same study reported that the mean C:N enzyme activity ratio in soils across 40 sampling sites spanning all major biomes was 1.41 (Sinsabaugh *et al.*, 2009). The C:N enzyme activity ratio of this study indicated that site 14 was the most C limited (average C:N activity = 1.26; ± 0.4 SD), and N demand was highest in the 'Fog Zone' (average C:N activity = 0.78; ± 0.40 SD) (Figure 36a). The mean C:N enzyme activity ratio across the transect was 0.84 (± 0.34 SD), indicating a higher demand for N relative to the demand for C overall (Bell *et al.*, 2013), although C:N enzyme activity did not vary significantly across the transect (ANOVA $p = 0.58$) (Figure 36a).

The C:P ratio of potential enzyme activity across the transect averaged 1.02 (± 0.38 SD), and the average ratio of C:P enzyme activity was lowest in the 'Fog Zone' (0.89; ± 0.38 SD) (Figure 36b). The ratio of 'Fog Zone' C:P enzyme activity varied significantly from the rest of the transect (ANOVA $p < 0.05$). The lower C:P enzyme activity ratio in the 'Fog Zone' indicated a higher demand for P relative to C (Figure 36b).

The ratio of potential N:P enzyme activity across the transect averaged 1.22 (± 0.30 SD) and did not vary significantly between the xeric zones (ANOVA $p = 0.37$) (Figure 36c). This average contrasted greatly with the global mean N:P enzyme activity ratio of 0.44 from soils in all major biomes (Sinsabaugh *et al.*, 2009) and indicated the demand for P was consistently higher relative to N across the transect (Figure 36c).

Interestingly, despite significant differences in soil organic matter content between the three xeric zones (ANOVA $p < 0.05$; Table 6) and low levels of soil organic carbon in the 'Fog Zone' (mean C = 0.12% ± 0.08; Table 5), the enzyme stoichiometric ratios indicated that the transect's microbial communities were not C limited.

Nutrient acquisition by oxidative enzymes is generally an indication of higher concentrations of recalcitrant organic matter (Sinsabaugh, 2010). The ratios of potential BG:PO, (NAG + LAP):PO, and AP:PO enzyme activity all differed significantly across the transect (ANOVA $p < 0.05$) and increased

from the coast inland, indicating a greater dependence on oxidative C, N, and P nutrient acquisition near the coast (Figure 37) (Sinsabaugh and Shah, 2011).

The ratio of BG:PO enzyme activity is also suggested to reflect the relative stoichiometric abundance of labile to recalcitrant carbon in a sample (Sinsabaugh, 2010; Sinsabaugh and Shah, 2011). The BG:PO ratio of the transect indicated an increase in labile carbon from the coast inland (Figure 37a). This would agree with the observed vegetation structure transition from bare ground in the 'Fog Zone', to grasslands in the 'Dry Zone', and sparse shrublands in the 'Rain Zone' (Figure 16; Appendix B).

Chapter 5: Bacterial community structure in the Namib Desert

5.1 Results

5.1.1 Bacterial diversity

Terminal restriction fragment length polymorphism (T-RFLP) analysis of the 16S rRNA gene yielded 50 unique bacterial OTUs from the 72 samples analyzed (Figure 38). The OTUs of the individual samples, or the α diversity, ranged from 5 to 19 OTUs and averaged 12.1 OTUs per sample across the entire transect (Table 13). The α diversity of the individual samples increased across the transect from the coast inland, and the mean α diversity of the 'Fog', 'Dry', and 'Rain' zones were 9.6, 12.3, and 13.4, respectively (Table 13). The total number of OTUs, or γ diversity, of the 'Fog', 'Dry', and 'Rain' zones was 34 OTUs each (Table 13; Figure 38). A total of 19 OTUs were shared between the three zones (36%; Table 13; Figure 38). The 'Dry' and 'Rain' zones shared 30 OTUs (79%; Figure 38). The 'Fog Zone' contained the highest number of unique OTUs of the three zones (12, i.e., 24%; Table 13; Figure 38). The 'Fog Zone' also presented the highest ß diversity of the three zones, calculated as γ diversity over the mean α diversity (ß = γ/ ᾱ; Table 13), indicating it contained the most diverse community of the three zones.

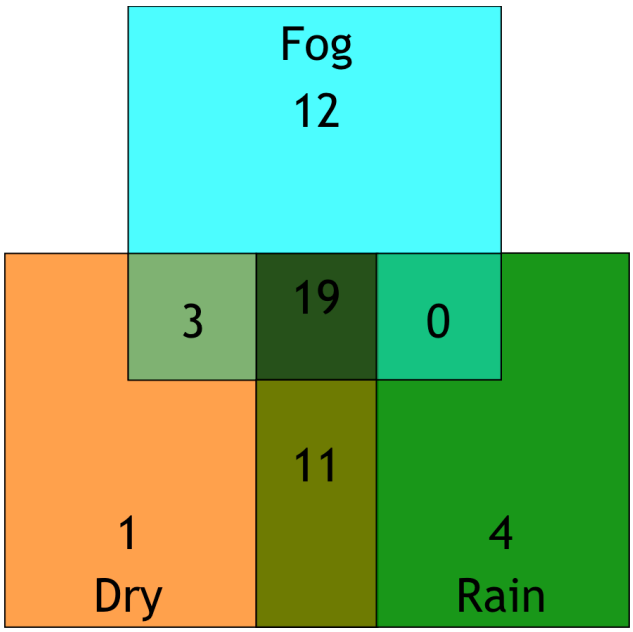

Figure 38: Venn diagram comparing the distribution of bacterial OTUs between the 'Fog' 'Dry', and 'Rain' zones.

Table 13: Descriptions of the 'Fog', 'Dry', and 'Rain' zones in terms of mean OTU abundance and diversity.

Environments	Mean OTUs (ᾱ)	Total OTUs (γ)	ß-diversity	Unique OTUs	OTUs shared across transect (%)
Fog Zone	9.63 (± 2.80)	34	3.53	12	68%
Dry Zone	12.31 (± 2.31)	34	2.76	1	66%
Rain Zone	13.38 (± 2.70)	34	2.54	4	60%

Species diversity was calculated using the Margalef's diversity index (Table 14). Species diversity ranged from 7.04 (sampling site 4, 'Fog Zone') to 11.36 (sampling site 15, 'Rain Zone'). The mean species diversity of the individual zones increased across the transect from the coast inland. The increasing species diversity from the 'Fog' to 'Rain' zones was also observed after applying the Shannon diversity index and Simpson's diversity index (Table 14).

Table 14: Descriptions of the 'Fog Zone', 'Dry Zone', and 'Rain Zone' in terms of diversity estimates.

Environments	Margalef's index (d)	Shannon index (H')	Simpson index (1-λ')
Fog Zone	8.42 (± 1.78)	2.11 (± 0.36)	1.38 (± 0.08)
Dry Zone	9.81 (± 1.30)	2.39 (± 0.19)	1.32 (± 0.03)
Rain Zone	10.54 (± 1.34)	2.45 (± 0.22)	1.31 (± 0.03)

5.1.2 Bacterial community structure and environmental drivers

The NMDS plot of bacterial community across the transect showed a separation in composition between the three *a priori* defined xeric zones (i.e., the 'Fog', 'Dry', and 'Rain' zones; Figure 39a), although some overlap of is evident between the 'Dry' and 'Rain' zone samples. The high percentage of shared OTUs may explain the close grouping of the 'Dry' and 'Rain' zones samples in the NMDS plot (Figure 38; Figure 39). Despite this overlap, PERMANOVA indicated a significant separation between the bacterial communities overall and for all pairwise combinations of xeric zones (PERMANOVA $p < 0.05$; Table 15). Additionally, soil organic matter content, C, Ca^{+}, CEC, K^{+}, Mg^{+}, Na^{+}, NO_3^{-}, P, pH, S, coarse sand, and silt were identified as significantly contributing to the structure of the bacterial community across the transect, accounting for 34.3% of the total observed variation (envfit $p < 0.05$; Table 16; Figure 39b).

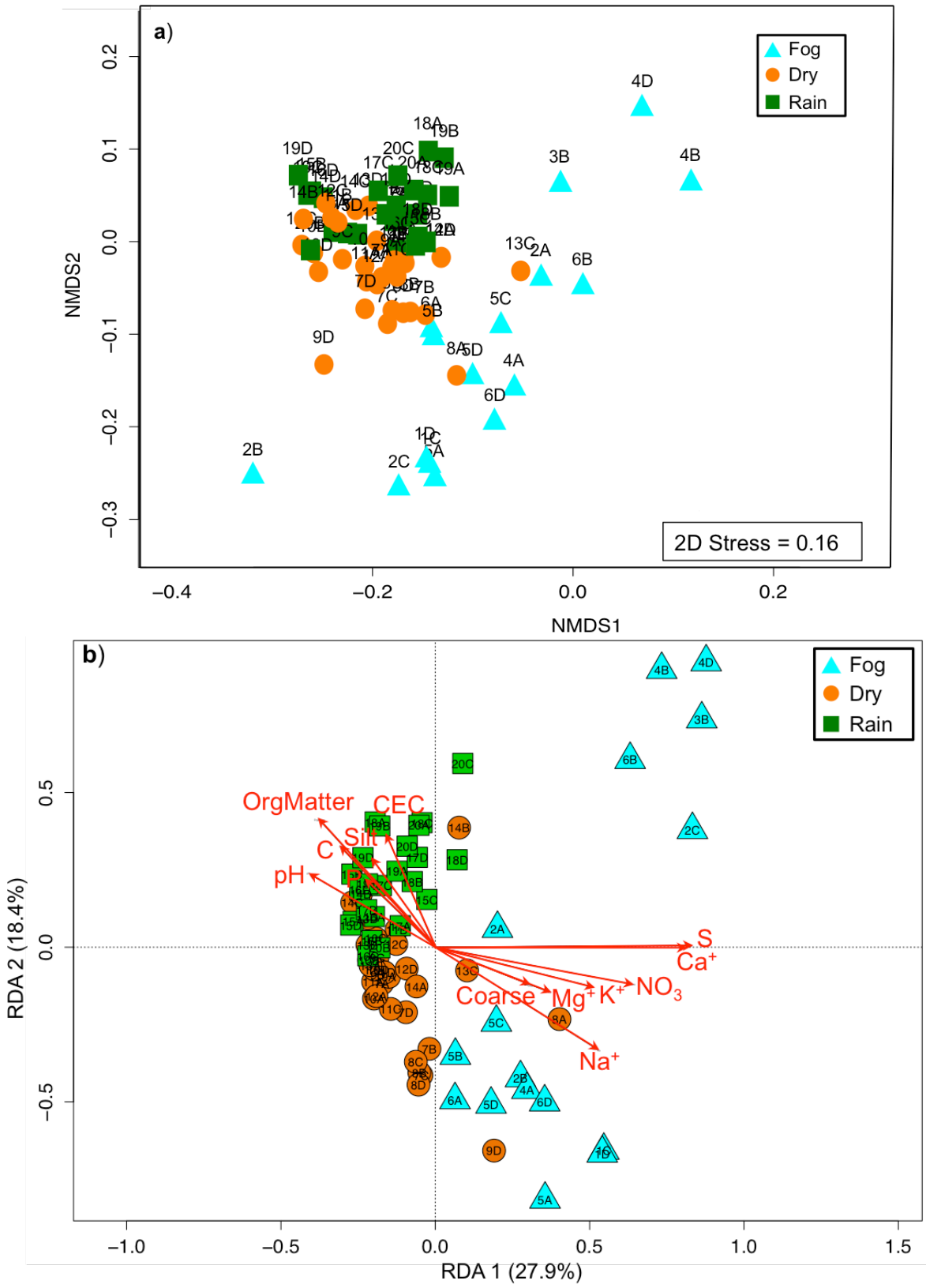

Figure 39: a) Non-metric multidimensional scaling (NMDS) of the Bray-Curtis dissimilarities of the bacterial community structure based on 16S rRNA gene T-RFLP profiles (Hellinger-transformed). b) RDA of the bacterial community structure. Arrows indicate significant correlations (envfit $p < 0.05$).

(C = carbon, Ca^+ = calcium, CEC = cation exchange capacity, Coarse = coarse sand, K^+ = potassium, Mg^+ = magnesium, Na^+ = sodium, NO_3 = nitrate, OrgMatter= organic matter content, ph = soil pH, P = phosphorus, S = sulfur, and Silt = silt content)

Table 15: PERMANOVA results showing differences in T-RFLP bacterial OTUs overall and between xeric zones. The adjusted p value of the Tukey test shows differences in the homogeneity of group dispersion (Tukey $p < 0.05$ indicates significant within group variation). Significant values ($p < 0.05$) are designated by an asterisk.

(Df = degree of freedom, F = F value, and p = p value)

	PERMANOVA Df	PERMANOVA F	PERMANOVA p	Tukey p
Overall	2,69	10.930	**0.001***	
Pairwise				
Fog – Dry	1,46	12.518	**0.001***	**0.000***
Fog – Rain	1,38	13.268	**0.001***	**0.000***
Dry – Rain	1,54	5.348	**0.001***	0.781

Table 16: Correlations (r^2) of environmental parameters with the NMDS plot of bacterial community composition. Significant correlations based on the envfit function ($p < 0.05$; 999 permutations) are denoted with an asterisk.

Parameter	r^2	p
Org. matter	0.312	**0.001***
C	0.201	**0.002***
NH_4^+	0.041	0.212
NO_3^-	0.423	**0.001***
P	0.102	**0.035***
pH	0.225	**0.001***
CEC	0.154	**0.005***
Ca^+	0.690	**0.001***
K^+	0.275	**0.001***
Mg^+	0.156	**0.001***
Na^+	0.392	**0.003***
S	0.697	**0.001***
Coarse sand	0.109	**0.015***
Med. sand	0.059	0.821
Fine Sand	0.054	0.154
Silt	0.120	**0.014***
Clay	0.008	0.755

(n=80; Org. matter = organic matter content, C = carbon, NH_4^+ = ammonium, NO_3 = nitrate, P = phosphorus, pH = soil pH, CEC = cation exchange capacity, Ca^+ = calcium, K^+ = potassium, Mg^+ = magnesium, Na^+ = sodium, S = sulfur, Coarse sand = coarse sand content, Med. sand =medium sand content, Fine sand = fine sand content, Silt = silt content, and Clay = clay content)

As with the functional analysis results, PERMANOVA of the T-RFLP bacterial community did not indicate a significant separation of the sampling site 1 into a 'Coastal Zone' (PERMANOVA p = 0.138; Figure 39). Wide dispersion of the 'Fog Zone' bacterial community compared to the 'Dry' and 'Rain'

zones is evident in the NMDS plot, with *post hoc* Tukey's HSD and betadisper tests indicating large within-group variation in the 'Fog Zone' (Tukey $p < 0.05$; Table 15).

To test for stochasticity in community assembly, the *raupcrick* function of the vegan package was used to create a Raup-Crick dissimilarity matrix relative to that generated under a neutral model (999 randomizations) (Raup and Crick, 1979; Hubbell, 2001; Oksanen *et al.*, 2007). Betadisper analyses of the Raup-Crick dissimilarity matrix showed a large degree of variability in the 'Fog Zone' bacterial community relative to the 'Dry' and 'Rain' zones (Figure 40). Post hoc Tukey's HSD tests signified the dispersion of 'Fog Zone' samples was significantly different to that of the 'Dry' and 'Rain' zones (Tukey $p < 0.05$; Table 15; Figure 40). This indicated that the 'Dry' and 'Rain' zone bacterial communities differed from the neutral model and were shaped by more deterministic forces, while the 'Fog Zone' bacterial community was shaped by more random, stochastic forces (Raup and Crick, 1979; Chase and Myers, 2011).

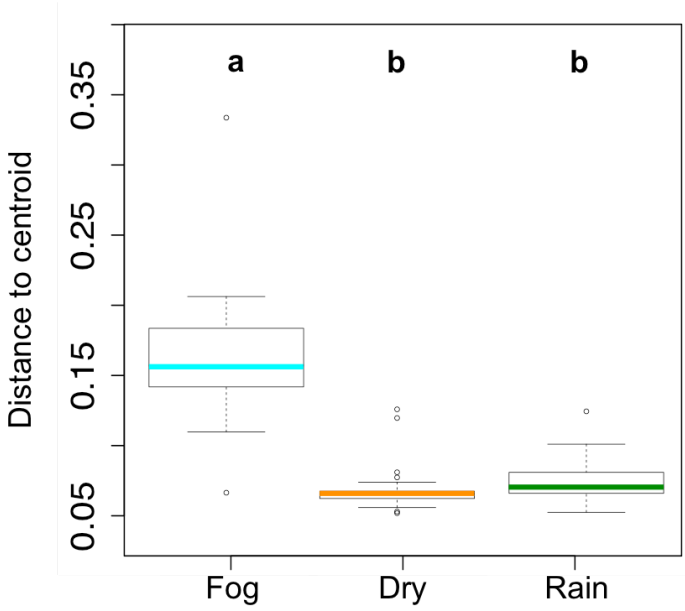

Figure 40: Boxplots of the betadisper analyses for the Raup-Crick dissimilarity matrix. Boxplots indicate the degree of homogeneity of group variances as the distance to the centroid.

Chapter 6: Discussion

6.1 Environmental gradient

The analyses of the environmental transect revealed four distinct zones (i.e., 'Coastal', 'Fog', 'Dry', and 'Rain' zones; Figure 24). The 'Coastal Zone' was comprised of site 1 and was characterized by high levels of sodium (Na^+) in the soil, probably due to the site's close proximity to the ocean (Na^+ = 11 000 mg·kg^{-1}; approximately 10 km inland; Table 5; Figure 12; Appendix A). The deposition of Na^+ was likely due to the combined processes of atmospherically transported marine aerosols and relict sea-salts remaining after oceanic regression (Chivas *et al.*, 1991). Atmospherically transported marine aerosols are also likely responsible for the deposition of Na^+ and sulfur (S) found in the 'Fog Zone' soils (sites 2 to 6; Table 5; Figure 19; Figure 27) (Goudie *et al.*, 1997). Interestingly, fog events likely played little role in the accumulation of gypsum ($CaSO_4 \cdot 2H_2O$) deposits, which were the most significant physicochemical characteristic of the 'Fog Zone' soil (Figure 15; Figure 19; Figure 27) (Eckardt and Spiro, 1999). Analysis of fog moisture from the Namib Desert have shown it to be low in salts and without the S levels necessary to facilitate gypsum formation (S = 3.2 ppm) (Eckardt and Schemenauer, 1998). Instead, the combination of the marine origin S and calcium (Ca^+) from secondary calcrete deposits are likely responsible for gypsum formation in the 'Fog Zone' (Table 5; Figure 15; Figure 19; Figure 27) (Eckardt and Spiro, 1999; Eckardt *et al.*, 2001).

Within the 'Coastal' and 'Fog' zones, the geochemical and climatic conditions of the soil are not favorable for higher plant growth and the vegetation coverage is essentially non-existent (Figure 16; Appendix B). Plant growth is impeded in this region by the high sulfate content in the soils, which create nutrient deficiencies at the root surface due to ion competition (Table 5; Figure 27) (Marschner, 2011). Although some plant species have adaptations to mitigate this stress (Escudero *et al.*, 2015), the low precipitation in the area further disrupts plant establishment and success (Figure 16; Figure 18; Appendix B) (Muller, 2015).

Outside the 'Fog Zone', the vegetation structure transitions from bare ground to sporadic grasslands in the 'Dry Zone', then to sparse shrublands in the 'Rain Zone' (Figure 16; Appendix B).

This transition corresponds to a shift in soil composition from gypsisols to calcisols (Figure 15). Calcisols have a greater degree of soil fertility than gypsisols (Mendlesohn *et al.*, 2002); however, the bioavailability of iron and zinc is low in calcisols which limits plant growth (Mendlesohn *et al.*, 2002).

Soil physicochemical characterization of 'Dry' and 'Rain' zone samples showed some degree of overlap near the Kuiseb River (sites 14 to 16; Figure 15; Figure 22; Figure 24). This portion of the transect was a transitional zone between the gravel plains of the 'Dry Zone', characterized by calcretes and low denudation rates (Bierman and Caffee, 2001; Viles and Goudie, 2013), and the Great Escarpment, characterized by high rates of erosion and regosol and leptosol soil types (Figure 15; Appendix B) (Mendlesohn *et al.*, 2002). Regosols and leptosols are fragmented soils that are highly dependent on consistent rainfall to sustain vegetation, as their loose composition has a low water holding capacity (Mendlesohn *et al.*, 2002).

A priori zonation of the transect was based on dominant water regime (i.e., fog or rainfall) and published climatic data for mean annual rainfall, dividing the transect into 3 zones of differing xeric stress (i.e., 'Fog', 'Dry', and 'Rain' zones; Figure 18; Figure 19; Appendix C; Appendix D) (Lancaster and Seely, 1984; Directorate of Environmental Affairs, 2002; Eckardt *et al.*, 2013b). However, gradients of soil physicochemistry, geology, and vegetation coverage were also evident across the transect after sampling (Figure 15; Figure 16; Figure 27; Appendix B). The combined effect of these environmental gradients in addition to xeric stress highlights the complexity of ecological transects and the multitudinal forces shaping microbial community structures and functions in soil (Smith *et al.*, 2002; Warren-Rhodes *et al.*, 2006; Hollister *et al.*, 2010).

6.2 Microbial community structure and function

Unlike the soil physicochemical properties, microbial community structures and microbial community functions (as determined by enzyme activity assays) did not position site 1 into a 'Coastal Zone' (PERMANOVA $p > 0.05$; Figure 24; Figure 33; Figure 39). Both microbial community structures and functions separated based on the three *a priori* defined xeric zones (i.e., 'Fog',

'Dry', and 'Rain' zones; Figure 33; Figure 39). Analysis of the bacterial community fingerprint and potential enzyme activity indicated water availability as significantly shaping the microbial community structure and function in the central Namib Desert.

6.2.1 Potential enzyme activity

The enzyme activities of ß-glucosidase (BG), ß-N-acetylglucosaminidase (NAG), leucine aminopeptidase (LAP), alkaline phosphatase (AP), phenol oxidase (PO), and fluorescein diacetate (FDA) hydrolysis generally increased from the coastal samples to the more inland samples (Figure 28; Appendix A). These enzymes are commonly used as indicators of C, N, and P cycling in soils (Steinweg *et al.*, 2012). Determining the relative rates of microbial activities in soils is important, as they are suggested to provide a sensitive and early indication of changes in soil quality (Landi *et al.*, 2000). This is of particular importance in arid environments due to the susceptibility of these regions to climatic change (Pointing and Belnap, 2012).

The stoichiometric ratios of potential enzyme activities indicates the relative reliance on oxidative over hydrolytic enzyme production for nutrient acquisition (Schnecker *et al.*, 2014). The stoichiometric ratios of this study indicated that the edaphic microbial communities in the 'Fog Zone' are dependent on the oxidative activity of PO for C, N, and P nutrient acquisition (Figure 37). This is consistent with studies in other arid environments that have linked substrate limitation with higher PO potential actives (Sinsabaugh, 2010).

In addition, Sinsabaugh and Shah (2011) have demonstrated the effectiveness of using the stoichiometric ratios of BG to PO potential enzyme activities as an indicator of the relative abundance of recalcitrant organic matter in a sample. The analysis of this stoichiometric ratio across the transect indicated that the 'Fog Zone' contained a higher proportion of recalcitrant organic matter than the 'Dry' and 'Rain' zones (Figure 37a). This corresponds with the gradient of increasing vegetation observed from the coast inland, as the concentration of labile organic matter in soil is primarily influenced by input from vegetation (Figure 16; Appendix B) (Haynes, 2000; Hoyle and Murphy, 2006). In the 'Dry' and 'Rain' zones, the higher ratio of labile organic coincided with greater BG, NAG, LAP, and AP activities (Figure 28; Figure 37). This would be expected, as

labile organic matter is preferentially degraded by these hydrolyzing enzymes (Sinsabaugh and Shah, 2011). Studies have shown soil enzyme activities to be dependent on the concentration as well as type of soil organic matter (i.e., recalcitrant or labile), and that organic matter degradation by microbial extracellular enzymes is a possible rate-limiting step for ecosystem productivity (Waldrop *et al.*, 2000; Allison *et al.*, 2007; Bell *et al.*, 2009).

However, a definitive relationship between enzyme activity and organic matter content has been difficult to determine as relationships between enzyme activity and nutrient availability have not been conclusively established (Stevenson and Mandelstam, 1965; Sinsabaugh *et al.*, 1993; Olander and Vitousek, 2000; Fontaine *et al.*, 2003; Allison *et al.*, 2007). Physical stability and spatial separation of organic matter based on soil particle size may be a more important determinant of enzymatic decomposition rates than organic matter content alone (Schnecker *et al.*, 2015). For example, the rate of organic matter decomposition in soils has been shown to be dependent on the availability of electron acceptors and binding sites within the soil matrix, as well as the amount of surface area available for these reactions (Boyd and Mortland, 1990; Huang, 1990; Sinsabaugh, 2010). As the silt fraction of soil has a greater surface area than the sand fraction, higher silt content in soils may be more conducive for the enzymatic degradation of organic matter (Huang, 1990; Sinsabaugh, 2010). The analysis of the Namib Desert transect samples backed these findings, as statistically significant correlations between soil particle size and enzyme activity were observed for all samples ($r_s > 0.3$; Table 9; Figure 30). Silt content showed a positive correlation with all enzyme activities, while sand content showed negative correlations (Table 9; Figure 30). It is important to note that this relationship may also be due to water availability, as small soil particles (i.e., silt; <53 µm) have a greater water holding capacity than the larger soil fractions (i.e., sand; >250 µm) (Van Gestel *et al.*, 1996; Kandeler *et al.*, 2000; Sessitsch *et al.*, 2001; Novak *et al.*, 2009). Furthermore, soil fractions of silt have been shown to contain higher levels of organic matter than soil fractions of sand (Van Gestel *et al.*, 1996; Kandeler *et al.*, 2000; Sessitsch *et al.*, 2001; Novak *et al.*, 2009).

In addition to the spatial conditions, soil chemical parameters are also an important determinant of soil enzyme function (Sinsabaugh, 2010). The chemical composition of the soil affects enzyme

kinetics and microbial function (Burns and Dick, 2002; Grandy *et al.*, 2008; Legg *et al.*, 2012). For example, the cation exchange capacity (CEC), a measurement of the retention capacity of cations by electrostatic forces on soil surfaces (Ross, 1995), must be suitable for proper enzyme catalysis (Burns and Dick, 2002). Soils with low CEC have been shown to have diminished enzyme activities (Juma and Tabatabai, 1977; Frankenberger and Tabatabai, 1981; Burns and Dick, 2002; Nannipieri *et al.*, 2002). As such, CEC is often used as a measure of soil quality and productivity (Ross, 1995). Statistically significant correlations between CEC and enzyme activity were observed for all transect samples (r_s > 0.4; Table 9; Figure 31). This may be due in part to the sequestering of positively charged metals in soils with high CEC that would otherwise be inhibitory to enzyme functioning (Lighthart *et al.*, 1983; Doelman and Haanstra, 1989; Burns and Dick, 2002; Nannipieri *et al.*, 2002).

Other soil chemical parameters, such as phosphorus (P), were not shown to have a strong correlation with any of the measured potential enzyme activities (r_s > 0.4; Table 12). This was unexpected, as P has repeatedly been shown to be negatively correlated with phosphatase activity, and variations in soil P levels have been shown to modify microbial functional properties in soil (McGill and Cole, 1981; Olander and Vitousek, 2000; Allison and Vitousek, 2005; Bell *et al.*, 2014). The lack of correlation with soil P and enzyme activity in this study may be due to the Bray-1 method used to measure soil P concentration (Section 2.3.3). In alkaline soils, Bray-1 can underestimate P content (Bowman and Vigil, 2002; Ronca *et al.*, 2015). The sodium bicarbonate extraction procedure would be a more appropriate method for determination of P content in alkaline desert soils (Olsen, 1954) and should be used in future studies of Namib Desert soil physicochemistry.

Within the Namib Desert transect, Ca^+, K^+, Mg^+, Na^+, NO_3^-, S, and pH were indicated to be significant drivers of microbial function (envfit $p < 0.05$; Table 12; Figure 35). These soil chemical parameters accounted for 10.7% of the variation observed in the functional community fingerprint (Table 12; Figure 35). The remaining variation may be explained by environmental factors that were not measured, and this degree of unexplained variation is not uncommon in studies of microbial ecology (Cottenie, 2005; Dumbrell *et al.*, 2010; Ronca *et al.*, 2015). Despite the

unexplained variation, the transect functional community fingerprint showed significant differentiation based on the three *a priori* xeric zones (i.e., 'Fog', 'Dry', and 'Rain' zones; PERMANOVA $p < 0.05$; Table 11; Figure 33). It is important to note that despite markedly different soil physicochemistry between the 'Coastal' and 'Fog' zones, the functional community fingerprint did not show a significantly differentiated structure at site 1 (PERMANOVA $p > 0.05$; Table 5; Figure 24; Figure 33). This result highlights the importance of water availability in shaping microbial function in the Namib Desert.

6.2.2 Bacterial community structure

The Namib Desert transect bacterial communities were analyzed using terminal restriction fragment length polymorphism (T-RFLP) fingerprinting analysis (Figure 39). Although next-generation sequencing (NGS) has become more widely available since this study was initiated, T-RFLP fingerprinting analysis has repeatedly been shown to produce community composition profiles that are comparable to those generated through NGS (Besemer *et al.*, 2012; Gobet *et al.*, 2014; Valverde *et al.*, 2014). T-RFLP fingerprinting is particularly useful for analyzing and comparing distinctive microbial community patterns, as well as correlating environmental variables with community structure (Tiquia, 2005; van Dorst *et al.*, 2014).

Analysis of the T-RFLP bacterial community fingerprint showed that each *a priori* defined xeric zone presented a unique and significantly differentiated phylogenetic profile (i.e., 'Fog', 'Dry', and 'Rain' zones; PERMANOVA $p < 0.05$; Table 15; Figure 39). Soil organic matter content, C, Ca^{+}, CEC, K^{+}, Mg^{+}, Na^{+}, NO_3^{-}, P, pH, S, coarse sand, and silt were identified as significantly contributing to the structure of the bacterial community across the transect, accounting for 34.3% of the total observed variation (envfit $p < 0.05$; Table 16; Figure 39). However, as with the functional community fingerprint, a significantly differentiated structure at site 1 was not observed despite markedly different soil physicochemistry between site 1 and the other 'Fog Zone' samples (PERMANOVA $p > 0.05$; Table 5; Figure 24; Figure 33; Figure 39). This result emphasizes the importance of water availability in shaping the microbial structure in the Namib Desert.

Comparison of the 'Fog', 'Dry', and 'Rain' zone bacterial community structures using the Raup-Crick dissimilarity metric indicated the 'Fog Zone' community structure did not deviate from the random variation predicted using the null model (999 randomizations; Figure 40) (Raup and Crick, 1979). In addition, the 'Fog Zone' samples showed the largest variation in community composition of all samples from the transect (Table 13; Figure 38; Figure 39; Figure 40). Together, these results suggest that stochastic processes are responsible for the bacterial community assembly in the 'Fog Zone'. This was unanticipated, as the high salt and gypsum content of the 'Fog Zone' soils were expected to act as an environmental filter, shaping the bacterial community deterministically (Chase, 2007; Chase and Myers, 2011; Muller, 2015). Globally, soil salinity has been identified as a dominant environmental physicochemical filter (Lozupone and Knight, 2007). Instead, 'Fog Zone' samples contained the highest percentage of unique OTUs of the three xeric zones (12%; Figure 38).

Several factors are likely to be responsible for the variation observed in the 'Fog Zone' bacterial community. For instance, a disparate gradient of solar radiation was present across the Namib Desert, and near the coast fog formation reduces the penetration of solar radiation (Figure 7) (Hewson, 1943). Beyond the 'Fog Zone' cloud coverage is rare, and solar radiation levels are in excess of 6 $kWh \cdot m^{-2} \cdot day^{-1}$ (Figure 7) (Mendlesohn *et al.*, 2002). Thus, fog formation reduces the selective pressure posed by solar radiation (Paul and Gwynn-Jones, 2003). In addition, strong onshore winds formed by the South Atlantic anticyclonic airflows are persistent throughout the year (Figure 8) (Mendlesohn *et al.*, 2002). These winds homogenize and disperse microbial communities throughout the 'Fog Zone', increasing the stochastic effects of chance colonization (Mouquet and Loreau, 2003; Chase and Myers, 2011). Linked to this, the marine aerosols that carry Na^+ and S sea salts into the 'Fog Zone' are also likely to impact the region with a consistent influx of marine bacteria, furthering the possibility of chance colonization (Burrows *et al.*, 2009). Marine aerosols have been shown to provide an influx of organic matter into soil systems, and microbial inputs to soil from bodies of water are not uncommon in desert environments (Cavalli *et al.*, 2004; Wood *et al.*, 2008b; Pointing *et al.*, 2009). Furthermore, the gypsum found in the 'Fog Zone' soils may support unique microbial communities (Wierzchos *et al.*, 2012). Deserts worldwide have shown diverse microbial populations within soils of high gypsum content (Schlesinger *et al.*, 1996; Yeager *et al.*, 2004; Nagy *et al.*, 2005; Drees *et al.*, 2006; Gundlapally and Garcia-Pichel, 2006; Oren *et*

al., 2009; Pointing *et al.*, 2009; López-Lozano *et al.*, 2012). Interestingly, microbially inhabited gypsum soils in arid environments are possible Martian soil analogues, as extensive gypsum deposits have been found on Mars (Davila *et al.*, 2010; Massé *et al.*, 2012). Fossilized microbes are detectable within gypsum deposits on Earth, warranting the investigation of Martian gypsum during near-term missions to Mars (Schopf *et al.*, 2012; Benison and Karmanocky, 2014). Finally, fog events provide a consistent source of moisture to an arid region of the Namib Desert with a mean annual rainfall of less than 40 mm (Figure 18; Figure 19; Appendix C; Appendix D) (Lancaster and Seely, 1984; Eckardt *et al.*, 2013b, 2013c). Utilization of fog moisture in the Namib Desert has been demonstrated with macroorganisms such as fog-harvesting beetles *(*including *Onymacris, Stenocara and Physasterna spp.)* and dune grasses (*S. sabulicola*), as well as for the hypolithic microbial communities that colonize the transverse side of translucent rocks (Hamilton and Seely, 1976; Henschel and Seely, 2008; Nørgaard and Dacke, 2010; Makhalanyane *et al.*, 2013). However, the degree to which edaphic microbial communities are able to utilize fog moisture has not been widely studied beyond refuge niches (Warren-Rhodes *et al.*, 2006; Pointing and Belnap, 2012). This is partially due to the difficulty in determining the amount of fog moisture that is made available to the edaphic microbial communities, as not all fog events intersect with the soil and a method for determining the volume of moisture input from fog is not standardized in literature (Lancaster and Seely, 1984; Olivier, 1995; Hachfeld, 2000; Eckardt *et al.*, 2013b). However, the indication that stochastic processes dominate the 'Fog Zone' bacterial community assembly suggests that fog moisture is in fact utilized by edaphic microbial communities outside of refuge niches, as rainfall in this area would likely be insufficient in supporting the varied community observed (Figure 18; Figure 19; Figure 39) (Navarro-Gonzalez *et al.*, 2003; Warren-Rhodes *et al.*, 2006; Caruso *et al.*, 2011).

Beyond the 'Fog Zone', moisture input is dependent upon seasonally regulated rainfall (Figure 18). Frequent drying of soils has been shown to affect microbial communities, and the deterministic filtering effects of arid conditions within the 'Dry Zone' are evident in the clustered composition of the bacterial community (Figure 39) (Schimel *et al.*, 2007; Burns *et al.*, 2013). Interestingly, 'Rain Zone' samples did not show a significant increase in community variation as compared to 'Dry Zone' samples, and the Raup-Crick dissimilarity metric indicated that deterministic processes

were likely shaping the bacterial community compositions in both the 'Dry' and 'Rain' zones (999 randomizations; Figure 40). This was despite the 'Rain Zone' receiving an average of 70 mm more rainfall annually and having significantly high concentrations of soil organic matter than the 'Dry Zone' (1.3%; ANOVA $p < 0.05$; Table 5; Table 6; Figure 18; Figure 20; Appendix A; Appendix C; Appendix D). The environmental filtering observed in the 'Rain Zone' is probably linked to the seasonality of the rainfall. In both the 'Dry' and 'Rain' zones, mean monthly rainfall is less than 10 mm during the six month long dry season (June to November) (Hachfeld, 2000; Mendlesohn *et al.*, 2002; Okitsu, 2005). A recent microcosm study of Namib Desert soils has shown the intensity of water input, rather than its frequency, to have a greater effect in shaping soil bacterial communities (Frossard *et al.*, 2015). Although the mean annual rainfall in the 'Fog Zone' was significantly less than the 'Dry' and 'Rain' zones, moisture input from fog events were more consistently spread throughout the year (Figure 18; Figure 19; Appendix C) (Lancaster and Seely, 1984). The episodic intensity of rainfall in the 'Dry' and 'Rain' zones may be another deterministic factor shaping the bacterial community in this region.

6.3 Conclusion

Taken as a whole, the microbial community structures and functions across the Namib Desert transect appear to be shaped by the degree of xeric stress imposed on the communities, as both microbial community structures and functions separated based on the three *a priori* defined xeric zones (i.e., 'Fog', 'Dry', and 'Rain' zones; Table 11; Table 15; Figure 33; Figure 39). Community assembly across the Namib Desert transect appears to result from the interaction of stochastic and deterministic processes, linked to differing degrees of xeric stress (Figure 40). Indeed, despite the high percentage of unique OTUs seen in the 'Fog Zone' (12%; Table 13; Figure 38), an even greater percentage of OTUs were shared between all three xeric zones (19%; Table 13; Figure 38). The high percentage of shared taxa highlights the important interplay between these two mechanisms of community assembly. Stochastic and deterministic processes are responsible for sustaining biodiversity and ecosystem functioning in arid environments that are threatened by climate change, and the unique members of stochastically assembled microbial communities may be particularly susceptible to extinction (Schnecker *et al.*, 2014). As such, fully understanding the drivers of

community structure and function is of considerable importance (Caruso *et al.*, 2011; Stomeo *et al.*, 2013).

In addition, to better understand ecosystem functioning and enable predictions of biotic and abiotic responses to environmental change, the relationship between community structure and ecosystem function must be understood (Fuhrman, 2009). However, there is currently a considerable gap in knowledge concerning the relationship between community composition and community functional capacity (Waldrop *et al.*, 2000). One suggested manner in which to expand on this knowledge is through the analysis of changes in microbial function related to community structure across environmental gradients (Findlay *et al.*, 2003; Docherty *et al.*, 2006; Findlay and Sinsabaugh, 2006; Comte and Del Giorgio, 2009; Frossard *et al.*, 2012). By focusing on environmental gradients in depauperate desert systems, where nutrient cycling rates are lower than more mesic environments, the linking of community structures and functions may be further facilitated as the complexity of the interactions is reduced (Fierer *et al.*, 2007; Fierer *et al.*, 2012b; Manzoni *et al.*, 2012; Paul, 2014; Makhalanyane *et al.*, 2015). In this study, a significant relationship between community structure and function was found (Mantel $r = 0.2$; $p < 0.01$), indicating changes in community structure coincided with changes in function. This relationship shows the importance of species composition in microbial community processes and has been observed in similar studies (Fierer *et al.*, 2012b; Valverde *et al.*, 2015).

As climatic variation is likely to intensify in the future, the findings outlined in the study are important for expanding our understanding of soil microbial community structures and functions, their relationships to each other, as well as their response to differing climatic regimes.

6.4 Future work

Future sampling campaigns across this environmental transect may be well served by further expanding the length of the transect. The physicochemical differentiation on the 'Coastal Zone' was unexpected, and finer sampling resolution closer to the coast would be interesting in more detailed comparisons of community structure and function. Similarly, extension of the transect further into the 'Rain Zone' may yield interesting results. As our transect did not reach past the Great Escarpment that marked the eastern-most boundary of the Namib Desert, the degree of community variability in the higher rainfall environment of the Central Plateau of Namibia is unknown.

A wider range of soil chemical analyses may also aid future studies of this edaphic environment. Additional measurements of soil heavy metal concentrations may have shed light on the enzyme activity patterns observed across the transect, as the inhibitory effects of heavy metals such as copper (Cu), iron (Fe), manganese (Mn), and zinc (Zn) on soil enzyme functioning are well documented (Tyler, 1974; Garcıa-Gil *et al.*, 2000; Burns and Dick, 2002; Burns *et al.*, 2013). As the concentrations of these metals were not measured in this study, their effect on the overall function of the microbial community across the transect is unknown. It is not unreasonable to assume that heavy metals had some effect on the potential enzyme activity in the soils of this study, as elevated levels of Cu, Fe, Mn, and Zn have been found in soils within 60 km of our transect sampling sites (Cu = 6.4 $mg \cdot kg^{-1}$, Fe = 66.1 $mg \cdot kg^{-1}$, Mn = 83.4 $mg \cdot kg^{-1}$, and Zn = 1.2 $mg \cdot kg^{-1}$) (Gombeer *et al.*, 2015). Further soil chemical analyses may help give a more complete picture of the environmental regulation of enzymes in Namib Desert soils.

Temporal analysis of microbial community structure and function may also further serve the understanding of this site. Namibia has the highest coefficient of variation of rainfall in all of southern Africa (Figure 11) (Directorate of Environmental Affairs, 2002), and year to year analysis may yield different results. The level of stochastic community assembly may shift with differing dispersion rates, recovery from disturbance, or shifts in climatic variance. Adding temporal analyses aids in circumventing the inherent weakness in one time studies (Schmidt *et al.*, 2007; Prosser, 2010; Knight *et al.*, 2012).

Finally, direct manipulation of soil samples would contribute to further understanding of the stochastic role of community assembly across the Namib Desert transect. For example, microcosm experiments in which soil samples from the 'Fog Zone' were placed in the 'Dry' and 'Rain' zones, as well as 'Dry' and 'Rain' zone samples placed within the 'Fog Zone', would provide valuable data on community structure and adaptations (Frossard *et al.*, 2015). 'Fog Zone' samples placed in the 'Dry' and 'Rain' zones would be outside the dispersion effects of marine aerosol and coastal winds, and under the same environmental filtering effects of increased solar radiation and aridity (while soil chemistry would remain constant). Likewise, 'Dry' and 'Rain' zone samples would be introduced to the effects of marine aerosols and aeolian dispersion when placed within the 'Fog Zone'. Comparison of the metagenome of nearby marine samples could further elucidate any inoculating effects of the ocean. Comparing shifts in community structure and function throughout a full rain-dry season could help explain the variation and clustering of microbial communities in the Namib Desert, as well as what process are responsible for the community assembly.

Appendices

Appendix A(i): Sampling information and soil structure for sites **1 to 10**.

Site	Rep	GPS coordinates		Date sampled	Time	Elevation (SRTM; m)	Coarse sand (<2mm; %)	Med. sand (<500um; %)	Fine sand (<250um; %)	Slit (<53um; %)	Clay (%)
1	A	S 22°58.712'	E014°35.046'	4/22/13	10:30	22.9	22.7	11.3	48.4	11.7	6
	B	S 22°58.763'	E014°35.031'	4/22/13		22	18.6	8.3	58.9	6.1	8
	C	S 22°58.810'	E014°35.013'	4/22/13		20.1	12.8	7.0	66.3	7.9	6
	D	S 22°58.863'	E014°34.995'	4/22/13		20.9	11.7	9.3	65.4	7.5	6
2	A	S 22°59.979'	E014°40.294'	4/22/13	11:03	117.9	17.0	9.5	57.2	12.3	4
	B	S 23°00.034'	E014°40.293'	4/22/13		117.6	18.2	9.6	53.2	17.0	2
	C	S 23°00.090'	E014°40.285'	4/22/13		116	17.8	11.2	52.3	12.7	6
	D	S 23°00.137'	E014°40.278'	4/22/13		115.1	25.1	11.2	51.9	7.9	4
3	A	S 23°00.841'	E014°45.992'	4/22/13	11:30	234	17.7	12.7	47.9	15.7	6
	B	S 23°00.879'	E014°45.971'	4/22/13		233.4	12.3	9.8	52.5	21.4	4
	C	S 23°00.930'	E014°45.960'	4/22/13		232.6	19.3	16.2	42.8	17.6	4
	D	S 23°00.972'	E014°45.973'	4/22/13		233.1	24.3	17.9	39.2	14.6	4
4	A	S 23°01.016'	E014°51.548'	4/22/13	12:00	312.9	10.4	14.1	52.9	14.5	8
	B	S 23°01.057'	E014°51.564'	4/22/13		313.7	12.7	13.5	55.5	12.2	6
	C	S 23°01.118'	E014°51.584'	4/22/13		315.5	11.8	14.9	53.9	15.3	4
	D	S 23°01.163'	E014°51.594'	4/22/13		314.9	11.8	14.1	47.7	16.5	10
5	A	S 23°02.074'	E014°57.022'	4/22/13	12:25	415.5	16.3	18.7	50.5	6.5	8
	B	S 23°02.116'	E014°57.004'	4/22/13		415.6	22.0	25.5	45.0	3.5	4
	C	S 23°02.173'	E014°56.977'	4/22/13		416	21.9	22.6	45.4	4.1	6
	D	S 23°02.217'	E014°56.961'	4/22/13		415.7	20.4	25.3	48.3	2.0	4
6	A	S 23°03.909'	E015°02.413'	4/22/13	13:45	529.3	19.1	13.6	51.3	8.0	8
	B	S 23°03.953'	E015°02.386'	4/22/13		528.4	21.1	15.6	43.9	15.4	4
	C	S 23°04.010'	E015°02.364'	4/22/13		527.3	24.7	15.1	47.8	6.4	6
	D	S 23°04.033'	E015°02.364'	4/22/13		527.3	29.9	17.8	42.8	5.5	4
7	A	S 23°05.932'	E015°07.704'	4/22/13	14:10	568.2	7.4	12.0	71.6	3.0	6
	B	S 23°05.973'	E015°07.679'	4/22/13		568	9.3	13.5	65.9	7.4	4
	C	S 23°06.028'	E015°07.649'	4/22/13		568.3	6.3	11.2	68.6	5.9	8
	D	S 23°06.070'	E015°07.636'	4/22/13		567.6	9.8	15.1	66.0	5.0	4
8	A	S 23°08.553'	E015°12.578'	4/22/13	14:35	613.2	10.0	13.6	64.3	8.1	4
	B	S 23°08.569'	E015°12.529'	4/22/13		613.2	13.9	16.7	60.3	5.1	4
	C	S 23°08.596'	E015°12.473'	4/22/13		610.9	7.5	12.3	68.5	7.7	4
	D	S 23°08.617'	E015°12.432'	4/22/13		609.5	11.2	14.5	64.8	5.6	4
9	A	S 23°11.719'	E015°16.930'	4/22/13	15:10	683.6	12.4	22.5	56.3	4.8	4
	B	S 23°11.751'	E015°16.897'	4/22/13		683.9	7.4	14.6	66.8	7.1	4
	C	S 23°11.796'	E015°16.856'	4/22/13		683.1	5.7	12.7	67.9	9.7	4
	D	S 23°11.841'	E015°16.843'	4/22/13		682.8	5.5	10.7	65.1	14.7	4
10	A	S 23°14.713'	E015°21.663'	4/22/13	15:36	748.9	11.5	11.8	50.7	18.0	8
	B	S 23°14.752'	E015°21.635'	4/22/13		747.4	15.2	9.5	45.2	22.1	8
	C	S 23°14.807'	E015°21.605'	4/22/13		747.3	11.8	12.0	49.0	21.3	6
	D	S 23°14.852'	E015°21.598'	4/22/13		746.8	11.8	13.7	54.3	14.2	6

Coarse sand = coarse sand content, Med. sand =medium sand content, Fine sand = fine sand content, Silt = silt content, and Clay = clay content

Appendix A(ii): Sampling information and soil structure for sites **11 to 20**.

Site	Rep	GPS coordinates		Date Sampled	Time	Elevation (SRTM; m)	Coarse Sand (<2mm; %)	Med. Sand (<500um; %)	Fine Sand (<250um; %)	Slit (<53um; %)	Clay (%)
11	A	S 23°17.424'	E015°26.586'	4/22/13	16:03	831.1	4.3	14.3	50.9	22.6	8
	B	S 23°17.468'	E015°26.568'	4/22/13		829.5	8.7	26.1	49.9	11.3	4
	C	S 23°17.515'	E015°26.528'	4/22/13		827.3	10.0	19.4	54.8	11.8	4
	D	S 23°17.560'	E015°26.520'	4/22/13		826.2	9.8	14.8	56.7	14.7	4
12	A	S 23°18.584'	E015°32.032'	4/22/13	16:30	935.5	9.1	6.1	50.1	26.7	8
	B	S 23°18.633'	E015°32.032'	4/22/13		934.5	8.7	8.4	60.1	16.8	6
	C	S 23°18.739'	E015°32.028'	4/22/13		934.3	18.6	7.6	65.7	4.1	4
	D	S 23°18.584'	E015°32.034'	4/22/13		935.4	21.6	7.9	56.6	9.9	4
13	A	S 23°19.189'	E015°37.433'	4/23/13	9:15	931.2	15.1	8.1	47.1	19.7	10
	B	S 23°19.223'	E015°37.402'	4/23/13		931.9	8.0	5.8	62.2	18.0	6
	C	S 23°19.284'	E015°37.365'	4/23/13		930.6	14.1	5.8	59.6	14.5	6
	D	S 23°19.334'	E015°37.358'	4/23/13		929.3	11.7	7.9	57.4	17.0	6
14	A	S 23°19.442'	E015°42.844'	4/23/13	10:00	879.1	22.5	11.3	48.9	11.3	6
	B	S 23°19.467'	E015°42.846'	4/23/13		880.2	24.0	9.6	49.3	13.1	4
	C	S 23°19.553'	E015°42.866'	4/23/13		885	8.4	13.5	57.7	16.4	4
	D	S 23°19.604'	E015°42.856'	4/23/13		886.1	10.2	13.8	62.2	9.8	4
15	A	S 23°18.123'	E015°47.429'	4/23/13	10:30	879.3	20.6	10.4	54.5	10.4	4
	B	S 23°18.129'	E015°47.425'	4/23/13		880.6	11.4	9.6	63.5	11.5	4
	C	S 23°18.161'	E015°47.436'	4/23/13		882.4	14.1	9.2	55.2	15.5	6
	D	S 23°18.175'	E015°47.436'	4/23/13		881.6	9.8	9.0	58.2	19.0	4
16	A	S 23°19.221'	E015°51.808'	4/23/13	11:00	959.4	12.2	5.2	43.6	33.0	6
	B	S 23°19.225'	E015°51.760'	4/23/13		956.7	10.6	8.4	51.4	25.6	4
	C	S 23°19.239'	E015°51.702'	4/23/13		954.9	15.7	11.4	47.1	21.8	4
	D	S 23°19.245'	E015°51.655'	4/23/13		953.3	25.9	12.3	40.1	17.7	4
17	A	S 23°20.596'	E015°55.160'	4/23/13	11:35	1022.9	8.7	7.5	61.7	18.1	4
	B	S 23°20.646'	E015°55.160'	4/23/13		1022.6	12.3	17.0	59.8	6.9	4
	C	S 23°20.699'	E015°55.177'	4/23/13		1022.7	11.0	14.3	67.4	3.3	4
	D	S 23°20.741'	E015°55.190'	4/23/13		1025.6	5.6	14.4	72.8	3.2	4
18	A	S 23°20.678'	E016°00.585'	4/23/13	12:00	1084	6.0	13.3	53.8	21.0	6
	B	S 23°20.715'	E016°00.610'	4/23/13		1084.5	6.4	20.3	50.2	17.0	6
	C	S 23°20.754'	E016°00.052'	4/23/13		1074.3	7.4	41.0	47.2	0.4	4
	D	S 23°20.780'	E016°00.691'	4/23/13		1082.9	8.0	40.2	47.5	0.3	4
19	A	S 23°17.785'	E016°04.361'	4/23/13	13:00	1077.2	5.9	9.0	62.0	17.2	6
	B	S 23°17.822'	E016°04.371'	4/23/13		1077.6	5.5	11.2	61.2	16.1	6
	C	S 23°17.871'	E016°04.404'	4/23/13		1078.8	5.3	8.7	56.0	22.1	8
	D	S 23°17.907'	E016°04.441'	4/23/13		1080.2	9.0	12.4	61.9	10.7	6
20	A	S 23°14.683'	E016°08.562'	4/23/13	13:35	1253.4	13.1	9.6	50.8	18.5	8
	B	S 23°14.715'	E016°08.600'	4/23/13		1251.1	4.5	12.4	63.7	13.4	6
	C	S 23°14.750'	E016°08.678'	4/23/13		1249	14.6	13.7	51.4	14.3	6
	D	S 23°14.783'	E016°08.674'	4/23/13		1247.3	6.3	11.7	61.3	14.7	6

Coarse sand = coarse sand content, Med. sand =medium sand content, Fine sand = fine sand content, Silt = silt content, and Clay = clay content

Appendix A(iii): Soil chemical parameters for sites **1 to 10**.

Site	Rep	pH	CEC ($cmol(+)\cdot kg^{-1}$)	Org. Matter (%OM)	C (%)	P ($mg\cdot kg^{-1}$)	NH_4^+ ($mg\cdot kg^{-1}$)	NO_3^- ($mg\cdot kg^{-1}$)	Na^+ ($mg\cdot kg^{-1}$)	Ca^+ ($mg\cdot kg^{-1}$)	S ($mg\cdot kg^{-1}$)	K^+ ($mg\cdot kg^{-1}$)	Mg^+ ($mg\cdot kg^{-1}$)
1	A	6.68	5.41	0.5384	0.153	20.25	8.38	42.66	5848.56	28016.03	19887.78	429.31	413.07
	B	6.73	4.96	0.3231	0.352	10.19	14.58	29.83	15710.02	19980.08	14581.67	508.02	427.03
	C	6.73	5.14	0.4019	0.232	9.55	9.24	60.00	12348.08	12599.21	7448.41	567.71	499.64
	D	6.66	5.02	0.4149	0.277	9.4	13.01	83.79	11523.91	13507.01	7196.39	586.43	498.64
2	A	7.35	5.97	0.3970	0.075	22.2	6.59	7.07	462.85	22828.69	14264.94	314.14	72.37
	B	6.73	6.06	0.4919	0.065	14.8	3.80	7.29	847.00	28220.00	16824.00	334.30	112.60
	C	7.4	6.05	0.4667	0.069	16.36	6.09	17.36	4179.28	26474.10	16179.28	348.11	166.63
	D	6.8	5.51	0.2931	0.037	17.19	4.44	4.74	371.81	28466.14	17139.44	202.39	57.67
3	A	7.22	6.89	0.4809	0.267	10.49	4.59	21.61	2588.82	27944.11	16538.92	410.78	239.82
	B	7.14	7.91	0.5581	0.188	1.1	3.88	5.27	536.20	25640.00	15532.00	434.40	104.80
	C	7.1	6.29	0.6697	0.168	11.39	3.04	13.13	831.18	28167.33	16840.64	280.58	260.06
	D	7.31	5.33	0.3994	0.210	18.78	4.05	3.53	285.36	27928.29	16832.67	204.28	57.56
4	A	7.49	7.55	0.5034	0.087	10.83	4.16	-	874.35	22885.77	13565.13	341.98	295.29
	B	7.03	6.71	0.3600	0.076	7.64	2.89	48.00	388.57	25566.60	15493.04	249.01	79.07
	C	7.37	6.62	0.3424	0.069	6.87	3.19	8.97	601.20	27960.00	16678.00	385.40	81.54
	D	7.07	7.91	0.4650	0.032	1.45	2.14	28.85	623.20	25880.00	15346.00	380.70	219.30
5	A	7.04	4.59	0.0873	0.107	9.44	3.42	25.95	6250.00	6210.00	2158.00	487.50	180.70
	B	7.12	4.67	0.1407	0.011	12.31	2.26	0.43	43.26	11950.10	7574.85	85.05	31.72
	C	6.76	4.13	0.1425	0.072	10.48	2.98	0.79	41.49	14042.00	8718.00	96.27	33.77
	D	6.72	5.43	0.1129	0.008	7.08	3.76	0.31	22.19	7133.73	4097.80	58.78	24.15
6	A	7.1	5.39	0.2481	0.022	9.34	3.06	1.44	123.26	7487.08	3029.82	220.87	47.36
	B	6.86	5.15	0.4898	0.155	8.98	5.38	16.01	408.48	28582.83	16908.18	217.56	67.10
	C	6.92	4.13	0.2280	0.021	15.16	4.29	2.01	43.43	19244.00	12474.00	120.30	24.76
	D	6.84	3.95	0.1395	0.007	9.36	4.99	0.74	29.83	21055.78	13404.38	95.73	22.94
7	A	9.59	3.54	0.2297	0.021	13.43	3.84	0.31	20.21	2722.55	83.77	76.54	28.55
	B	6.86	4.15	0.1993	0.047	10.94	4.38	0.31	22.30	5226.00	2170.00	80.19	23.75
	C	6.88	4.42	0.2441	0.035	16.01	3.94	0.31	28.08	9532.93	5582.83	101.70	22.92
	D	6.94	4.10	0.1900	0.019	11.32	3.85	0.31	22.08	1457.09	1665.27	64.62	19.55
8	A	7.14	3.50	0.4675	0.097	5.47	3.46	15.40	1648.80	2762.00	102.70	256.10	175.50
	B	6.9	3.59	0.1588	0.105	10.14	3.68	0.26	43.93	5623.51	2515.94	95.83	27.42
	C	6.81	4.27	0.2420	0.060	12.34	2.79	0.00	28.48	7308.76	3517.93	91.21	26.78
	D	7.26	3.74	0.1543	0.055	11.84	3.37	0.39	27.65	2351.30	451.20	77.38	30.76
9	A	7.61	4.14	0.1725	0.030	15.03	3.79	1.57	20.77	2776.00	39.30	74.67	38.86
	B	9.44	5.44	0.3251	0.113	6.66	3.44	1.39	26.10	1636.27	85.21	119.04	45.59
	C	7.28	4.81	0.3403	0.080	9.29	3.19	1.09	35.57	1707.17	125.40	152.59	61.37
	D	6.86	6.22	0.4244	0.078	11.28	3.74	1.26	41.70	1934.00	314.00	173.80	51.32
10	A	7.73	7.28	0.7205	0.239	6.74	3.68	0.66	16.51	4435.13	7.61	260.53	89.89
	B	7.54	7.98	0.7726	0.318	2.64	3.81	0.96	18.15	4538.00	14.37	242.26	72.61
	C	9.5	7.67	0.5950	0.314	5.84	3.02	2.10	17.05	4402.39	7.53	229.34	71.35
	D	7.42	7.43	0.6190	0.267	7.56	3.46	0.57	26.83	4334.00	14.20	199.26	70.21

pH = soil pH, CEC = cation exchange capacity, Org. matter = organic matter content, C = carbon, P. = phosphorus, NH_4^+ = ammonium, NO_3^- = nitrate, Na^+ = sodium, Ca^+ = calcium, S = sulfur, K^+ = potassium, and Mg^+ = magnesium

Appendix A(iv): Soil chemical parameters for sites **11 to 20**.

Site	Rep	pH	CEC ($cmol(+)\cdot kg^{-1}$)	Org. Matter (%OM)	C (%)	P ($mg\cdot kg^{-1}$)	NH_4^+ ($mg\cdot kg^{-1}$)	NO_3^- ($mg\cdot kg^{-1}$)	Na^+ ($mg\cdot kg^{-1}$)	Ca^+ ($mg\cdot kg^{-1}$)	S ($mg\cdot kg^{-1}$)	K^+ ($mg\cdot kg^{-1}$)	Mg^+ ($mg\cdot kg^{-1}$)
11	A	7.57	7.68	0.6996	0.162	17.55	5.03	1.62	31.69	1123.25	43.04	337.58	106.71
	B	7.3	5.32	0.5332	0.089	6.13	3.98	0.88	28.22	1808.15	79.64	128.03	69.84
	C	7.52	6.07	0.4261	0.081	8.38	3.85	2.01	26.79	1634.00	90.31	170.60	74.75
	D	7.6	5.76	0.4943	0.028	13.05	5.29	0.96	24.77	2067.00	37.83	202.10	81.63
12	A	9.29	8.83	0.8246	0.243	3.43	7.82	2.40	74.97	1069.86	38.76	473.55	94.75
	B	7.38	6.39	0.8091	0.282	7.18	3.84	1.00	22.24	1232.60	77.26	185.59	66.74
	C	7.37	5.74	0.5270	0.071	1.32	4.60	1.18	23.00	1499.00	108.00	131.30	55.50
	D	7.44	6.20	0.8809	0.257	0.16	3.41	1.35	26.84	1362.73	64.03	186.17	66.62
13	A	6.56	6.84	0.8835	0.248	7.56	4.03	3.33	46.10	1061.00	55.80	413.60	109.20
	B	7.4	8.24	0.7963	0.183	9.93	5.66	1.39	25.37	1233.07	34.05	198.31	93.22
	C	8.61	6.77	0.6757	0.203	9.57	3.85	2.06	28.22	1452.00	36.34	225.10	95.80
	D	7.19	7.03	0.9800	0.337	13.9	4.59	6.26	41.59	1488.05	54.95	301.00	108.47
14	A	7.38	7.15	1.0918	0.350	3.87	5.95	6.83	30.15	1712.15	40.84	253.88	157.67
	B	7.25	5.71	1.1207	0.458	11.45	7.26	6.91	108.50	1800.00	101.10	214.30	177.00
	C	7.96	5.19	0.9616	0.349	10.84	3.88	1.92	28.95	1845.69	33.88	209.52	143.09
	D	7.54	4.57	0.7340	0.252	9.67	3.80	1.05	28.14	1936.00	25.20	183.00	143.60
15	A	9.08	3.99	0.5665	0.120	10.26	3.72	1.31	19.69	1993.00	27.26	112.50	104.30
	B	7.92	5.32	0.6692	0.222	12.49	4.33	2.23	20.27	2059.88	30.31	133.13	112.18
	C	7.6	6.54	0.8647	0.445	14.36	5.68	3.10	27.70	1954.18	40.47	179.58	121.12
	D	7.34	6.62	0.8330	0.277	19.4	3.45	1.92	20.18	2198.00	24.17	150.10	119.90
16	A	7.12	8.98	1.4525	0.593	16.54	5.78	2.71	23.37	2779.56	6.72	175.65	131.66
	B	5.62	7.60	1.1991	0.486	8.7	4.46	0.92	22.87	1447.90	18.42	147.19	177.86
	C	8.64	7.82	1.2382	0.459	3.89	6.40	3.33	21.72	1412.35	25.98	151.99	276.10
	D	9.47	6.74	1.1481	0.483	11.4	6.40	3.95	27.65	2169.32	27.32	133.17	212.95
17	A	8.72	7.65	1.4361	0.567	29.36	9.64	4.65	20.20	1653.69	7.94	198.00	101.10
	B	7.59	6.78	0.9828	0.238	11.59	7.07	3.25	22.87	2476.00	11.53	185.10	87.99
	C	7.45	5.70	0.6560	0.270	8.49	5.48	4.78	27.38	2413.35	14.59	162.05	67.10
	D	7.82	6.32	0.5205	0.141	8.48	4.42	2.32	22.71	2380.76	11.09	160.32	72.46
18	A	7.13	6.09	1.0175	0.381	61.09	5.08	2.10	18.95	908.98	2.94	104.89	68.31
	B	8.85	6.87	0.6069	0.165	28.14	3.38	1.75	19.28	1139.72	1.22	88.27	50.31
	C	9.2	3.92	0.2395	0.138	11.85	3.15	3.15	16.63	555.89	1.66	36.91	19.89
	D	8.63	3.49	0.3048	0.023	8.94	5.99	3.24	20.43	377.25	3.98	51.29	26.36
19	A	8.88	7.74	1.7003	1.376	32.9	3.64	3.99	16.50	1434.00	7.29	126.80	78.24
	B	8.49	6.12	1.0874	0.440	35.49	2.66	1.26	15.07	840.76	0.72	90.02	45.86
	C	9.01	6.00	0.8721	0.167	30.94	2.48	2.00	11.52	1434.87	1.59	75.88	50.80
	D	8.6	7.17	0.9072	0.322	19.41	2.63	1.10	15.47	1566.00	1.15	65.93	45.03
20	A	7.3	10.59	2.8912	1.137	25.04	3.89	7.04	3.11	2162.00	0.00	341.56	141.24
	B	7.75	6.93	1.0943	0.356	6.47	2.94	2.02	2.65	3836.33	0.00	102.75	49.13
	C	7.12	7.19	1.7152	0.738	21.14	3.84	4.58	1.83	1234.00	0.26	180.56	79.76
	D	7.64	8.21	1.4592	0.612	40.74	4.35	3.96	2.68	1710.58	0.00	145.26	62.11

pH = soil pH, CEC = cation exchange capacity, Org. matter = organic matter content, C = carbon, P. = phosphorus, NH_4^+ = ammonium, NO_3^- = nitrate, Na^+ = sodium, Ca^+ = calcium, S = sulfur, K^+ = potassium, and Mg^+ = magnesium

Appendix A(v): Soil enzyme assay results for sites **1 to 10**.

Site	Rep	FDA		BG		AP		NAG		LAP		PO	
		µmol/(h·gDS)	µmol/(h·gOM)	µmol/(h·gDS)	µmol/(h·gOM)	µmol/(h·gDS)	µmol/(h·gOM)	µmol/(h·gDS)	µmol/(h·gOM)	µmol/(h·gDS)	µmol/(h·gOM)	µmol/(h·gDS)	µmol/(h·gOM)
1	A	0.148	4.528	1.267	237.249	0.364	68.112	0.455	85.182	1.008	188.754	6.403	1198.671
	B	0.008	0.372	0.234	72.909	0.567	176.737	0.554	172.692	0.000	0.000	2.385	743.258
	C	0.060	3.757	1.458	364.223	2.764	690.684	2.667	666.315	4.673	1167.653	5.867	1466.163
	D	0.070	4.674	1.092	265.845	0.683	166.173	0.488	118.855	0.251	61.195	15.338	3734.492
2	A	0.973	42.196	0.480	120.128	0.415	103.838	0.262	65.644	1.591	398.052	10.129	2534.589
	B	0.071	1.834	0.000	0.000	0.353	72.388	0.107	21.925	0.069	14.050	3.444	705.432
	C	0.302	8.889	0.930	200.742	1.935	417.867	1.952	421.401	5.850	1263.040	12.153	2623.967
	D	0.661	15.338	0.161	54.827	0.199	67.726	0.178	60.511	0.096	32.750	3.194	1087.494
3	A	0.446	10.532	1.062	220.932	1.369	284.738	1.388	288.685	2.644	549.765	13.162	2737.170
	B	1.225	42.189	0.334	60.328	2.305	416.693	1.819	328.824	2.707	489.304	6.426	1161.484
	C	2.216	22.769	1.926	289.348	4.055	609.335	2.961	444.841	5.284	793.945	18.643	2801.217
	D	1.867	26.031	0.087	21.768	0.356	89.207	1.342	336.621	0.271	67.959	4.314	1082.347
4	A	0.607	28.099	0.192	38.532	1.139	228.433	0.541	108.477	0.196	39.329	5.391	1081.052
	B	1.061	40.957	0.368	101.897	0.217	60.200	0.000	0.000	0.676	187.449	1.477	409.384
	C	0.586	21.518	0.000	0.000	1.164	343.134	1.915	564.634	3.475	1024.497	7.481	2205.243
	D	0.551	21.942	0.803	173.676	1.824	394.454	2.025	437.965	10.221	2210.536	12.101	2617.069
5	A	0.188	2.212	0.522	182.912	0.453	158.834	0.197	69.060	0.000	0.000	2.766	969.675
	B	0.645	65.018	0.262	187.405	0.323	230.551	0.556	397.425	0.757	540.530	4.910	3507.460
	C	0.542	47.283	0.404	284.701	1.158	815.314	0.404	284.459	1.150	809.148	0.000	0.000
	D	0.568	98.258	1.623	1387.727	0.064	54.295	0.264	226.037	0.599	512.528	0.410	350.518
6	A	1.096	150.044	0.709	286.813	1.253	506.414	1.716	693.555	1.947	787.077	4.518	1826.387
	B	1.829	36.095	0.381	77.577	0.000	0.000	0.000	0.000	0.306	62.211	0.558	113.479
	C	2.032	130.854	1.031	453.236	0.286	125.554	0.388	170.418	1.279	562.043	1.682	739.266
	D	0.044	3.033	0.146	105.120	0.247	178.031	0.000	0.000	0.046	32.805	0.685	493.439
7	A	1.131	295.951	1.802	786.476	0.159	69.562	0.707	308.439	0.000	0.000	2.918	1273.203
	B	2.936	475.988	0.000	0.000	0.000	0.000	0.236	118.607	0.999	502.849	4.299	2163.774
	C	6.020	568.656	1.443	596.623	0.857	354.181	0.273	112.651	3.289	1359.306	1.227	506.988
	D	3.073	631.723	0.938	492.667	0.000	0.000	0.389	204.321	1.118	587.491	0.320	168.272
8	A	0.907	144.311	0.192	41.517	0.340	73.444	0.000	0.000	1.665	359.830	0.000	0.000
	B	2.280	443.012	1.812	1144.582	1.411	891.062	0.313	197.386	1.765	1114.685	2.085	1316.460
	C	2.635	380.998	0.000	0.000	0.074	30.708	0.134	55.605	0.110	45.487	0.767	317.956
	D	3.511	1163.828	1.981	1288.596	0.198	129.069	1.259	818.629	4.758	3094.066	5.051	3284.533
9	A	4.675	1579.655	0.000	0.000	0.000	0.000	0.575	333.885	0.487	282.672	1.922	1116.232
	B	10.720	1845.445	1.282	395.640	0.115	35.455	0.000	0.000	0.000	0.000	0.875	270.159
	C	8.281	1451.567	2.137	629.567	0.076	22.405	0.132	38.772	1.199	353.298	1.785	525.959
	D	1.854	252.206	1.167	275.823	1.183	279.631	2.385	563.964	4.278	1011.482	10.369	2451.567
10	A	15.198	1211.824	1.373	191.726	2.269	316.925	0.553	77.235	1.072	149.735	4.018	561.189
	B	15.429	1190.700	0.302	39.393	0.000	0.000	1.266	165.103	3.674	479.261	9.379	1223.337
	C	15.768	1394.199	0.637	107.809	0.218	36.889	0.000	0.000	1.055	178.469	0.000	0.000
	D	11.414	1095.957	1.414	229.761	1.447	235.119	0.518	84.176	2.101	341.234	12.402	2014.654

FDA = fluorescein diacetate hydrolysis, BG = ß-glucosidase, AP = alkaline phosphatase, NAG = ß-N-acetylglucosaminidase, LAP = leucine aminopeptidase, and PO = phenol oxidase

Appendix A(vi): Soil enzyme assay results for sites **11 to 20**.

Site	Rep	FDA		BG		AP		NAG		LAP		PO	
		µmol/(h·gDS)	µmol/(h·gOM)	µmol/(h·gDS)	µmol/(h·gOM)	µmol/(h·gDS)	µmol/(h·gOM)	µmol/(h·gDS)	µmol/(h·gOM)	µmol/(h·gDS)	µmol/(h·gOM)	µmol/(h·gDS)	µmol/(h·gOM)
11	A	18.812	1591.482	2.239	321.413	4.279	614.228	1.893	271.732	3.276	470.287	21.077	3025.382
	B	12.671	1627.007	3.119	587.003	1.809	340.442	0.040	7.482	2.553	480.499	3.300	620.969
	C	1.745	233.365	0.916	215.650	1.925	453.225	0.208	48.923	3.556	837.456	0.254	59.724
	D	7.738	890.946	1.408	285.621	0.501	101.674	0.000	0.000	2.000	405.663	5.269	1068.788
12	A	31.014	2363.282	3.639	442.540	1.328	161.541	0.000	0.000	7.744	941.796	5.904	718.017
	B	21.822	1722.732	4.456	552.263	2.870	355.671	0.580	71.848	7.386	915.406	7.130	883.594
	C	4.408	452.429	0.470	89.390	0.224	42.709	0.304	57.874	1.654	314.783	0.625	118.928
	D	9.021	621.226	2.091	237.730	2.264	257.324	0.000	0.000	3.315	376.856	13.167	1496.865
13	A	21.700	1484.191	5.422	615.266	3.690	418.736	2.979	338.044	11.878	1347.839	25.317	2872.862
	B	19.077	1452.667	4.332	544.453	1.305	164.045	0.170	21.424	4.884	613.936	4.716	592.806
	C	17.939	1743.889	4.796	710.040	5.539	819.979	2.437	360.806	6.477	958.945	9.697	1435.636
	D	20.175	1400.097	5.782	591.146	1.533	156.753	2.203	225.215	3.371	344.630	0.383	39.157
14	A	10.909	640.209	1.063	97.289	0.000	0.000	0.000	0.000	0.081	7.396	0.995	91.086
	B	14.441	932.500	3.835	341.783	2.390	213.052	2.733	243.563	6.705	597.590	8.506	758.143
	C	3.629	253.319	3.116	323.625	1.005	104.393	0.790	82.002	5.789	601.286	9.603	997.409
	D	11.244	1017.401	1.634	222.702	0.714	97.376	0.050	6.795	2.644	360.327	3.709	505.587
15	A	3.475	458.646	0.699	123.592	0.572	101.097	0.000	0.000	2.505	442.865	8.043	1421.752
	B	12.164	1423.002	4.672	698.535	0.833	124.592	1.718	256.874	3.589	536.561	4.890	730.987
	C	18.893	1669.817	6.386	739.168	2.259	261.503	1.474	170.620	7.420	858.842	3.902	451.608
	D	3.939	355.032	0.756	91.017	0.508	61.138	0.246	29.606	1.804	217.229	6.603	795.180
16	A	27.979	1456.484	2.078	142.967	4.936	339.540	1.988	136.782	6.824	469.452	1.823	125.400
	B	3.800	221.497	3.446	287.261	2.284	190.389	2.614	217.926	3.015	251.285	2.236	186.366
	C	16.176	880.574	1.756	141.822	4.554	367.810	0.781	63.111	6.714	542.242	1.860	150.231
	D	13.632	863.131	2.532	220.033	1.833	159.248	0.699	60.771	5.028	436.924	1.730	150.340
17	A	21.546	1235.600	3.220	223.755	6.670	463.458	1.792	124.519	5.979	415.436	2.187	151.988
	B	11.820	990.298	5.790	587.369	4.167	422.705	3.780	383.453	8.327	844.814	9.657	979.746
	C	10.200	1116.481	4.694	714.220	2.806	427.001	3.433	522.300	4.259	647.945	10.818	1645.872
	D	11.215	1452.381	1.678	321.786	2.197	421.399	0.648	124.266	2.974	570.270	5.416	1038.717
18	A	20.700	1702.918	3.073	301.467	10.208	1001.441	1.278	125.329	5.711	560.308	27.483	2696.176
	B	4.115	525.685	2.817	463.853	4.916	809.399	1.073	176.677	8.153	1342.327	5.915	973.887
	C	2.066	684.733	0.082	34.261	0.781	326.004	0.028	11.727	2.081	868.918	0.000	0.000
	D	4.210	1223.784	1.318	431.800	0.463	151.674	0.218	71.514	1.044	342.062	3.841	1258.505
19	A	23.816	1225.340	7.270	424.421	18.453	1077.330	2.508	146.426	13.015	759.809	13.973	815.743
	B	6.149	502.009	1.095	100.270	12.708	1164.176	1.474	135.052	5.040	461.729	21.408	1961.196
	C	4.009	381.762	0.702	80.438	4.844	554.982	0.126	14.471	3.545	406.174	17.133	1963.140
	D	14.461	1346.332	2.749	302.638	0.987	108.599	0.545	60.032	0.892	98.148	11.494	1265.283
20	A	33.486	1000.355	10.631	363.390	7.450	254.643	2.839	97.055	11.689	399.555	16.327	558.068
	B	16.739	1254.253	1.847	168.249	0.670	61.052	0.035	3.183	3.962	360.779	15.303	1393.651
	C	6.226	313.854	9.341	540.875	7.773	450.116	2.123	122.950	13.182	763.291	8.807	509.958
	D	6.249	339.207	6.571	449.731	5.420	370.934	2.470	169.065	8.098	554.233	7.652	523.724

FDA = fluorescein diacetate hydrolysis, BG = ß-glucosidase, AP = alkaline phosphatase, NAG = ß-N-acetylglucosaminidase, LAP = leucine aminopeptidase, and PO = phenol oxidase

Appendix B(i): Transect sites 1 to 4, and replicate sampling points (labeled A, B, C, and D).

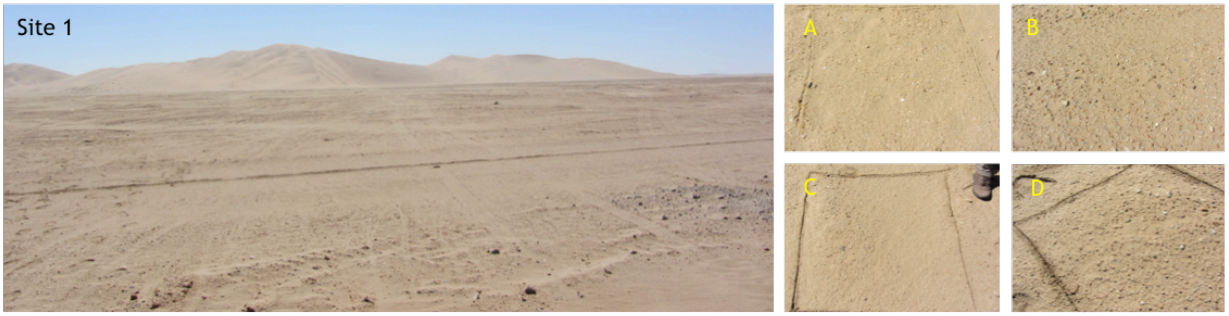

Appendix B(ii): Transect sites 5 to 8, and replicate sampling points (labeled A, B, C, and D).

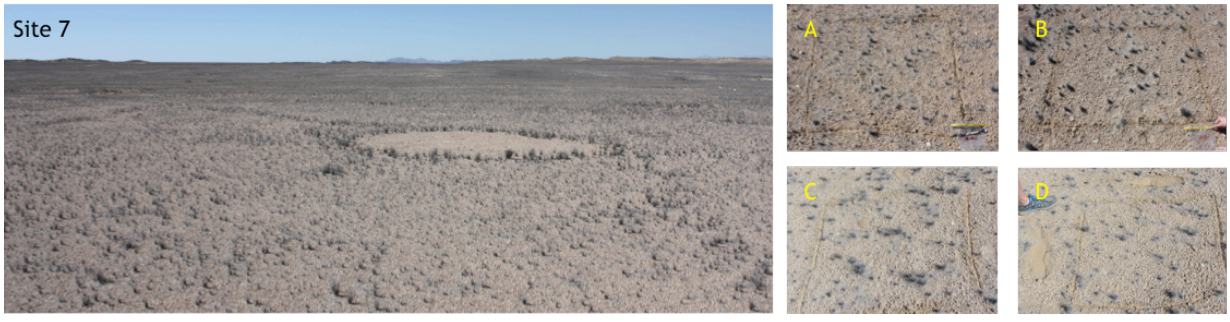

Appendix B(iii): Transect sites 9 to 12, and replicate sampling points (labeled A, B, C, and D).

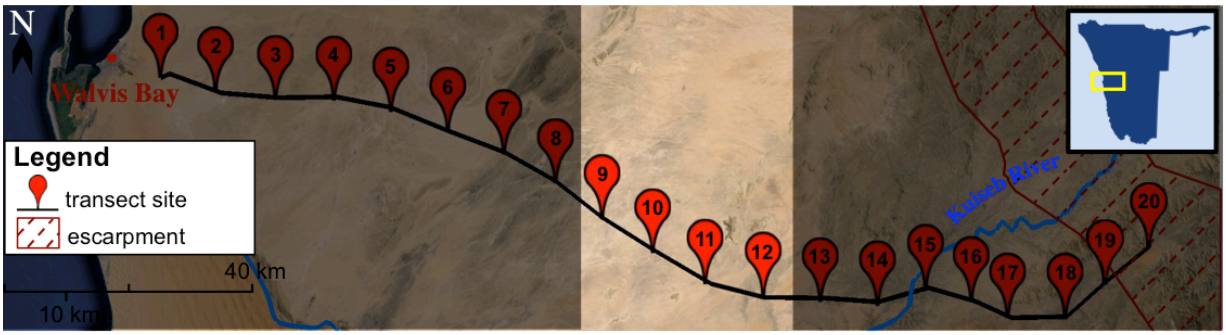

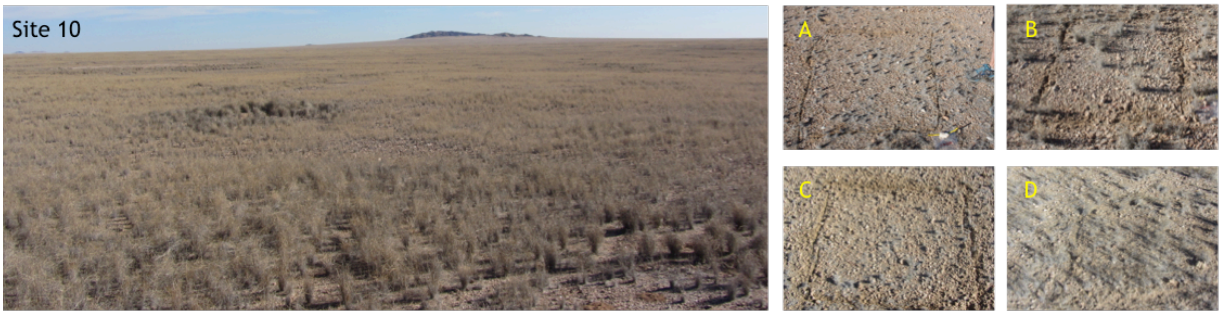

Appendix B(iv): Transect sites 13 to 16, and replicate sampling points (labeled A, B, C, and D).

Appendix B(v): Transect sites 17 to 20, and replicate sampling points (labeled A, B, C, and D).

Appendix C: Mean annual rainfall data (Lancaster and Seely, 1984; Eckardt *et al.*, 2013c)

	Rain gauge location site	GPS of rain gauge		GPS of transect site		Distance from rain gauge to transect Site	Data source	Years of data collection	Mean annual rainfall (mm)	Std. D
1	Pelican Point	S 22°58.953'	E 14°30.994'	S 22°58.784'	E 014°35.022'	6.8 km	Lancaster, 1984	18	15.2	na
2	Rooihank	S 23°10.986'	E 14°38.003'	S 23°00.037'	E 014°40.288'	20.5 km	Lancaster, 1984	12	16.7	na
3	Swartbank	S 23°19.980'	E 14°50.003'	S 23°00.903'	E 014°45.963'	36.2 km	Lancaster, 1984	8	18.8	na
4	Vogelfederberg	S 23°04.983'	E 14°59.997'	S 23°01.080'	E 014°51.571'	16.0 km	Lancaster, 1984	4	21.5	na
5	GW00RG	S 23°33.593'	E 15°02.483'	S 23°02.136'	E 014°56.990'	60.2 km	Eckardt et al., 2013	4	25.5	±45.8
6	GW01RG	S 23°33.678'	E 15°05.496'	S 23°03.980'	E 015°02.376'	54.9 km	Eckardt et al., 2013	4	40	±50
7	GW02RG	S 23°32.960'	E 15°08.124'	S 23°05.997'	E 015°07.662'	49.5 km	Eckardt et al., 2013	4	55.5	±42.4
8	GW05RG	S 23°30.014'	E 15°15.944'	S 23°08.577'	E 015°12.504'	39.8 km	Eckardt et al., 2013	4	59	±41.8
9	GW06RG	S 23°29.173'	E 15°18.550'	S 23°11.763'	E 015°16.878'	32 km	Eckardt et al., 2013	4	59.8	±34.9
10	GW07RG	S 23°28.149'	E 15°21.264'	S 23°14.777'	E 015°21.623'	26 km	Eckardt et al., 2013	4	62	±41.7
11	GW10RG	S 23°24.756'	E 15°28.933'	S 23°17.487'	E 015°26.549'	15.5 km	Eckardt et al., 2013	4	61.8	±63.8
12	GW13RG	S 23°18.668'	E 15°34.463'	S 23°18.659'	E 015°32.031'	4.3 km	Eckardt et al., 2013	4	78.8	±74.3
13	GW14RG	S 23°19.137'	E 15°37.167'	S 23°19.189'	E 015°37.433'	0.3 km	Eckardt et al., 2013	4	87.5	±67.4
14	GW17RG	S 23°18.451'	E 15°44.698'	S 23°19.521'	E 015°42.857'	3.7 km	Eckardt et al., 2013	4	100.5	±60
15	GW19RG	S 23°17.427'	E 15°49.514'	S 23°18.125'	E 015°47.427'	4.2 km	Eckardt et al., 2013	4	101.5	±60.6
16	GW21RG	S 23°21.182'	E 15°51.563'	S 23°19.225'	E 015°51.737'	3.4 km	Eckardt et al., 2013	4	133	±69.9
17	GW22RG	S 23°20.981'	E 15°54.181'	S 23°20.676'	E 015°55.165'	1.5 km	Eckardt et al., 2013	4	131.5	±77.3
18	GW25RG	S 23°19.905'	E 16°01.529'	S 23°20.729'	E 016°00.630'	2.3 km	Eckardt et al., 2013	4	169.3	±117.4
19	GW27RG	S 23°17.365'	E 16°06.212'	S 23°17.844'	E 016° 04.381'	3.3 km	Eckardt et al., 2013	4	165.3	±136.8
20	GW28RG	S 23°15.355'	E 16°08.034'	S 23°14.733'	E 016°08.617'	1.5 km	Eckardt et al., 2013	4	184.8	±80.9

Appendix D: Location of rain gauges in relation to transect sites.

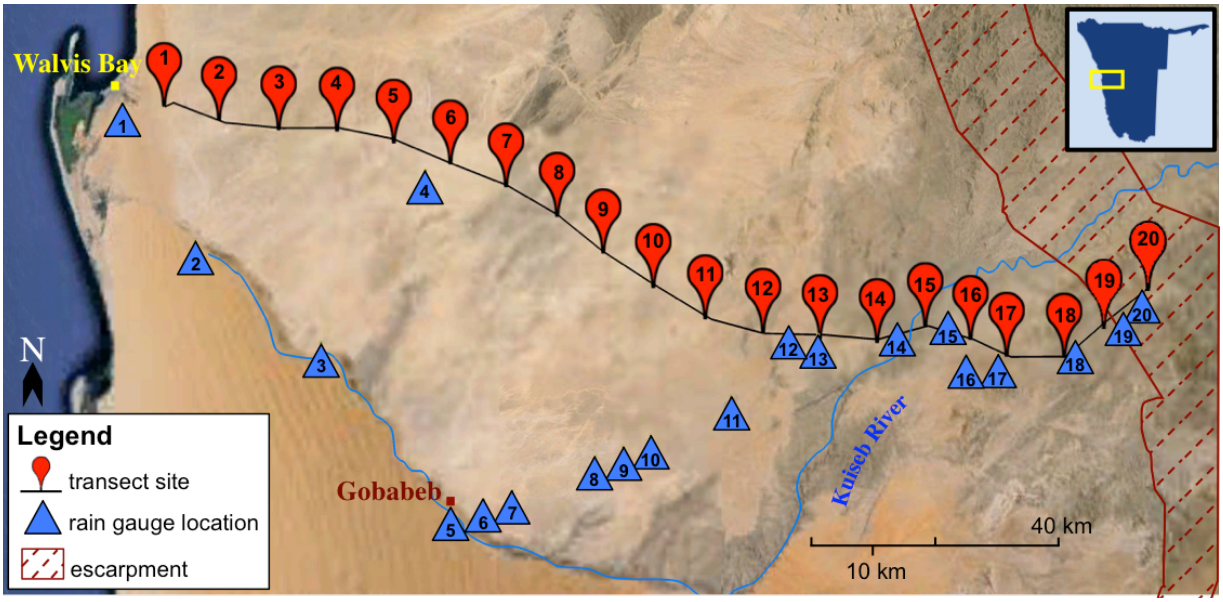

References

Abdo, Z., Schüette, U., Bent, S., Williams, C., Forney, L. and Joyce, P. (2006). "Statistical methods for characterizing diversity of microbial communities by analysis of terminal restriction fragment length polymorphisms of 16s rRNA genes." Environmental microbiology **8**(5): 929-938.

Acosta-Martínez, V., Cruz, L., Sotomayor-Ramirez, D. and Pérez-Alegría, L. (2007). "Enzyme activities as affected by soil properties and land use in a tropical watershed." Applied Soil Ecology **35**(1): 35-45.

Adriaenssens, E., Van Zyl, L., De Maayer, P., Rubagotti, E., Rybicki, E., Tuffin, M. and Cowan, D. (2014). "Metagenomic analysis of the viral community in Namib Desert hypoliths." Environmental microbiology.

Ahrens, C. D. (2011). Essentials of meteorology: An invitation to the atmosphere, Cengage Learning.

ALASA (2004). "Agrilasa soil handbook." Agri Laboratory Association of South Africa.

Allison, S. and Vitousek, P. (2004). "Extracellular enzyme activities and carbon chemistry as drivers of tropical plant litter decomposition." Biotropica **36**(3): 285-296.

Allison, S. and Vitousek, P. (2005). "Responses of extracellular enzymes to simple and complex nutrient inputs." Soil Biology and Biochemistry **37**(5): 937-944.

Allison, V., Condron, L., Peltzer, D., Richardson, S. and Turner, B. (2007). "Changes in enzyme activities and soil microbial community composition along carbon and nutrient gradients at the Franz Josef Chronosequence, New Zealand." Soil Biology and Biochemistry **39**(7): 1770-1781.

Alpert, P. (2005). "Sharing the secrets of life without water." Integrative and comparative biology **45**(5): 683-684.

Amann, R. I., Binder, B. J., Olson, R. J., Chisholm, S. W., Devereux, R. and Stahl, D. A. (1990). "Combination of 16s rRNA-targeted oligonucleotide probes with flow cytometry for analyzing mixed microbial populations." Applied and environmental microbiology **56**(6): 1919-1925.

An, S., Couteau, C., Luo, F., Neveu, J. and DuBow, M. (2013). "Bacterial diversity of surface sand samples from the Gobi and Taklamaken Deserts." Microbial ecology **66**(4): 850-860.

ASTM D (2007). "Standard test method for particle-size analysis of soils."

Aukerman, M. J., Schmidt, R. J., Burr, B. and Burr, F. A. (1991). "An arginine to lysine substitution in the bzip domain of an opaque-2 mutant in maize abolishes specific DNA binding." Genes & development **5**(2): 310-320.

Austin, A., Yahdjian, L., Stark, J., Belnap, J., Porporato, A., Norton, U., Ravetta, D. and Schaeffer, S. (2004). "Water pulses and biogeochemical cycles in arid and semiarid ecosystems." Oecologia **141**(2): 221-235.

Azua-Bustos, A., Urrejola, C. and Vicuña, R. (2012). "Life at the dry edge: Microorganisms of the Atacama Desert." FEBS letters **586**(18): 2939-2945.

Bahl, J., Lau, M., Smith, G., Vijaykrishna, D., Cary, S., Lacap, D., Lee, C., Papke, R., Warren-Rhodes, K., Wong, F., McKay, C. and Pointing, S. (2011). "Ancient origins determine global biogeography of hot and cold desert cyanobacteria." Nature communications **2**: 163.

Bakken, L. R. (1985). "Separation and purification of bacteria from soil." Applied and environmental microbiology **49**(6): 1482-1487.

Bell, C., Acosta-Martinez, V., McIntyre, N., Cox, S., Tissue, D. and Zak, J. (2009). "Linking microbial community structure and function to seasonal differences in soil moisture and temperature in a Chihuahuan Desert grassland." Microbial ecology **58**(4): 827-842.

Bell, C., Fricks, B., Rocca, J., Steinweg, J., McMahon, S. and Wallenstein, M. (2013). "High-throughput fluorometric measurement of potential soil extracellular enzyme activities." Journal of visualized experiments: JoVE(81).

Bell, C., Tissue, D., Loik, M., Wallenstein, M., Acosta‐Martinez, V., Erickson, R. and Zak, J. (2014). "Soil microbial and nutrient responses to 7 years of seasonally altered precipitation in a Chihuahuan Desert grassland." Global change biology **20**(5): 1657-1673.

Belnap, J. (2003). "The world at your feet: desert biological soil crusts." Frontiers in Ecology and the Environment **1**(4): 181-189.

Benison, K. and Karmanocky, F. (2014). "Could microorganisms be preserved in Mars gypsum? Insights from terrestrial examples." Geology **42**(7): 615-618.

Besemer, K., Peter, H., Logue, J., Langenheder, S., Lindström, E., Tranvik, L. and Battin, T. (2012). "Unraveling assembly of stream biofilm communities." The ISME journal **6**(8): 1459-1468.

Bierman, P. and Caffee, M. (2001). "Slow rates of rock surface erosion and sediment production across the Namib Desert and escarpment, southern Africa." American Journal of Science **301**(4-5): 326-358.

Billi, D., Friedmann, E. I., Hofer, K. G., Caiola, M. G. and Ocampo-Friedmann, R. (2000). "Ionizing-radiation resistance in the desiccation-tolerant cyanobacteriumchroococcidiopsis." Applied and environmental microbiology **66**(4): 1489-1492.

Black, C. A. and Dinauer, R. (1969). Methods of soil analysis, American Society of Agronomy Madison, Wisconsin.

Blackwood, C., Marsh, T., Kim, S.-H. and Paul, E. (2003). "Terminal restriction fragment length polymorphism data analysis for quantitative comparison of microbial communities." Applied and environmental microbiology **69**(2): 926-932.

Bluck, B., Ward, J., Cartwright, J. and Swart, R. (2007). "The Orange River, southern Africa: An extreme example of a wave-dominated sediment dispersal system in the south Atlantic Ocean." Journal of the Geological Society **164**(2): 341-351.

Boerner, R., Brinkman, J. and Smith, A. (2005). "Seasonal variations in enzyme activity and organic carbon in soil of a burned and unburned hardwood forest." Soil Biology and Biochemistry **37**(8): 1419-1426.

Borcard, D., Gillet, F. and Legendre, P. (2011). Numerical ecology with R, Springer Science & Business Media.

Bouyoucos, G. J. (1962). "Hydrometer method improved for making particle size analyses of soils." Agronomy Journal **54**(5): 464-465.

Bowman, R. and Vigil, M. (2002). "Soil testing for different phosphorus pools in cropland soils of the Great Plains." Journal of soil and water conservation **57**(6): 479-485.

Boyd, S. and Mortland, M. (1990). "Enzyme interactions with clays and clay-organic matter complexes." Soil biochemistry **6**: 1-28.

Bray, J. and Curtis, J. (1957). "An ordination of the upland forest communities of southern Wisconsin." Ecological monographs **27**(4): 325-349.

Bray, R. H. and Kurtz, L. (1945). "Determination of total, organic, and available forms of phosphorus in soils." Soil science **59**(1): 39-46.

Bruenken, W. (1996). Butter tree. South African Wild Flower Guide, The Botanical Society of South Africa.

Burke, A. (2004). "A preliminary account of patterns of endemism in Namibia's Sperrgebiet–the Succulent Karoo." Journal of biogeography **31**(10): 1613-1622.

Burns, R., DeForest, J., Marxsen, J., Sinsabaugh, R., Stromberger, M., Wallenstein, M., Weintraub, M. and Zoppini, A. (2013). "Soil enzymes in a changing environment: Current knowledge and future directions." Soil Biology and Biochemistry **58**: 216-234.

Burns, R. and Dick, R. (2002). Enzymes in the environment: activity, ecology, and applications, CRC Press.

Burrows, S., Elbert, W., Lawrence, M. and Pöschl, U. (2009). "Bacteria in the global atmosphere–part 1: Review and synthesis of literature data for different ecosystems." Atmospheric Chemistry and Physics **9**(23): 9263-9280.

Calderon, F., Jackson, L., Scow, K. and Rolston, D. (2001). "Short-term dynamics of nitrogen, microbial activity, and phospholipid fatty acids after tillage." Soil Science Society of America Journal **65**(1): 118-126.

Caruso, T., Chan, Y., Lacap, D., Lau, M., McKay, C. and Pointing, S. (2011). "Stochastic and deterministic processes interact in the assembly of desert microbial communities on a global scale." The ISME journal **5**(9): 1406-1413.

Cary, S., McDonald, I., Barrett, J. and Cowan, D. (2010). "On the rocks: The microbiology of Antarctic Dry Valley soils." Nature Reviews Microbiology **8**(2): 129-138.

Castillo-Monroy, A., Maestre, F., Delgado-Baquerizo, M. and Gallardo, A. (2010). "Biological soil crusts modulate nitrogen availability in semi-arid ecosystems: Insights from a mediterranean grassland." Plant and Soil **333**(1-2): 21-34.

Cavalli, F., Facchini, M., Decesari, S., Mircea, M., Emblico, L., Fuzzi, S., Ceburnis, D., Yoon, Y., O'Dowd, C. and Putaud, J. P. (2004). "Advances in characterization of size‐resolved organic matter in marine aerosol over the North Atlantic." Journal of Geophysical Research: Atmospheres (1984–2012) **109**(D24).

Chan, Y., Lacap, D., Lau, M., Ha, K., Warren‐Rhodes, K., Cockell, C., Cowan, D., McKay, C. and Pointing, S. (2012). "Hypolithic microbial communities: Between a rock and a hard place." Environmental microbiology **14**(9): 2272-2282.

Chanal, A., Chapon, V., Benzerara, K., Barakat, M., Christen, R., Achouak, W., Barras, F. and Heulin, T. (2006). "The desert of Tataouine: an extreme environment that hosts a wide diversity of microorganisms and radiotolerant bacteria." Environmental microbiology **8**(3): 514-525.

Chase, J. (2007). "Drought mediates the importance of stochastic community assembly." Proceedings of the National Academy of Sciences of the United States of America **104**(44): 17430-17434.

Chase, J. (2010). "Stochastic community assembly causes higher biodiversity in more productive environments." Science **328**(5984): 1388-1391.

Chase, J. and Myers, J. (2011). "Disentangling the importance of ecological niches from stochastic processes across scales." Philosophical transactions of the Royal Society B: Biological sciences **366**(1576): 2351-2363.

Chater, K. and Chandra, G. (2006). "The evolution of development in streptomyces analysed by genome comparisons." FEMS microbiology reviews **30**(5): 651-672.

Chivas, A., Andrews, A., Lyons, W., Bird, M. and Donnelly, T. (1991). "Isotopic constraints on the origin of salts in Australian playas. 1. Sulphur." Palaeogeography, Palaeoclimatology, Palaeoecology **84**(1): 309-332.

Clarke, K. and Ainsworth, M. (1993). "A method of linking multivariate community structure to environmental variables." Marine Ecology-Progress Series **92**: 205-205.

Clarke, K. and Warwick, R. (2001). "An approach to statistical analysis and interpretation." Change in Marine Communities **2**.

Cockell, C. S. and Stokes, M. D. (2004). "Ecology: Widespread colonization by polar hypoliths." Nature **431**(7007): 414-414.

Coleman, M. and Chisholm, S. (2010). "Ecosystem-specific selection pressures revealed through comparative population genomics." Proceedings of the National Academy of Sciences **107**(43): 18634-18639.

Collet, O. (2011). "How does the first water shell fold proteins so fast?" The Journal of chemical physics **134**(8): 085107.

Comte, J. and Del Giorgio, P. (2009). "Links between resources, C metabolism and the major components of bacterioplankton community structure across a range of freshwater ecosystems." Environmental microbiology **11**(7): 1704-1716.

Connon, S., Lester, E., Shafaat, H., Obenhuber, D. and Ponce, A. (2007). "Bacterial diversity in hyperarid Atacama Desert soils." Journal of Geophysical Research: Biogeosciences (2005–2012) **112**(G4).

Corbett, I. (1993). "The modern and ancient pattern of sandflow through the southern Namib deflation basin." Aeolian Sediments: Ancient and Modern: 45-60.

Corvalan, C., Hales, S. and McMichael, A. J. (2005). Ecosystems and human well-being: Health synthesis, World health organization.

Cottenie, K. (2005). "Integrating environmental and spatial processes in ecological community dynamics." Ecology letters **8**(11): 1175-1182.

Cowan, D. (2009). "Cryptic microbial communities in Antarctic deserts." Proceedings of the National Academy of Sciences of the United States of America **106**(47): 19749-19750.

Cowan, D., Pointing, S., Stevens, M., Craig, C., Stomeo, F. and Tuffin, I. (2010). "Distribution and abiotic influences on hypolithic microbial communities in an Antarctic dry valley." Polar Biology **34**(2): 307-311.

Cunha, A., Almeida, A., Coelho, F., Gomes, N., Oliveira, V. and Santos, A. (2010). "Bacterial extracellular enzymatic activity in globally changing aquatic ecosystems." Current research, technology and education topics in applied microbiology and microbial biotechnology. Badajoz, Spain: Formatex Research Center: 124-135.

Davila, A., Duport, L., Melchiorri, R., Jänchen, J., Valea, S., de los Rios, A., Fairén, A., Möhlmann, D., McKay, C. and Ascaso, C. (2010). "Hygroscopic salts and the potential for life on Mars." Astrobiology **10**(6): 617-628.

Didrik, J. (2014). Aerial of Zeila shipwreck on Skeleton Coast Namibia. Namibia Air Safari.

Directorate of Environmental Affairs (2002). "Atlas of Namibia project. Ministry of Environment and Tourism.". from http://www.uni-koeln.de/sfb389/e/e1/download/atlas_namibia/index_e.htm.

Dirks, P., Blenkinsop, T. G. and Jelsma, H. A. (2003). "The geological evolution of Africa." Encylopedia of life support systems. UNESCO Publishing, EOLSS Publishers Co Ltd. Oxford, UK. http://www. eolss. net.

Docherty, K., Young, K., Maurice, P. and Bridgham, S. (2006). "Dissolved organic matter concentration and quality influences upon structure and function of freshwater microbial communities." Microbial ecology **52**(3): 378-388.

Doelman, P. and Haanstra, L. (1989). "Short-and long-term effects of heavy metals on phosphatase activity in soils: An ecological dose-response model approach." Biology and Fertility of Soils **8**(3): 235-241.

Doran, J. and Zeiss, M. (2000). "Soil health and sustainability: Managing the biotic component of soil quality." Applied Soil Ecology **15**(1): 3-11.

Drees, K. P., Neilson, J. W., Betancourt, J. L., Quade, J., Henderson, D. A., Pryor, B. M. and Maier, R. M. (2006). "Bacterial community structure in the hyperarid core of the Atacama Desert, Chile." Applied and environmental microbiology **72**(12): 7902-7908.

Drenovsky, R., Vo, D., Graham, K. and Scow, K. (2004). "Soil water content and organic carbon availability are major determinants of soil microbial community composition." Microbial ecology **48**(3): 424-430.

Dumbrell, A., Nelson, M., Helgason, T., Dytham, C. and Fitter, A. (2010). "Relative roles of niche and neutral processes in structuring a soil microbial community." The ISME journal **4**(3): 337-345.

Dunbar, J., Barns, S. M., Ticknor, L. O. and Kuske, C. R. (2002). "Empirical and theoretical bacterial diversity in four Arizona soils." Applied and environmental microbiology **68**(6): 3035-3045.

Eckardt, F., Drake, N., Goudie, A., White, K. and Viles, H. (2001). "The role of playas in pedogenic gypsum crust formation in the central Namib Desert: A theoretical model." Earth Surface Processes and Landforms **26**(11): 1177-1193.

Eckardt, F., Livingstone, I., Seely, M. and Von Holdt, J. (2013a). "The surface geology and geomorphology around Gobabeb, Namib Desert, Namibia." Geografiska Annaler: Series A, Physical Geography **95**(4): 271-284.

Eckardt, F. and Schemenauer, R. (1998). "Fog water chemistry in the Namib Desert, Namibia." Atmospheric Environment **32**(14): 2595-2599.

Eckardt, F., Soderberg, K., Coop, L., Muller, A., Vickery, K., Grandin, R., Jack, C., Kapalanga, T. and Henschel, J. (2013b). "The nature of moisture at Gobabeb, in the central Namib Desert." Journal of arid environments **93**: 7-19.

Eckardt, F., Soderberg, K., Coop, L., Muller, A., Vickery, K., Grandin, R., Jack, C., Kapalanga, T. and Henschel, J. (2013c). "The nature of moisture at Gobabeb, in the central Namib Desert, unpublished raw data." Journal of arid environments **93**: 7-19.

Eckardt, F. and Spiro, B. (1999). "The origin of sulphur in gypsum and dissolved sulphate in the central Namib Desert, Namibia." Sedimentary Geology **123**(3): 255-273.

Ekenler, M. and Tabatabai, M. (2002). "B-glucosaminidase activity of soils: Effect of cropping systems and its relationship to nitrogen mineralization." Biology and Fertility of Soils **36**(5): 367-376.

Elbert, W., Weber, B., Burrows, S., Steinkamp, J., Büdel, B., Andreae, M. and Pöschl, U. (2012). "Contribution of cryptogamic covers to the global cycles of carbon and nitrogen." Nature Geoscience **5**(7): 459-462.

Emmerich, M., Bhansali, A., Lösekann-Behrens, T., Schröder, C., Kappler, A. and Behrens, S. (2012). "Abundance, distribution, and activity of Fe (ii)-oxidizing and Fe (iii)-reducing microorganisms in hypersaline sediments of Lake Kasin, southern Russia." Applied and environmental microbiology **78**(12): 4386-4399.

Ensign, J. (1978). "Formation, properties, and germination of actinomycete spores." Annual Reviews in Microbiology **32**(1): 185-219.

Escudero, A., Palacio, S., Maestre, F. and Luzuriaga, A. (2015). "Plant life on gypsum: A review of its multiple facets." Biological Reviews **90**(1): 1-18.

Faramarzi, M., Abbaspour, K., Vaghefi, S., Farzaneh, M., Zehnder, A., Srinivasan, R. and Yang, H. (2013). "Modeling impacts of climate change on freshwater availability in Africa." Journal of hydrology **480**: 85-101.

Farrelly, V., Rainey, F. A. and Stackebrandt, E. (1995). "Effect of genome size and rrn gene copy number on PCR amplification of 16s rRNA genes from a mixture of bacterial species." Applied and environmental microbiology **61**(7): 2798-2801.

Fierer, N., Bradford, M. and Jackson, R. (2007). "Toward an ecological classification of soil bacteria." Ecology **88**(6): 1354-1364.

Fierer, N. and Jackson, R. B. (2006). "The diversity and biogeography of soil bacterial communities." Proceedings of the National Academy of Sciences of the United States of America **103**(3): 626-631.

Fierer, N., Lauber, C., Ramirez, K., Zaneveld, J., Bradford, M. and Knight, R. (2012a). "Comparative metagenomic, phylogenetic and physiological analyses of soil microbial communities across nitrogen gradients." The ISME journal **6**(5): 1007-1017.

Fierer, N., Leff, J. W., Adams, B. J., Nielsen, U. N., Bates, S. T., Lauber, C. L., Owens, S., Gilbert, J. A., Wall, D. H. and Caporaso, J. G. (2012b). "Cross-biome metagenomic analyses of soil microbial communities and their functional attributes." Proceedings of the National Academy of Sciences **109**(52): 21390-21395.

Fierer, N., Strickland, M., Liptzin, D., Bradford, M. and Cleveland, C. (2009). "Global patterns in belowground communities." Ecology letters **12**(11): 1238-1249.

Findlay, S. and Sinsabaugh, R. (2006). "Large-scale variation in subsurface stream biofilms: A cross-regional comparison of metabolic function and community similarity." Microbial ecology **52**(3): 491-500.

Findlay, S., Sinsabaugh, R., Sobczak, W. and Hoostal, M. (2003). "Metabolic and structural response of hyporheic microbial communities to variations in supply of dissolved organic matter." Limnology and oceanography **48**(4): 1608-1617.

Fisher, M. and Triplett, E. (1999). "Automated approach for ribosomal intergenic spacer analysis of microbial diversity and its application to freshwater bacterial communities." Applied and environmental microbiology **65**(10): 4630-4636.

Fontaine, S., Mariotti, A. and Abbadie, L. (2003). "The priming effect of organic matter: A question of microbial competition?" Soil Biology and Biochemistry **35**(6): 837-843.

Forney, L. J., Zhou, X. and Brown, C. J. (2004). "Molecular microbial ecology: Land of the one-eyed king." Current opinion in microbiology **7**(3): 210-220.

Frankenberger, W. and Tabatabai, M. (1981). "Amidase activity in soils: Iv. Effects of trace elements and pesticides." Soil Science Society of America Journal **45**(6): 1120-1124.

Friedmann, E. and Ocampo, R. (1976). "Endolithic blue-green algae in the dry valleys: Primary producers in the Antarctic desert ecosystem." Science **193**(4259): 1247-1249.

Frossard, A., Gerull, L., Mutz, M. and Gessner, M. (2012). "Disconnect of microbial structure and function: enzyme activities and bacterial communities in nascent stream corridors." The ISME journal **6**(3): 680-691.

Frossard, A., Ramond, J., Seely, M. and Cowan, D. (2015). "Water regime history drives responses of soil Namib Desert microbial communities to wetting events." Scientific reports **5**.

Fuhrman, J. (2009). "Microbial community structure and its functional implications." Nature **459**(7244): 193-199.

Gao, Q. and Garcia-Pichel, F. (2011). "Microbial ultraviolet sunscreens." Nature Reviews Microbiology **9**(11): 791-802.

Garcıa-Gil, J., Plaza, C., Soler-Rovira, P. and Polo, A. (2000). "Long-term effects of municipal solid waste compost application on soil enzyme activities and microbial biomass." Soil Biology and Biochemistry **32**(13): 1907-1913.

Garzanti, E., Andò, S., Vezzoli, G., Lustrino, M., Boni, M. and Vermeesch, P. (2012). "Petrology of the Namib Sand Sea: Long-distance transport and compositional variability in the wind-displaced Orange delta." Earth-Science Reviews **112**(3): 173-189.

Garzanti, E., Vermeesch, P., Andò, S., Lustrino, M., Padoan, M. and Vezzoli, G. (2014). "Ultra-long distance littoral transport of Orange sand and provenance of the Skeleton Coast erg (Namibia)." Marine Geology **357**: 25-36.

Gehring, A. U., Riahi, N., Kind, J., Almqvist, B. S. and Weidler, P. G. (2014). "The formation of the Namib Sand Sea inferred from the spatial pattern of magnetic rock fragments." Earth and Planetary Science Letters **395**: 168-172.

Gobet, A., Boetius, A. and Ramette, A. (2014). "Ecological coherence of diversity patterns derived from classical fingerprinting and next generation sequencing techniques." Environmental microbiology **16**(9): 2672-2681.

Gombeer, S., Ramond, J., Eckardt, F., Seely, M. and Cowan, D. (2015). "The influence of surface soil physicochemistry on the edaphic bacterial communities in contrasting terrain types of the central Namib Desert." Geobiology.

Goswami, D., Pithwa, S., Dhandhukia, P. and Thakker, J. (2014). "Delineating kocuria turfanensis 2m4 as a credible pgpr: A novel iaa-producing bacteria isolated from saline desert." Journal of Plant Interactions **9**(1): 566-576.

Goudie, A. and Eckardt, F. (1999). "The evolution of the morphological framework of the central Namib Desert, Namibia, since the early Cretaceous." Geografiska Annaler. Series A, Physical Geography **81**(3): 443-458.

Goudie, A. and Viles, H. (2015). Landscapes and landforms of Namibia, Springer.

Goudie, A., Viles, H. and Parker, A. (1997). "Monitoring of rapid salt weathering in the central Namib Desert using limestone blocks." Journal of Arid Environments **37**(4): 581-598.

Grandy, A., Sinsabaugh, R., Neff, J., Stursova, M. and Zak, D. (2008). "Nitrogen deposition effects on soil organic matter chemistry are linked to variation in enzymes, ecosystems and size fractions." Biogeochemistry **91**(1): 37-49.

Gray, D., Foster, D., Meert, J., Goscombe, B., Armstrong, R., Trouw, R. and Passchier, C. (2008). "A Damara Orogen perspective on the assembly of southwestern Gondwana." Geological Society, London, Special Publications **294**(1): 257-278.

Green, P. (2006). Methylobacterium. The prokaryotes, Springer: 257-265.

Green, V., Stott, D. and Diack, M. (2006). "Assay for fluorescein diacetate hydrolytic activity: Optimization for soil samples." Soil Biology and Biochemistry **38**(4): 693-701.

Gundlapally, S. and Garcia-Pichel, F. (2006). "The community and phylogenetic diversity of biological soil crusts in the Colorado Plateau studied by molecular fingerprinting and intensive cultivation." Microbial ecology **52**(2): 345-357.

Hachfeld, B. (2000). "Rain, fog and species richness in the central Namib Desert in the exceptional rainy season of 1999/2000." Dinteria(26): 113-146.

Hamilton, W. and Seely, M. (1976). "Fog basking by the Namib Desert beetle, onymacris unguicularis."

Hanson, C., Fuhrman, J., Horner-Devine, M. and Martiny, J. (2012). "Beyond biogeographic patterns: Processes shaping the microbial landscape." Nature Reviews Microbiology **10**(7): 497-506.

Haynes, R. (2000). "Labile organic matter as an indicator of organic matter quality in arable and pastoral soils in New Zealand." Soil Biology and Biochemistry **32**(2): 211-219.

Henschel, J. and Lancaster, N. (2013). "Gobabeb–50 years of Namib Desert research." Journal of Arid Environments **93**: 1-6.

Henschel, J. and Seely, M. (2008). "Ecophysiology of atmospheric moisture in the Namib Desert." Atmospheric Research **87**(3): 362-368.

Hewson, E. (1943). "The reflection, absorption, and transmission of solar radiation by fog and cloud." Quarterly Journal of the Royal Meteorological Society **69**(298): 47-62.

Hollister, E., Engledow, A., Hammett, A., Provin, T., Wilkinson, H. and Gentry, T. (2010). "Shifts in microbial community structure along an ecological gradient of hypersaline soils and sediments." The ISME journal **4**(6): 829-838.

Hoyle, F. and Murphy, D. (2006). "Seasonal changes in microbial function and diversity associated with stubble retention versus burning." Soil Research **44**(4): 407-423.

Huang, P. (1990). "Role of soil minerals in transformations of natural organics and xenobiotics in soil." Soil biochemistry **6**: 29-115.

Hubbell, S. (2001). The unified neutral theory of biodiversity and biogeography (mpb-32), Princeton University Press.

Ishii, K. and Fukui, M. (2001). "Optimization of annealing temperature to reduce bias caused by a primer mismatch in multitemplate PCR." Applied and environmental microbiology **67**(8): 3753-3755.

Jones, R. T., Robeson, M. S., Lauber, C. L., Hamady, M., Knight, R. and Fierer, N. (2009). "A comprehensive survey of soil acidobacterial diversity using pyrosequencing and clone library analyses." The ISME journal **3**(4): 442-453.

Juma, N. and Tabatabai, M. (1977). "Effects of trace elements on phosphatase activity in soils." Soil Science Society of America Journal **41**(2): 343-346.

Jürgens, N., Burke, A., Seely, M. and Jacobson, K. (1997). "Desert." Vegetation of southern Africa: 189-214.

Kandeler, E., Tscherko, D., Bruce, K., Stemmer, M., Hobbs, P. J., Bardgett, R. D. and Amelung, W. (2000). "Structure and function of the soil microbial community in microhabitats of a heavy metal polluted soil." Biology and fertility of soils **32**(5): 390-400.

Keith-Roach, M., Bryan, N., Bardgett, R. D. and Livens, F. (2002). "Seasonal changes in the microbial community of a salt marsh, measured by phospholipid fatty acid analysis." Biogeochemistry **60**(1): 77-96.

Kemp, D. J., Smith, D. B., Foote, S. J., Samaras, N. and Peterson, M. G. (1989). "Colorimetric detection of specific DNA segments amplified by polymerase chain reactions." Proceedings of the National Academy of Sciences **86**(7): 2423-2427.

Khan, N., Tuffin, I., Stafford, W., Cary, C., Lacap, D., Pointing, S. and Cowan, D. (2011). "Hypolithic microbial communities of quartz rocks from Miers Valley, McMurdo Dry Valleys, Antarctica." Polar Biology **34**(11): 1657-1668.

Klappenbach, J., Dunbar, J. and Schmidt, T. (2000). "Rrna operon copy number reflects ecological strategies of bacteria." Applied and environmental microbiology **66**(4): 1328-1333.

Knight, R., Jansson, J., Field, D., Fierer, N., Desai, N., Fuhrman, J., Hugenholtz, P., van der Lelie, D., Meyer, F. and Stevens, R. (2012). "Unlocking the potential of metagenomics through replicated experimental design." Nature biotechnology **30**(6): 513-520.

Krapf, C. B., Stollhofen, H. and Stanistreet, I. G. (2003). "Contrasting styles of ephemeral river systems and their interaction with dunes of the Skeleton Coast erg (Namibia)." Quaternary International **104**(1): 41-52.

Lacap, D., Warren-Rhodes, K., McKay, C. and Pointing, S. (2011). "Cyanobacteria and chloroflexi-dominated hypolithic colonization of quartz at the hyper-arid core of the Atacama Desert, Chile." Extremophiles : life under extreme conditions **15**(1): 31-38.

Laity, J. J. (2009). Deserts and desert environments, John Wiley & Sons.

Lancaster, N. (1989). The Namib Sand Sea: Dune forms, processes and sediments, Balkema.

Lancaster, N. (2002). "How dry was dry?—late Pleistocene palaeoclimates in the Namib Desert." Quaternary Science Reviews **21**(7): 769-782.

Lancaster, N. and Seely, M. (1984). "Climate of the central Namib Desert." Madoqua **14**(1): 5-61.

Landi, L., Renella, G., Moreno, J., Falchini, L. and Nannipieri, P. (2000). "Influence of cadmium on the metabolic quotient, l-: D-glutamic acid respiration ratio and enzyme activity: Microbial biomass ratio under laboratory conditions." Biology and Fertility of Soils **32**(1): 8-16.

Lane, D. J., Pace, B., Olsen, G. J., Stahl, D. A., Sogin, M. L. and Pace, N. R. (1985). "Rapid determination of 16s ribosomal RNA sequences for phylogenetic analyses." Proceedings of the National Academy of Sciences **82**(20): 6955-6959.

Lauber, C. L., Hamady, M., Knight, R. and Fierer, N. (2009). "Pyrosequencing-based assessment of soil pH as a predictor of soil bacterial community structure at the continental scale." Applied and environmental microbiology **75**(15): 5111-5120.

Legendre, P. and Gallagher, E. (2001). "Ecologically meaningful transformations for ordination of species data." Oecologia **129**(2): 271-280.

Legg, T., Zheng, Y., Simone, B., Radloff, K., Mladenov, N., González, A., Knights, D., Siu, H., Rahman, M. and Ahmed, K. (2012). "Carbon, metals, and grain size correlate with bacterial community structure in sediments of a high arsenic aquifer." Frontiers in microbiology **3**.

Lester, E., Satomi, M. and Ponce, A. (2007). "Microflora of extreme arid Atacama Desert soils." Soil Biology and Biochemistry **39**(2): 704-708.

Li, W. J., Chen, H. H., Zhang, Y. Q., Kim, C. J., Park, D. J., Lee, J. C., Xu, L. H. and Jiang, C. L. (2005). "Citricoccus alkalitolerans sp. Nov., a novel actinobacterium isolated from a desert soil in Egypt." Int J Syst Evol Microbiol **55**(Pt 1): 87-90.

Li, W. J., Zhang, Y. Q., Schumann, P., Chen, H. H., Hozzein, W. N., Tian, X. P., Xu, L. H. and Jiang, C. L. (2006). "Kocuria aegyptia sp. Nov., a novel actinobacterium isolated from a saline, alkaline desert soil in Egypt." Int J Syst Evol Microbiol **56**(Pt 4): 733-737.

Lighthart, B., Baham, J. and Volk, V. (1983). "Microbial respiration and chemical speciation in metal-amended soils." Journal of environmental quality **12**(4): 543-548.

Lindström, E. and Langenheder, S. (2012). "Local and regional factors influencing bacterial community assembly." Environmental microbiology reports **4**(1): 1-9.

Liu, M., Peng, F., Wang, Y., Zhang, K., Chen, G. and Fang, C. (2009). "Kineococcus xinjiangensis sp. Nov., isolated from desert sand." International journal of systematic and evolutionary microbiology **59**(5): 1090-1093.

Liu, W.-T., Marsh, T. L., Cheng, H. and Forney, L. J. (1997). "Characterization of microbial diversity by determining terminal restriction fragment length polymorphisms of genes encoding 16s rRNA." Applied and environmental microbiology **63**(11): 4516-4522.

Livingstone, I. (2013). "Aeolian geomorphology of the Namib Sand Sea." Journal of Arid Environments **93**: 30-39.

López-Lozano, N., Eguiarte, L., Bonilla-Rosso, G., García-Oliva, F., Martínez-Piedragil, C., Rooks, C. and Souza, V. (2012). "Bacterial communities and the nitrogen cycle in the gypsum soils of Cuatro Ciénegas Basin, Coahuila: A Mars analogue." Astrobiology **12**(7): 699-709.

López-Lozano, N., Heidelberg, K., Nelson, W., García-Oliva, F., Eguiarte, L. and Souza, V. (2013). "Microbial secondary succession in soil microcosms of a desert oasis in the Cuatro Cienegas Basin, Mexico." PeerJ **1**: e47.

Lozupone, C. and Knight, R. (2007). "Global patterns in bacterial diversity." Proceedings of the National Academy of Sciences **104**(27): 11436-11440.

Luo, X., Wang, J., Zeng, X. C., Wang, Y., Zhou, L., Nie, Y., Dai, J. and Fang, C. (2012). "Mycetocola manganoxydans sp. Nov., an actinobacterium isolated from the Taklamakan Desert." Int J Syst Evol Microbiol **62**(Pt 12): 2967-2970.

Lynch, R., Darcy, J., Kane, N., Nemergut, D. and Schmidt, S. (2014). "Metagenomic evidence for metabolism of trace atmospheric gases by high-elevation desert actinobacteria." Frontiers in microbiology **5**.

Macherey-Nagel (2012). "PCR clean-up gel extraction, user manual Nucleospin® gel and PCR clean up." Retrieved July 1, 2014, from http://www.mn-net.com.

Makhalanyane, T., Valverde, A., Gunnigle, E., Frossard, A., Ramond, J. and Cowan, D. (2015). "Microbial ecology of hot desert edaphic systems." FEMS microbiology reviews.

Makhalanyane, T., Valverde, A., Lacap, D., Pointing, S., Tuffin, M. and Cowan, D. (2013). "Evidence of species recruitment and development of hot desert hypolithic communities." Environmental microbiology reports **5**(2): 219-224.

Manzoni, S., Schimel, J. and Porporato, A. (2012). "Responses of soil microbial communities to water stress: Results from a meta-analysis." Ecology **93**(4): 930-938.

Mardis, E. (2008). "The impact of next-generation sequencing technology on genetics." Trends in genetics **24**(3): 133-141.

Marschner, H. (2011). Marschner's mineral nutrition of higher plants, Academic press.

Martin, H. and Porada, H. (1977). "The intracratonic branch of the Damara Orogen in south west Africa i. Discussion of geodynamic models." Precambrian Research **5**(4): 311-338.

Massé, M., Bourgeois, O., Le Mouélic, S., Verpoorter, C., Spiga, A. and Le Deit, L. (2012). "Wide distribution and glacial origin of polar gypsum on Mars." Earth and Planetary Science Letters **317**: 44-55.

Matsui, M., Fowler, J. H. and Walling, L. L. (2006). "Leucine aminopeptidases: Diversity in structure and function." Biological chemistry **387**(12): 1535-1544.

Mayilraj, S., Krishnamurthi, S., Saha, P. and Saini, H. S. (2006). "Rhodococcus kroppenstedtii sp. Nov., a novel actinobacterium isolated from a cold desert of the Himalayas, India." Int J Syst Evol Microbiol **56**(Pt 5): 979-982.

McCarthy, A. and Williams, S. (1992). "Actinomycetes as agents of biodegradation in the environment—a review." Gene **115**(1): 189-192.

McGill, W. and Cole, C. (1981). "Comparative aspects of cycling of organic C, N, S and P through soil organic matter." Geoderma **26**(4): 267-286.

Mendlesohn, J., Jarvis, A., Roberts, C. and Robertson, T. (2002). Atlas of Namibia, David Philip Publishers, Cape Town.

Mildrexler, D. J., Zhao, M. and Running, S. W. (2006). "Where are the hottest spots on Earth?" EOS, Transactions American Geophysical Union **87**(43): 461-467.

Milner, S., Duncan, A. and Ewart, A. (1992). "Quartz latite rheoignimbrite flows of the Etendeka formation, north-western Namibia." Bulletin of Volcanology **54**(3): 200-219.

MO BIO Laboratories (2013). "Powersoil® DNA isolation kit, instruction manual." Version: 11212013. Retrieved July 1, 2014, from www.mobio.com.

Mooney, H. A., Gulmon, S., Rundel, P. W. and Ehleringer, J. (1980). "Further observations on the water relations ofprosopis tamarugo of the northern Atacama Desert." Oecologia **44**(2): 177-180.

Mouquet, N. and Loreau, M. (2003). "Community patterns in source – sink metacommunities." The american naturalist **162**(5): 544-557.

Muller, A., Reason, C. and Fauchereau, N. (2008). "Extreme rainfall in the Namib Desert during late summer 2006 and influences of regional ocean variability." International Journal of Climatology **28**(8): 1061-1070.

Muller, C. (2015). "Plant-soil relations on gypsum and non-gypsum soils of the Chihuahuan Desert." Plant-soil.

Muyzer, G., De Waal, E. and Uitterlinden, A. (1993). "Profiling of complex microbial populations by denaturing gradient gel electrophoresis analysis of polymerase chain reaction-amplified genes coding for 16s rRNA." Applied and environmental microbiology **59**(3): 695-700.

Myers, N., Mittermeier, R. A., Mittermeier, C. G., Da Fonseca, G. A. and Kent, J. (2000). "Biodiversity hotspots for conservation priorities." Nature **403**(6772): 853-858.

Nagy, M., Pérez, A. and Garcia-Pichel, F. (2005). "The prokaryotic diversity of biological soil crusts in the Sonoran Desert (Organ Pipe Cactus National Monument, AZ)." FEMS microbiology ecology **54**(2): 233-245.

Nannipieri, P., Ascher, J., Ceccherini, M., Landi, L., Pietramellara, G. and Renella, G. (2003). "Microbial diversity and soil functions." European Journal of Soil Science **54**(4): 655-670.

Nannipieri, P., Giagnoni, L., Landi, L. and Renella, G. (2011). Role of phosphatase enzymes in soil. Phosphorus in action, Springer: 215-243.

Nannipieri, P., Giagnoni, L., Renella, G., Puglisi, E., Ceccanti, B., Masciandaro, G., Fornasier, F., Moscatelli, M. and Marinari, S. (2012). "Soil enzymology: Classical and molecular approaches." Biology and fertility of soils **48**(7): 743-762.

Nannipieri, P., Kandeler, E. and Ruggiero, P. (2002). "Enzyme activities and microbiological and biochemical processes in soil." Enzymes in the environment. Marcel Dekker, New York: 1-33.

Nannipieri, P. and Smalla, K. (2006). Nucleic acids and proteins in soil, Springer Science & Business Media.

NASA (2013). NASA-USGS landsat 8 satellite pinpoints coldest spots on earth.

Navarro-Gonzalez, R., Rainey, F. A., Molina, P., Bagaley, D. R., Hollen, B. J., de la Rosa, J., Small, A. M., Quinn, R. C., Grunthaner, F. J., Caceres, L., Gomez-Silva, B. and McKay, C. P. (2003). "Mars-like soils in the Atacama Desert, Chile, and the dry limit of microbial life." Science **302**(5647): 1018-1021.

Non-Affiliated Soil Analysis Work Committee (1990). Handbook of standard soil testing methods for advisory purposes, Soil Science Society of South Africa.

Nørgaard, T. and Dacke, M. (2010). "Fog-basking behaviour and water collection efficiency in Namib Desert darkling beetles." Frontiers in zoology **7**(1): 23.

Novak, J. M., Lima, I., Xing, B., Gaskin, J. W., Steiner, C., Das, K., Ahmedna, M., Rehrah, D., Watts, D. W. and Busscher, W. J. (2009). "Characterization of designer biochar produced at different temperatures and their effects on a loamy sand." Annals of Environmental Science **3**(1): 2.

Okitsu, S. (2005). "Factors controlling geographical distribution in savanna vegetation in Namibia."

Oksanen, J., Kindt, R., Legendre, P., O'Hara, B., Stevens, M. H. H., Oksanen, M. J. and Suggests, M. (2007). "The vegan package." Community ecology package: 631-637.

Olander, L. P. and Vitousek, P. M. (2000). "Regulation of soil phosphatase and chitinase activityby N and P availability." Biogeochemistry **49**(2): 175-191.

Olivier, J. (1995). "Spatial distribution of fog in the Namib." Journal of Arid Environments **29**(2): 129-138.

Olsen, S. (1954). "Estimation of available phosphorus in soils by extraction with sodium bicarbonate."

Oren, A., Sørensen, K., Canfield, D., Teske, A., Ionescu, D., Lipski, A. and Altendorf, K. (2009). "Microbial communities and processes within a hypersaline gypsum crust in a saltern evaporation pond (Eilat, Israel)." Hydrobiologia **626**(1): 15-26.

Osborn, A., Moore, E. and Timmis, K. (2000). "An evaluation of terminal – restriction fragment length polymorphism (T – RFLP) analysis for the study of microbial community structure and dynamics." Environmental microbiology **2**(1): 39-50.

Pace, N., Stahl, D., Lane, D. and Olsen, G. (1986). The analysis of natural microbial populations by ribosomal RNA sequences. Advances in microbial ecology, Springer: 1-55.

Pallett, J. (1995). "The Sperrgebiet: Namibia's least known wilderness." An environmental profile of the Sperrgebiet or Diamond Area **1**.

Paul, E. (2014). Soil microbiology, ecology and biochemistry, Academic press.

Paul, N. and Gwynn-Jones, D. (2003). "Ecological roles of solar UV radiation: Towards an integrated approach." Trends in Ecology & Evolution **18**(1): 48-55.

Peel, M. C., Finlayson, B. L. and McMahon, T. A. (2007). "Updated world map of the Köppen-Geiger climate classification." Hydrology and earth system sciences discussions **4**(2): 439-473.

Petrosino, J., Highlander, S., Luna, R., Gibbs, R. and Versalovic, J. (2009). "Metagenomic pyrosequencing and microbial identification." Clinical chemistry **55**(5): 856-866.

Pickford, M., Senut, B. and Dauphin, Y. (1995). "Biostratigraphyof the Tsondab sandstone (Namibia) based on gigantic avian eggshells." Geobios **28**(1): 85-98.

Pointing, S. and Belnap, J. (2012). "Microbial colonization and controls in dryland systems." Nature reviews. Microbiology **10**(8): 551-562.

Pointing, S., Chan, Y., Lacap, D., Lau, M., Jurgens, J. and Farrell, R. (2009). "Highly specialized microbial diversity in hyper-arid polar desert." Proceedings of the National Academy of Sciences: pnas. 0908274106.

Prestel, E., Salamitou, S. and DuBow, M. S. (2008). "An examination of the bacteriophages and bacteria of the Namib Desert." Journal of microbiology **46**(4): 364-372.

Pretty, J., Olsson, L., Farage, P., Warren, A., Tschakert, P. and Ardö, J. (2005). "Carbon sequestration in dryland soils." World Soil Resources Report.

Prosser, J. (2010). "Replicate or lie." Environmental microbiology **12**(7): 1806-1810.

Ramette, A. (2009). "Quantitative community fingerprinting methods for estimating the abundance of operational taxonomic units in natural microbial communities." Applied and environmental microbiology **75**(8): 2495-2505.

Raup, D. and Crick, R. (1979). "Measurement of faunal similarity in paleontology." Journal of Paleontology: 1213-1227.

RCD Team (2013). R: A language and environment for statistical computing.

Reysenbach, A., Pace, N., Robb, F. and Place, A. (1995). "Archaea: A laboratory manual—thermophiles." Cold Spring Harbour Laboratory Press, New York, NY, USA.

Ringnér, M. (2008). "What is principal component analysis?" Nature biotechnology **26**(3): 303-304.

Robertson, T. (2012). "Namibia's coast: Ocean riches and desert treasures."

Robinson, C., Wierzchos, J., Black, C., Crits‐Christoph, A., Ma, B., Ravel, J., Ascaso, C., Artieda, O., Valea, S. and Roldán, M. (2015). "Microbial diversity and the presence of algae in halite endolithic communities are correlated to atmospheric moisture in the hyper‐arid zone of the Atacama Desert." Environmental microbiology **17**(2): 299-315.

Robinson, M. D. and Barrows, C. W. (2013). "Namibian and north american sand-diving lizards." Journal of Arid Environments **93**(0): 116-125.

Romero, H. (2008). "Irradiancia solar en territorios de la República de Chile." Santiago, CNE/PNUD/UTFSM.

Ronca, S., Ramond, J., Jones, B., Seely, M. and Cowan, D. (2015). "Namib Desert dune/interdune transects exhibit habitat-specific edaphic bacterial communities." Frontiers in microbiology **6**.

Ross, D. S. (1995). "Recommended methods for determining soil cation exchange capacity." Recommended Soil Testing Procedures for the Northeastern United States. Northeastern Regional Publication(493): 62-69.

Rothschild, L. J. and Mancinelli, R. L. (2001). "Life in extreme environments." Nature **409**(6823): 1092-1101.

Santhanam, R., Rong, X., Huang, Y., Andrews, B. A., Asenjo, J. A. and Goodfellow, M. (2013). "Streptomyces bullii sp. Nov., isolated from a hyper-arid Atacama Desert soil." Antonie van Leeuwenhoek **103**(2): 367-373.

Schimel, J., Balser, T. and Wallenstein, M. (2007). "Microbial stress-response physiology and its implications for ecosystem function." Ecology **88**(6): 1386-1394.

Schlesinger, W., Raikes, J., Hartley, A. and Cross, A. (1996). "On the spatial pattern of soil nutrients in desert ecosystems." Ecology **77**(2): 364-374.

Schmidt, S., Costello, E., Nemergut, D., Cleveland, C. C., Reed, S., Weintraub, M., Meyer, A. and Martin, A. (2007). "Biogeochemical consequences of rapid microbial turnover and seasonal succession in soil." Ecology **88**(6): 1379-1385.

Schnecker, J., Wild, B., Hofhansl, F., Alves, R. J. E., Bárta, J., Capek, P., Fuchslueger, L., Gentsch, N., Gittel, A. and Guggenberger, G. (2014). "Effects of soil organic matter properties and microbial community composition on enzyme activities in cryoturbated arctic soils." PloS one **9**(4).

Schnecker, J., Wild, B., Takriti, M., Alves, R. J. E., Gentsch, N., Gittel, A., Hofer, A., Klaus, K., Knoltsch, A. and Lashchinskiy, N. (2015). "Microbial community composition shapes enzyme patterns in topsoil and subsoil horizons along a latitudinal transect in western Siberia." Soil Biology and Biochemistry **83**: 106-115.

Schopf, J., Farmer, J., Foster, I., Kudryavtsev, A., Gallardo, V. and Espinoza, C. (2012). "Gypsum-permineralized microfossils and their relevance to the search for life on Mars." Astrobiology **12**(7): 619-633.

Schumacher, B. A. (2002). "Methods for the determination of total organic carbon (TOC) in soils and sediments." Ecological Risk Assessment Support Center: 1-23.

Scientific, T. (2012a). "Fast digestion of DNA." Retrieved July 1, 2014, from www.thermoscientificbio.com/uploadedFiles/Resources/fast-digestion-dna.pdf.

Scientific, T. (2012b). "Scaling up DNA digestion reaction." Retrieved July 1, 2014, from www.thermoscientificbio.com/uploadedFiles/Resources/scaling-up-dna-digestion-reaction.pdf.

Scola, V. (2012). Gobabeb dune.

Seely, M. (2012). Namib sand sea world heritage nomination, Windhoek: UNESCO Namibian National Committee for World Heritage.

Seely, M. and Pallett, J. (2008). Namib: Secrets of a desert uncovered, Venture.

Senut, B. and Pickford, M. (1995). "Fossil eggs and cenozoic continental biostratigraphy of Namibia." Palaeontologia Africana **32**: 33-37.

Sessitsch, A., Weilharter, A., Gerzabek, M. H., Kirchmann, H. and Kandeler, E. (2001). "Microbial population structures in soil particle size fractions of a long-term fertilizer field experiment." Applied and environmental microbiology **67**(9): 4215-4224.

Seth, B., Kröner, A., Mezger, K., Nemchin, A., Pidgeon, R. and Okrusch, M. (1998). "Archaean to neoproterozoic magmatic events in the Kaoko belt of NW Namibia and their geodynamic significance." Precambrian Research **92**(4): 341-363.

Sexstone, A. J., Revsbech, N. P., Parkin, T. B. and Tiedje, J. M. (1985). "Direct measurement of oxygen profiles and denitrification rates in soil aggregates." Soil science society of America journal **49**(3): 645-651.

Siesser, W. (1978). "Aridification of the Namib Desert: Evidence from oceanic cores." Antarctic glacial history and world palaeoenvironments. Balkema, Rotterdam: 105-113.

Siesser, W. G. (1980). "Late Miocene origin of the Benguela upswelling system off northern Namibia." Science **208**(4441): 283-285.

Sinsabaugh, R. (2010). "Phenol oxidase, peroxidase and organic matter dynamics of soil." Soil Biology and Biochemistry **42**(3): 391-404.

Sinsabaugh, R., Antibus, R., Linkins, A., McClaugherty, C., Rayburn, L., Repert, D. and Weiland, T. (1993). "Wood decomposition: Nitrogen and phosphorus dynamics in relation to extracellular enzyme activity." Ecology: 1586-1593.

Sinsabaugh, R., Hill, B. and Shah, J. J. F. (2009). "Ecoenzymatic stoichiometry of microbial organic nutrient acquisition in soil and sediment." Nature **462**(7274): 795-798.

Sinsabaugh, R. and Shah, J. J. F. (2011). "Ecoenzymatic stoichiometry of recalcitrant organic matter decomposition: The growth rate hypothesis in reverse." Biogeochemistry **102**(1-3): 31-43.

Smith, J., Halvorson, J. and Bolton, H. (2002). "Soil properties and microbial activity across a 500m elevation gradient in a semi-arid environment." Soil Biology and Biochemistry **34**(11): 1749-1757.

Southgate, R., Masters, P. and Seely, M. (1996). "Precipitation and biomass changes in the Namib Desert dune ecosystem." Journal of Arid Environments **33**(3): 267-280.

Souvignet, M., Penedo, S., Künne, A., Krause, P., Flügel, W. and Freer, J. (2012). Model comparison for climate change impact prediction: Does complexity actually matter? EGU General Assembly Conference Abstracts.

Stahl, D., Lane, D., Olsen, G. and Pace, N. (1985). "Characterization of a Yellowstone hot spring microbial community by 5s rRNA sequences." Applied and environmental microbiology **49**(6): 1379-1384.

Steinweg, J., Dukes, J. and Wallenstein, M. (2012). "Modeling the effects of temperature and moisture on soil enzyme activity: Linking laboratory assays to continuous field data." Soil Biology and Biochemistry **55**: 85-92.

Sterner, R. and Elser, J. (2002). Ecological stoichiometry: The biology of elements from molecules to the biosphere, Princeton University Press.

Stevenson, I. and Mandelstam, J. (1965). "Induction and multi-sensitive end-product repression in two converging pathways degrading aromatic substances in pseudomonas fluorescens." Biochem. J **96**: 354-362.

Stomeo, F., Valverde, A., Pointing, S., McKay, C., Warren-Rhodes, K., Tuffin, M., Seely, M. and Cowan, D. (2013). "Hypolithic and soil microbial community assembly along an aridity gradient in the Namib Desert." Extremophiles : life under extreme conditions **17**(2): 329-337.

Stone, A. E. C. and Thomas, D. S. G. (2013). "Casting new light on late quaternary environmental and palaeohydrological change in the Namib Desert: A review of the application of optically stimulated luminescence in the region." Journal of Arid Environments **93**(0): 40-58.

Tamames, J., Abellán, J., Pignatelli, M., Camacho, A. and Moya, A. (2010). "Environmental distribution of prokaryotic taxa." BMC microbiology **10**(1): 85.

Tankard, A. J. and Rogers, J. (1978). "Late Cenozoic palaeoenvironments on the west coast of southern Africa." Journal of Biogeography: 319-337.

Technicon (1977). "Individual/simultaneous determination of nitrogen and/or phosphorus in BD acid digests." Industrial method(329-74).

Thornthwaite, C. W. (1948). "An approach toward a rational classification of climate." Geographical review: 55-94.

Tiquia, S. (2005). "Microbial community dynamics in manure composts based on 16s and 18s rDNA T-RFLP profiles." Environmental technology **26**(10): 1101-1114.

Torsvik, V., Goksøyr, J. and Daae, F. (1990). "High diversity in DNA of soil bacteria." Applied and environmental microbiology **56**(3): 782-787.

Torsvik, V. and Øvreås, L. (2002). "Microbial diversity and function in soil: From genes to ecosystems." Current opinion in microbiology **5**(3): 240-245.

Tracy, C. R., Streten-Joyce, C., Dalton, R., Nussear, K. E., Gibb, K. S. and Christian, K. A. (2010). "Microclimate and limits to photosynthesis in a diverse community of hypolithic cyanobacteria in northern Australia." Environmental microbiology **12**(3): 592-607.

Trumper, K., Ravilious, C. and Dickson, B. (2008). "Carbon in drylands: Desertification, climate change and carbon finance." A UNEP-UNDPUNCCD Technical note for discussions at CRIC **7**: 1-12.

Tyler, G. (1974). "Heavy metal pollution and soil enzymatic activity." Plant and Soil **41**(2): 303-311.

UNEP (1992). World atlas of desertification / UNEP, United Nations Environment Programme. London ; Baltimore, Edward Arnold.

UNEP (2006). UNEP 2006 annual report.

Urich, T., Lanzén, A., Qi, J., Huson, D., Schleper, C. and Schuster, S. (2008). "Simultaneous assessment of soil microbial community structure and function through analysis of the meta-transcriptome." PloS one **3**(6): e2527-e2527.

Valverde, A., Makhalanyane, T. and Cowan, D. (2014). "Contrasting assembly processes in a bacterial metacommunity along a desiccation gradient." Frontiers in microbiology **5**.

Valverde, A., Makhalanyane, T., Seely, M. and Cowan, D. (2015). "Cyanobacteria drive community composition and functionality in rock–soil interface communities." Molecular ecology **24**(4): 812-821.

Van der Wateren, F. M. and Dunai, T. J. (2001). "Late neogene passive margin denudation history—cosmogenic isotope measurements from the central Namib Desert." Global and Planetary Change **30**(3–4): 271-307.

van Dorst, J., Bissett, A., Palmer, A., Brown, M., Snape, I., Stark, J., Raymond, B., McKinlay, J., Ji, M. and Winsley, T. (2014). "Community fingerprinting in a sequencing world." FEMS microbiology ecology **89**(2): 316-330.

Van Gestel, M., Merckx, R. and Vlassak, K. (1996). "Spatial distribution of microbial biomass in microaggregates of a silty-loam soil and the relation with the resistance of microorganisms to soil drying." Soil Biology and Biochemistry **28**(4): 503-510.

Van Zinderen Bakker, E. (1984). "Aridity along the Namibian coast." Palaeoecology of Africa **16**(1984): 149-160.

Vaneechoutte, M., Rossau, R., De Vos, P., Gillis, M., Janssens, D., Paepe, N., De Rouck, A., Fiers, T., Claeys, G. and Kersters, K. (1992). "Rapid identification of bacteria of the comamonadaceae with amplified ribosomal DNA-restriction analysis (ARDRA)." FEMS microbiology letters **93**(3): 227-233.

Vermeesch, P., Fenton, C., Kober, F., Wiggs, G., Bristow, C. S. and Xu, S. (2010). "Sand residence times of one million years in the Namib Sand Sea from cosmogenic nuclides." Nature Geoscience **3**(12): 862-865.

Viles, H. and Goudie, A. (2013). "Weathering in the central Namib Desert, Namibia: Controls, processes and implications." Journal of Arid Environments **93**: 20-29.

Vinardell, M., Ugartondo, V. and Mitjans, M. (2008). "Potential applications of antioxidant lignins from different sources." Industrial Crops and Products **27**(2): 220-223.

Waldrop, M., Balser, T. and Firestone, M. (2000). "Linking microbial community composition to function in a tropical soil." Soil Biology and Biochemistry **32**(13): 1837-1846.

Walkley, A. (1947). "A critical examination of a rapid method for determining organic carbon in soils-effect of variations in digestion conditions and of inorganic soil constituents." Soil Science **63**(4): 251-264.

Walkley, A. and Black, I. A. (1934). "An examination of the Degtjareff method for determining soil organic matter, and a proposed modification of the chromic acid titration method." Soil science **37**(1): 29-38.

Walter, H., Giess, W., Scholz, H., von Schwind, H., Seely, M., Walter, E. and Evenari, M. (1986). "The Namib Desert." Ecosystems of the World **12**: 245-282.

Wang, J., Shen, J., Wu, Y., Tu, C., Soininen, J., Stegen, J., He, J., Liu, X., Zhang, L. and Zhang, E. (2013). "Phylogenetic beta diversity in bacterial assemblages across ecosystems: Deterministic versus stochastic processes." The ISME journal **7**(7): 1310-1321.

Wanke, H. and Wanke, A. (2007). "Lithostratigraphy of the Kalahari Group in northeastern Namibia." Journal of African Earth Sciences **48**(5): 314-328.

Ward, J. (1987). The cenozoic succession in the Kuiseb Valley, central Namib Desert, Geological Survey, Department of Economic Affairs.

Ward, J. and Corbett, I. (1990). "Towards an age for the Namib." Namib ecology **25**: 17-26.

Ward, J., Seely, M. and Lancaster, N. (1983). "On the antiquity of the Namib." South African Journal of Science **79**(5): 175-183.

Warren-Rhodes, K., Rhodes, K., Pointing, S., Ewing, S., Lacap, D., Gómez-Silva, B., Amundson, R., Friedmann, E. and McKay, C. (2006). "Hypolithic cyanobacteria, dry limit of photosynthesis, and microbial ecology in the hyperarid Atacama Desert." Microbial ecology **52**(3): 389-398.

Wharton, D. A. (2002). "Life at the limits: Organisms in extreme environments." Cambridge university press Cambridge **14**: 427-431.

White, K., Walden, J. and Gurney, S. D. (2007). "Spectral properties, iron oxide content and provenance of Namib dune sands." Geomorphology **86**(3): 219-229.

Whitman, W. B., Coleman, D. C. and Wiebe, W. J. (1998). "Prokaryotes: The unseen majority." Proceedings of the National Academy of Sciences **95**(12): 6578-6583.

Wichern, F. and Joergensen, R. G. (2009). "Soil microbial properties along a precipitation transect in southern Africa." Arid Land Research and Management **23**(2): 115-126.

Wierzchos, J., Davila, A., Sánchez-Almazo, I., Hajnos, M., Swieboda, R. and Ascaso, C. (2012). "Novel water source for endolithic life in the hyperarid core of the Atacama Desert." Biogeosciences **9**(6): 2275-2286.

Wilkinson, M. J. (1990). Paleoenvironments in the Namib Desert: The lower tumas basin in the late Cenozoic, University of Chicago Press.

Woese, C. (1987). "Bacterial evolution." Microbiological reviews **51**(2): 221.

Wong, F., Lacap, D., Lau, M., Aitchison, J., Cowan, D. and Pointing, S. (2010). "Hypolithic microbial community of quartz pavement in the high-altitude tundra of central Tibet." Microbial ecology **60**(4): 730-739.

Wood, S., Mountfort, D., Selwood, A., Holland, P., Puddick, J. and Cary, S. (2008a). "Widespread distribution and identification of eight novel microcystins in Antarctic cyanobacterial mats." Applied and environmental microbiology **74**(23): 7243-7251.

Wood, S., Rueckert, A., Cowan, D. and Cary, S. (2008b). "Sources of edaphic cyanobacterial diversity in the dry valleys of eastern Antarctica." The ISME journal **2**(3): 308-320.

Wynn-Williams, D. (2002). Cyanobacteria in deserts—life at the limit? The ecology of cyanobacteria, Springer: 341-366.

Yao, H., He, Z., Wilson, M. and Campbell, C. (2000). "Microbial biomass and community structure in a sequence of soils with increasing fertility and changing land use." Microbial ecology **40**(3): 223-237.

Yeager, C., Kornosky, J., Housman, D., Grote, E., Belnap, J. and Kuske, C. (2004). "Diazotrophic community structure and function in two successional stages of biological soil crusts from the Colorado Plateau and Chihuahuan Desert." Applied and environmental microbiology **70**(2): 973-983.